Dynamics of Cortical Decision Circuits during Changes in the Fidelity of Sensory Representations

Dissertation Advisor: Dr. Richard T. Born Alexandra Smolyanskaya

Dynamics of cortical decision circuits during changes in the fidelity of sensory representations

Abstract

Every waking moment, we make decisions, from where to move our eyes to what to eat for dinner. The ease and speed with which we do this belie the complexity of the underlying neuronal processing. In the visual system, every scene is processed via a complicated network of neurons that extends from the retina through multiple areas in the visual cortex. Each decision requires rapid coordination of signals from the relevant neurons. Deficits in this integration are likely causes of debilitating learning disorders, yet we know little about the processes involved.

Previous studies of the macaque visual cortex indicate that as monkeys learn a new task the parts of the brain involved in decision making select which neurons they "listen to": the most informative neurons become more strongly associated with the animal's decisions as it learns. However, this process has only been studied over the course of several months as monkeys gradually learn a complex task. We set out to probe the dynamics of this relationship on a shorter timescale. We studied the middle temporal area (MT) of the visual cortex, where neurons are selective for binocular disparity (a depth cue) and motion direction; they have also been shown to contribute to perceptual decisions during motion- and depth-based tasks. After training monkeys on motion and depth detection tasks, we degraded the sensitivity of MT neurons for depth more than motion by reversibly inactivating two major inputs to MT—visual areas V2 and V3—by cooling. We hypothesized that degrading depth information more than motion would lead to bigger changes in the extent to which MT neurons contributed to decisions during the

depth task than the motion task. We monitored this contribution to decisions, as measured by *detect probability* (DP), prior to and during daily inactivation sessions. We found that neuronal DP decreased during the depth task, indicating that neurons became less involved in these decisions. DP did not change during the motion task, suggesting that these changes can be specific to one feature. Our results revealed a level of fast, selective flexibility in the decision circuitry.

Table of Contents

List of Figures

Acknowledgments

My experience in the Harvard Program in Neuroscience has been both a humbling and confidence-building experience. I have grown as a scientist and as a person while having a truly great time. I owe that to the many wonderful people who supported me along the way.

I am extremely grateful to my advisor, Rick Born, who challenged me and provided the freedom to let me grow as a scientist. He has been and will continue to be a role model in science and in life.

I am grateful to the past and present members of the Born Lab: Nic Price, Carlos Ponce, Nick Hunter, Vladimir Berezovskii, Andrew Zaharia, JoJo Nassi, Doug Ruff, Mari Sosa, Alex Trott, Till Hartmann, and Lexie Smith. In particular, thanks to Vladimir's patient teaching, I will forever be able to find MT in my sleep. Thanks to Nic Price for always being at the other end of the rope. Thanks to Doug Ruff for his infinite support as a colleague and a friend. I am immensely grateful to Lexie Smith for her help with my experiments and her friendship.

Thanks to all the people who make the Systems Club a fun, stimulating environment. A special thanks to Marlene Cohen, for her generosity and encouragement. Thanks to the Monkey Ladies for the chocolate, wine, and excellent stories. Thanks to John Maunsell, Marge Livingstone, and John Assad for their guidance and support.

Thanks to everyone who has helped make the Program in Neuroscience a truly supportive place to grow up: Karen Harmin, Rick Born, Rachel Wilson, Gina Conquest, Gary Yellen, and Roz Segal.

Thanks to my parents, grandparents, Sasha, and Tanya who left their lives behind and brought me to this country. Thanks to Dima, whose courage will always inspire.

Thanks to Dan for his kindness, cheerfulness, and companionship.

I have made some of the best friends I have ever had during my time here and I look to the future with excitement, knowing that I will have their continued friendship and support.

Introduction

We are confronted with a variety of new sights, sounds, and sensations every second. Without much effort, we can quickly use this information to respond to the world around us—move out of the way of an oncoming car, turn toward a singing bird, or learn to play a video game. The ease and speed with which we do these things belie the complexity of the underlying neuronal processing. In the visual system, every image that falls on our retina is processed via a complicated network of neurons that extends from the retina to the visual cortex—the part of the brain that is believed to endow us with visual perception. As the information proceeds through various pathways, the image is segmented into components—orientations, colors, speeds, and locations in space—different combinations of which are processed by different groups of neurons. A single decision, move right or move left, requires rapid coordination of outputs from the relevant neurons. This rapid flexibility implies that there are mechanisms in the brain that can select these relevant neurons very quickly. Yet we know little about the mechanisms and dynamics of how such neurons are selected.

What little we know about the cortical mechanisms underlying this flexibility has come primarily from experiments in monkeys that have been trained to perform demanding cognitive tasks. In particular, the visual system has been a particularly fruitful substrate for studies of cortical mechanisms because of how well we understand some of its basic properties. In a recent investigation into the dynamics accompanying learning in visual cortex, Law and Gold (2008) trained macaque monkeys on a motion-based task in which the animals discriminated the direction of motion of a visual stimulus presented on a screen. Monkeys master such tasks through daily training sessions over the course of several months, and Law and Gold recorded neurons in visual cortical area MT (and LIP), an area highly sensitive to motion, during every

such training session. They found that as the monkeys' behavioral performance improved, the MT neurons did not get any more sensitive to motion; they were just as informative about the visual stimulus at the beginning as they were after months of training. Instead, what seemed to change was how much these neurons contributed to the animals' decisions. In particular, as the animal learned, the more informative neurons became more involved in the monkey's decisions. These results indicate that one way to account for the animal's behavioral improvement is via the preferential selection of the most useful neurons through training. We set out to determine whether this selection process can happen more quickly, within about an hour. To do this, we inverted the question to ask: Can neurons be "de-selected" if they become less useful (*i.e.* less informative about the visual stimulus)? Does the decision circuitry adapt by no longer monitoring these neurons? Or stated differently, when the circuitry is forced to search for new neurons, as might happen when a monkey learns a new task, can we observe this change in the time course of an hour? Stating the question this way allowed us to use well-trained animals with established decision circuitry. Instead of training animals on a new task, which may take months, we degraded the sensitivity of neurons embedded within that circuitry on the time scale of a few minutes, thereby encouraging the decision circuitry to adapt.

To degrade neuronal sensitivity, we used cortical cooling (Lomber et al., 1999; Ponce et al., 2008) to inactivate two of the inputs to MT, the same brain area where Law and Gold observed long-timescale changes in decision circuits. In addition to being sensitive to motion direction, neurons in MT are sensitive to an important depth cue, binocular disparity. Ponce and colleagues (2008) showed that reversibly inactivating V2 and V3—two of the major cortical inputs to MT—degrades MT neurons' sensitivity for binocular disparity more so than for direction of motion. Using this technique, we asked whether such disproportionate changes in

MT neuron's "informativeness" can lead to disproportionate changes in decision circuits during motion and depth tasks. Since binocular disparity sensitivity is affected more than motion, we hypothesized that decision circuitry will also be affected more during depth tasks than motion tasks.

In the following sections I will briefly discuss the properties of MT neurons, focusing on their involvement in motion and depth processing as well as behavioral decisions during motion- and depth-based tasks. Furthermore, I will discuss potential mechanisms for how they become involved in behavioral decisions and present a plausible hypothesis for the results of degrading neuronal sensitivity for depth more than motion in MT.

The middle temporal area

MT of the macaque monkey visual cortex is located in the posterior bank of the superior temporal sulcus (Dubner and Zeki, 1971). Its connections with other cortical areas place it in the dorsal, or 'where' processing stream of the visual hierarchy (Ungerleider and Mishkin, 1982). Accordingly, neurons encode information about the location and motion of visual stimuli but are relatively insensitive to form and color (Albright, 1992; Gegenfurtner et al., 1994).

Anatomical connectivity

The two major sources of cortical input to MT originate from distinct but intermingled cells in layer 4B in V1 (Figure 1; reviewed in Born and Bradley, 2005). From layer 4B, spiny stellate cells provide the majority of the direct monosynaptic input to MT. In contrast, signals from the pyramidal 4B neurons proceed to MT indirectly via cortical areas V2 and V3 (Maunsell and Van Essen, 1983c; Shipp and Zeki, 1985, 1989; DeYoe and Van Essen, 1988; Sincich and Horton, 2003). Although these cortical inputs from V1 predominate, MT also receives

subcortical input from the lateral and inferior pulvinar (Glickstein et al., 1980; Maunsell and Van Essen, 1983c; Stepniewska et al., 1999) as well as directly from the lateral geniculate nucleus (Sincich et al., 2004). As a result, some MT neurons can remain somewhat responsive following lesions or inactivation of V1 (Rodman et al., 1989; Girard et al., 1992). As output, MT sends feed-forward projections to areas involved in optic flow processing (e.g. MST, VIP) and the generation of eye movements (e.g. LIP, FEF, SC, dorsolateral pons) as well as feedback connections to earlier visual areas (Maunsell and Van Essen, 1983c; Ungerleider and Desimone, 1986).

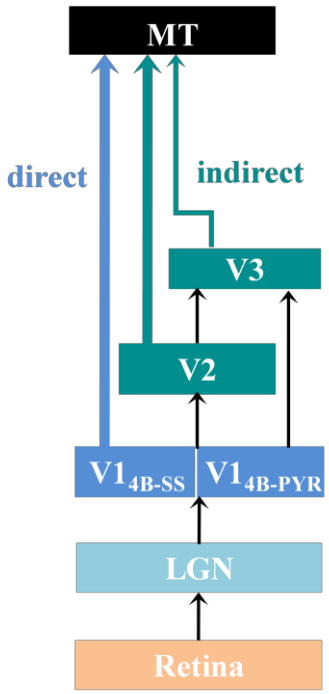

Figure 1: Schematic of the major cortical inputs to MT The "direct" pathway from V1 is shown in blue and the "indirect pathway" through V2 and V3 is in green.

Basic visual response properties

Macaque MT was originally identified by its large proportion of strongly direction-selective cells (Dubner and Zeki, 1971). The difference between an MT neuron's response to a stimulus moving in its preferred direction and one moving in the opposite direction can exceed 200 action potentials per second. This is one of the most pronounced forms of selectivity in visual cortex and has served as the substrate for studies of a variety of cortical mechanisms including noise reduction, perception, and attention (reviewed in Born and Bradley, 2005). MT neurons are also strongly selective for retinal position: a preferred-direction stimulus will have no effect on the neuron's response if placed outside of its classical receptive field (RF). Furthermore, MT neurons are selective for stimulus size, speed, and binocular disparity (Maunsell and Van Essen, 1983a, 1983b). Binocular disparity is an important

depth cue that arises because of the horizontal separation of the two eyes (Figure 2). When gaze is directed at a particular point in space (red circle), the image of that point falls on the foveae of the two eyes; however, the image of any object nearer or farther to the observer than that point, will fall on slightly different positions on the two retinae. The small difference between these two positions (d and d') gives the binocular disparity. For our purposes, we are most concerned with MT's responses to motion direction ("direction", for brevity) and binocular disparity.

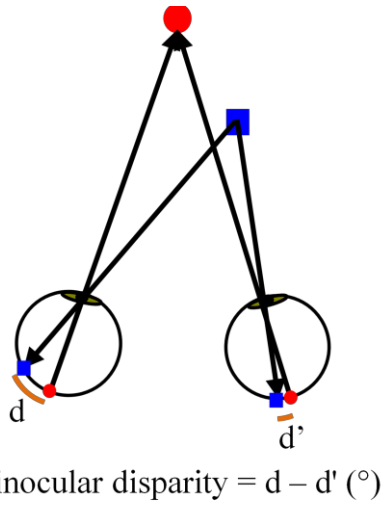

Figure 2: Geometry of binocular disparity

When gaze is directed at a point in space (red circle) the image falls on the foveae of the two eyes. An object nearer to the observer than the fixation plane (blue square) will fall on slightly different locations in the two retinae relative to each fovea, indicated by d and d'. The difference in these distances (d-d') is the binocular disparity in degrees of visual angle. By convention, negative binocular disparities indicate objects nearer to the observer than the plane of fixation and positive values indicate objects farther from the observer.

Sources of direction and disparity information in MT

Anatomical and functional evidence suggests that direction and disparity may be conveyed through somewhat anatomically distinct pathways. In particular, some segregation may occur along the direct and indirect cortical pathways (discussed above) such that the direct pathway conveys more direction information and the indirect pathway more binocular disparity information. Historically, it has proved challenging to determine both the anatomical connectivity and functional properties of individual neurons. Nevertheless, in one study, all of the V1 neurons that were identified as directly projecting to MT, were very direction selective (Movshon and Newsome, 1996). Furthermore, most of MT neurons' velocity tuning properties

appear to be inherited from their V1 inputs (Pack et al., 2003, 2006; Churchland et al., 2005), obviating the need for intermediate processing stages. In contrast, it seems that MT's disparity tuning preferences are different enough from V1's to require an additional processing step (Cumming and DeAngelis, 2001). For example, MT neurons are sensitive to larger disparities than V1 neurons, which would require a *de novo* combination of inputs from the two eyes (DeAngelis and Uka, 2003). Moreover, neurons in MT and V1 tend to have differently shaped disparity tuning curves: when classified by symmetry around its center (even or odd) V1 neurons tend to exhibit even-symmetric tuning curves while MT neurons mostly exhibit odd symmetry (DeAngelis and Uka, 2003). Although disparity sensitivity may be computed *de novo* in MT, an alternative possibility is that it is conveyed via V2 and the indirect pathway (Roe et al., 2007). Indeed, the V2 compartments that provide the majority of the input to MT have a high preponderance of disparity selectivity (DeYoe and Essen, 1985; Hubel and Livingstone, 1987; Peterhans and von der Heydt, 1993). Functional evidence for this contribution comes from recent experiments by Ponce and colleagues who inactivated the major components of the indirect pathway—V2 and V3—by cooling (Ponce et al., 2008). Concurrent recordings of neurons in MT revealed that despite a ~20% reduction in overall firing rate, MT neurons retained their direction tuning selectivity and bandwidth, consistent with a large proportion of motion information arriving directly from V1. In contrast, disparity tuning selectivity was usually significantly reduced and sometimes eliminated. Importantly, the effects on binocular disparity tuning were bigger than those predicted by the reduction in firing rate alone. These results indicate that V2 and V3 play an important role in conveying disparity information to MT. In the context of our experiments, this method gives us the means to disproportionately degrade the representation of these two features.

Role of MT in behavioral reports during motion and depth tasks

It has been proposed that in order to establish a link between perception and the activity of a particular group of neurons, several criteria must be met: 1) neurons should be sensitive to the parameters of the task, 2) lesions of the candidate set of neurons should lead to behavioral deficits, 3) electrical stimulation of the candidate neurons should bias the subject's decisions, and 4) neuronal activity should be predictive of the subject's decision (Parker and Newsome, 1998). Over the past several decades, MT neurons have met most of these criteria for both motion- and depth-based tasks. As discussed in a previous section, MT neurons are tuned—*i.e*. sensitive—to both direction and binocular disparity (criterion #1). To determine their relationship to behavior, researchers have employed a task in which animals are trained to report the direction or depth of a random dot stimulus. The stimulus in the direction of motion task consists of a patch of dozens of moving dots and looks like snowflakes during a windy Nor'easter: some fall downward, some fly up, and many seem to dance around randomly. The monkeys' task is a discrimination: report whether the dots move in one specific direction or the opposite. This stimulus has the advantages of eliciting high levels of activity from MT neurons and allowing the experimenter to control the task difficulty by changing the proportion of dots moving in one direction relative to those moving in the opposite. Analogously, in the depth task, the subject reports whether the patch of dots is nearer or farther than the fixation plane and the difficulty can be titrated by changing the proportion of dots drawn in each plane. This task design has been used by multiple laboratories for several decades to satisfy the criteria listed above.

First, it was established that lesions in MT impair monkeys' performance during the motion discrimination task described above (criterion #2; Newsome and Pare, 1988). Importantly, these lesions spared the monkeys' performance in a similarly designed contrast

discrimination task, indicating the impairment was not due to loss of basic visual sensitivity or due to deficits in making the behavioral response. Subsequent experiments showed that electrically stimulating groups of MT neurons biases animal's judgments during the motion discrimination task toward the preferences of the neurons being stimulated (criterion #3; Salzman et al., 1990): when stimulation targeted a cluster of upward-preferring neurons, animals more frequently reported seeing the stimulus move up than down, even though this reduced their success rate, and thereby reward frequency. Finally, methods from signal detection theory were implemented to measure the degree to which the activity of individual neurons correlated with perceptual decisions (Britten et al., 1996). Remarkably, individual neurons were weakly correlated with behavioral reports on the same motion discrimination task, suggesting that they contribute to the behavioral decision (criterion #4). The metric used to determine this correlation was termed "choice probability" because it measures the probability with which an ideal observer can predict the animal's behavioral choice from the response of a single neuron. A choice probability-like metric, called detect probability, has subsequently been used to implicate MT neurons on another variant of a motion task, a detection task, in which the animals report detecting onset of motion in a noisy patch of dots (Cook and Maunsell, 2002b).

A similar series of experiments was later performed while animals performed a depth discrimination task in which monkeys were trained to report whether a stimulus was near or far relative to the plane of gaze fixation. Similarly, electrically stimulating groups of neurons in MT led to biases in the animals' choices toward the preferences of the neurons being stimulated (DeAngelis et al., 1998). In addition, MT neurons exhibit choice probability greater than 0.5 during the depth discrimination task (Uka and DeAngelis, 2004). However, lesions in MT did not always lead to impairments during depth discrimination tasks. In one case, permanent lesions

led to no discernible deficits during depth discrimination or detection tasks (Schiller, 1993). However, the monkeys were only required to indicate which one of several stimuli was different, not to give information about its actual depth, a task that is possible to solve using binocular rivalry cues. A subsequent study demonstrated that MT inactivation impaired depth discrimination performance in a manner dependent on the animal's training history (Chowdhury and DeAngelis, 2008). When animals were only trained to perform a depth task optimized for MT neurons, MT inactivation devastated performance. However, when those same animals were trained on a variant of the task that required contribution from other cortical areas—*i.e*. a task where MT neurons were not sufficiently informative—MT inactivation no longer impaired performance on *either* version, suggesting processing for the original task had "moved" to another brain area. These results reveal a level of flexibility in the contribution of neurons to behavioral reports—one that can occur if neurons in other areas are also sensitive to the task demands. Importantly, MT lesions continued to cause impairments in performance during a motion discrimination task, indicating that MT was not entirely ignored in decision making.

Together, these results indicate that MT neurons are critically involved in both motion and depth based tasks. Importantly, choice probability-like measures allow us to assess the contribution of MT neurons to these behavioral tasks without having to interfere with the neurons' normal function (*e.g*. with electrical stimulation).

How do MT neurons come to be involved in behavioral decisions?

The results of Chowdhury and DeAngelis (2008) hint at another important feature of decision circuit formation: it can be selective. The original variant of the depth task required discriminating weak signals in noise—a task for which MT neurons may be especially well suited (Born and Bradley, 2005). On the other hand, both variants of the depth task can be solved

by neurons in other areas such as V4 or inferotemporal cortex (Janssen et al., 2000, 2001; Umeda et al., 2007). Why weren't these other areas used to begin with? It seems there may be an ongoing optimization process to select some relevant neurons but not all. Indeed, it has often been observed that, in the context of both motion and depth tasks, the MT neurons that are most sensitive to the task exhibit higher choice probabilities than those less sensitive, suggesting they are more strongly weighted in the decision process (Britten et al., 1996; Cook and Maunsell, 2002b; Uka and DeAngelis, 2004; Smith et al., 2011). In other words, the most sensitive, or useful, neurons seem to be prioritized in the decision. This relationship was not found at the start of behavioral training on a motion discrimination task in the one study that monitored choice probability throughout training (Law and Gold, 2008): few neurons in MT exhibited choice probabilities significantly different from chance in the first few weeks of training, even though the animals seemed to know the task rule. As animals' behavioral performance improved over many weeks, neurons most sensitive to the task tended to exhibit increasing choice probabilities. These results suggest that these slow behavioral improvements—typically called "perceptual learning"—can be accompanied by changes in the decision circuitry such that the most relevant neurons contribute more to the behavioral decision. In a follow-up computational study, the same authors showed that this relationship can develop by strengthening the connections between the most sensitive neurons and the "decision pool," which acts to collect sensory information to inform a decision (Law and Gold, 2009). These changes occurred even though the sensitivity of the MT population did not change over the course of many behavioral sessions, a change that could presumably also lead to improvements in behavioral performance. This is in contrast to a report that neuronal sensitivity improved in another mid-level visual cortical area, V4, following extensive training on an orientation discrimination task (Yang and Maunsell, 2004). Since

training on the same orientation task produced no changes in earlier visual areas V1 and V2 (Ghose et al., 2002), it is possible that changes of neuronal sensitivity happen only at specific stages of visual processing. Both findings are consistent with models that posit that improvements in behavioral performance can occur as a result of increases in the weighting of the responses of the most informative neurons (Dosher and Lu, 1998; Law and Gold, 2009).

Since most neurons in visual cortex are sensitive to multiple visual features, another question arises about how these neurons contribute to tasks that are dependent on each feature. Do neurons contribute to all tasks in which they are relevant? Do they do this if the animal switches quickly between such tasks? These questions have begun to be addressed with regard to MT neurons' sensitivity for direction and binocular disparity. In general, the contribution of individual MT neurons to motion and depth tasks seems to depend on the animal's strategy (DeAngelis and Newsome, 2004; Sasaki and Uka, 2009).

In addition to being retinotopically organized, MT neurons are functionally organized by both direction and binocular disparity, such that preferences for each feature vary smoothly among nearby neurons (Albright et al., 1984; DeAngelis and Newsome, 1999). DeAngelis and Newsome (2004) applied electrical microstimulation to regions of MT with varying degrees of disparity sensitivity as monkeys performed a *direction* discrimination task. They found that stimulating regions that were most sensitive for binocular disparity had the smallest effects on direction judgments (in 2 out of 3 animals); stimulating sites that were poorly tuned for binocular disparity had the biggest effect on direction judgments. This was true even though all experiments were performed at sites with strong direction tuning. In other words, it seemed that neurons that were well tuned for binocular disparity contributed little to direction judgments, even though they contained direction information. This was interpreted as resulting from a

strategy employed by the monkeys to pool the most versatile set of neurons: since these neurons were less sensitive to binocular disparity, they were equally informative at all stimulus depths. However, little is known about the interactions of MT's topographic maps, so it is also possible that regions less sensitive to binocular disparity had more variable direction preferences, leading to dilution of the microstimulation effects during direction decisions. An approach that monitored the activity of single neurons was needed to distinguish between these possibilities. Sasaki and Uka (2009) measured choice probability of individual MT neurons as animals performed interleaved trials of motion and depth discrimination tasks. Although the monkey could not anticipate whether the upcoming trial would be a direction or depth trial, the animal was cued to the dimension to be discriminated at the start of each trial. Importantly, visual stimuli during both tasks contained information about motion and depth but the animal was only rewarded for responding correctly to the cued feature. The response targets for the two tasks had the same appearance but corresponded to different answers: the target at the top of the screen corresponded to 'up' or 'far' responses and the target at the bottom of the screen corresponded to 'down' or 'near', depending on the cued task. Animals indicated their response during each task by looking at one of two targets. Since most MT neurons are tuned for both features, depending on the neurons' preferences, a higher firing rate might indicate only responses to one target (*e.g.* if the neuron preferred up and far a high firing rate always indicated the top target) or might be different depending on the task (*e.g.* if the neuron preferred up and near then a higher firing rate indicated opposite targets). As animals performed this difficult switching task, neurons that signaled behavioral responses to the same target had high choice probability during both tasks. However, choice probability for neurons that signaled opposite motor responses was mutually exclusive: it was significantly different from chance during only one of the two tasks. These

results indicated that neurons that contributed to opposite behavioral decisions were used in only one of the two tasks. The task to which each neuron contributed depended on its sensitivity: neurons more sensitive to the depth task contributed only during the depth task and neurons more sensitive to the motion task contributed only to the motion task (their Supplementary Figure 8; Chowdhury and DeAngelis, 2008). Therefore, although neurons contained information for both tasks, they were selectively used for just one of them. This might reflect temporal limits on reading out information from relevant neurons: the decision circuitry may not be able to switch quickly enough to use increases in firing rate from a single neuron for opposite behavioral responses. In both of these studies, the dynamics underlying neuronal contribution to behavioral decisions depend on a relationship between neuronal sensitivity and task demands that were likely established during months of training. For example, connections between the pool of relevant neurons and the downstream decision mechanisms for each task may have been strengthened over months. The relevant decision circuit for each task may have then been recruited by fast mechanisms such as feature attention (Cohen and Newsome, 2008). It was not known whether changes in the relationship between a neuron's *sensitivity* and its contribution to a task could change quickly.

In sum, decades of research indicate that MT neurons are important not only for processing motion and binocular disparity, but play an important role in behavioral decisions based on these two features. In some cases, changes in the degree to which the activity of MT neurons was correlated with behavioral decisions hint at the flexibility of the decision circuitry. In particular, the sensitivity of neurons to the particular task demands appears to play an important role in the degree to which neurons contribute to behavior.

Caution in interpreting choice probability

Although I have been using the presence of significant choice probability to implicate MT neurons in behavioral judgments, it is important to note that because neurons within MT share noise correlations, choice probability likely reflects the causal contribution of a local group of neurons rather than any individual neuron. In a simple pooling model, Cohen and Newsome (2009) showed that choice-related activity for neurons *not* causally involved in a task approaches that of neurons that *are* causally involved, if the two groups are even weakly correlated with each other. As a result, the magnitude of choice probability reflects the maximum decision weight of any neuron within the correlated group, rather than the weight of the single neuron being recorded. Since inter-neuronal correlations tend to be highest for neurons that are spatially near each other and have similar tuning preferences (Cohen and Kohn, 2011), this correlated group is mostly confined to a local cluster of neurons within MT (but see Smith and Kohn, 2008). Furthermore, there is some debate about whether choice probability reflects only causal fluctuations in neuronal activity or contains a component of post-decision feedback signals (Nienborg and Cumming, 2009, 2010). Therefore, I simply use choice probability as a measure of involvement in behavioral decisions, whether it is entirely causal or not.

Summary of dissertation research

Neurons in MT have served as an important substrate for studies of integration of neuronal signals for decision making. They contribute to perceptual decisions during motion and depth based tasks in a manner dependent on their task relevance. However, most studies to examine the relationship between neuronal sensitivity and their contribution to behavioral tasks were performed after animals had been trained and much of the circuitry may have already been established. We set out to determine whether changing neuronal sensitivity on a short timescale

would lead to changes in their contribution to behavioral reports. We accomplished this by reversibly inactivating two of the inputs to MT—V2 and V3—by cooling, which has been shown to degrade their sensitivity to depth more than motion. We then measured neurons' correlation with behavior while animals performed motion and depth detection tasks using a metric analogous to choice probability, called “detect probability” (DP).

Our first goal was to determine the effects of this reversible inactivation on behavioral performance during motion and depth detection tasks. The disproportionate disruption of selectivity for depth in MT led us to hypothesize that we might see bigger behavioral impairments during the depth task that during the motion task. Our results indicate that monkeys are indeed impaired during the depth task. However, one of the two animals was also substantially affected on the motion task, suggesting that the effects on MT neurons do not give a complete picture of the underlying impairment. These expectations, results, and implications are discussed in detail in Chapter 1.

Importantly, behavioral performance during both tasks was sufficiently high during inactivation to allow us to measure MT neurons’ correlation with behavioral reports using DP. We found that during the daily inactivation sessions, which lasted about an hour, MT neurons’ DP during the depth task was reduced relative to immediately before the inactivation while DP did not change for the motion task. These results indicate fast, selective changes in cortical decision circuitry. We elaborate on these results in Chapter 2.

Methods

General Overview

We recorded MT neurons in two experimentally naïve adult male macaque monkeys (*Macaca mulatta*, 10 and 12 kg) while they performed signal detection tasks. During many sessions, we also reversibly inactivated V2 and V3 by cooling. Before task training, each animal was trained to sit in a custom-made primate chair. Each animal was then implanted with a custom titanium head-post and a scleral search coil in each eye, to monitor eye position and vergence. Following a brief period of fixation training, animals were trained on a motion and then a depth signal detection task. After training we implanted a Cilux recording cylinder (Crist Instrument Co.) in the right hemisphere to access MT via an anterior approach. This was followed by recovery, several recording days to locate and map MT, and then by implantation of cryoloops, the devices used for cooling. Cooling sessions began after complete recovery, at most within a month after the implant surgery. All animal procedures complied with the National Institutes of Health Guide for Care and Use of Laboratory Animals, and were approved by the Harvard Medical Area Standing Committee on Animals.

Behavioral Tasks and Visual Stimuli

Animals were seated comfortably in primate chairs while performing two tasks: a motion detection task and a depth detection task. Both tasks began with the appearance of a single patch of random dots and the animals' task was to detect signal among noise in this patch. In the motion task, all the dots started out moving in random directions (motion noise) and the animal was rewarded for responding when a proportion of these dots began to move in one direction (the signal direction). Analogously, in the depth task, the dots started out scattered in different depth

planes and the animal was rewarded for responding when a proportion of these dots appeared in one depth plane (the signal depth). We will refer to this change from noise to signal as "signal onset" for both tasks. We titrated difficulty by changing the proportion of signal dots—the signal strength.

Each trial began after an animal maintained fixation on a central marker for 500 ms, after which a random dot stimulus appeared. Stimuli always contained either motion or depth noise dots at the start and after a random time (0.5-5.5 seconds, exponentially distributed with a mean of 1.4-1.6 seconds) changed to contain signal dots ("signal onset"). Animals were rewarded by making an eye movement toward the stimulus between 200 and 650 ms after signal onset. The 200 ms minimum was imposed as the minimum plausible reaction time based on the distributions of the animal's reaction times during the task. If the animal responded before signal onset or less than 200 ms after signal onset the trial was counted as a false alarm and no reward was given. If the animal did not respond within 650 ms, the trial was counted as a miss and no reward was given. When animals' fixation deviated from the 0.8-1.2° diameter window around the fixation point at any time other than after signal onset, the trial was aborted and no reward was given. We used a uniform distribution of waiting times in the first 17 experiments in one animal (monkey Q) but this had no obvious effects on the behavior.

The stimulus was presented in one of two locations, located symmetrically on either side of the fixation point. On days when we recorded neuronal activity, one of these was centered on the receptive field of the neuron and the other was in a mirror-symmetric location in the opposite visual hemifield. Since the cryoloops were implanted unilaterally, we expected cooling to affect behavioral performance only in the contralateral visual hemifield. Therefore, behavioral performance in the ipsilateral visual field served as a negative control for behavioral

performance. Stimulus location alternated on every trial or in a 2-to-1 fashion such that two consecutive trials were presented in the part of the visual field affected by cooling followed by one on the other side.

The tasks were interleaved in blocks of 25 trials per task. The animal was cued to the task by the shape of the fixation point. In addition, the two tasks' stimuli had a different starting appearance, which served as an additional cue to the dimension of the expected change (see *Visual Stimulus* below). After each task switch, the animal was given practice trials at the easiest signal strength, which were not included in the subsequent analysis. The difficulty increased only after two such trials were correctly completed.

One of the two animals (monkey Q) was also trained on a modified version of the detection tasks three months after neuronal recording was completed. In this "fine change" version of the task, the animal was rewarded for detecting a small change in the direction or depth of the random dot stimulus. All stimuli were presented at the maximal signal strength and difficulty was titrated by modulating the magnitude of the direction or disparity change. These stimuli also had a different starting appearance from the stimuli in the signal detection tasks. In all other respects, the task structure was identical.

Visual Stimulus

Visual stimuli were presented through a Wheatstone stereoscope (Wheatstone, 1838) on two Viewsonic 21" G220F CRT monitors. The image was presented to each eye via a mirror positioned at a 45° angle to a dedicated monitor. The stereoscope was calibrated daily such that the virtual image of the fixation point was in the same depth plane as a fixation point 57 cm in front of the monkey's eyes. The display subtended 39 x 29 degrees of visual angle at a resolution of 1600 x 1200 and was updated at 75 Hz. All visual stimuli were drawn using the Cogent

Graphics Matlab toolbox, developed by John Romaya at the LON at the Wellcome Department of Imaging Neuroscience (http://www.vislab.ucl.ac.uk/cogent.php).

Stimuli were random dot kinetograms (RDKs) drawn with the red phosphor on both monitors with a luminance of 6.97 cd/m^2 as seen in the mirrors. Binocular disparity stimuli were generated by drawing the image of a single dot with a horizontal offset between the two monitors. The magnitude and sign of this offset, in degrees, specifies the depth of the stimulus. By convention, negative disparities are nearer to the observer than the fixation plane and positive disparities are farther.

During receptive field mapping, neuronal tuning properties were measured with a random dot stimulus at 100% coherence with a dot lifetime of 150 ms.

The stimuli in the signal-detection tasks comprised 0.1° dots presented at a density of 1-2 dots/deg^2 with a 3-frame (40 ms) dot lifetime. The motion stimulus was adapted from the one described by Cook and Maunsell (2002a). Briefly, before signal onset all dots moved in random directions at a fixed speed (*i.e*. they were all noise dots). After signal onset, some proportion of the dots became signal dots, which all moved in one particular direction at a fixed speed; the rest remained noise dots. The proportion of signal dots dictated the motion signal strength. Speed was specified by the spatial displacement of the dots between successive video frames. The stimulus employed here differed from Cook and Maunsell's (2002b) only in that we used a 3-frame dot lifetime (they used 2-frame lifetime). The lifetime specifies the duration (in number of refresh frames) that each dot was displaced by a fixed distance within the aperture; after it "died" it was re-plotted in a new location and effectively became a new dot. Dots maintained their direction, whether signal or noise, for their entire 3-frame lifetime such that no dot ever changed direction. In other words, the stimulus was composed of many dots, each of which moved in one direction

for 3 video frames and then disappeared, to be re-drawn in a new location as a new dot. The change from noise to signal was smooth and happened for each dot only after it "died" and was re-plotted in a new location, therefore the change happened over the course of 3 video frames (40 ms). This eliminated the possibility that monitoring a single dot might give away the time of the change. Note that because of the limited lifetime, on every frame a third of the dots was re-plotted in a new location, therefore the true motion signal (or, the actual percentage of signal dots compared to total dots at a given moment) between any two frames was at most 66%. Throughout this text, we will always report the true motion signal. Motion task stimuli were presented at one constant binocular disparity in any given session.

The binocular disparity stimulus was designed analogously to the motion stimulus. The dots all moved in one unchanging direction throughout both noise and signal epochs. Signal dots were all presented at a particular binocular disparity (i.e. depth plane) and noise dots were scattered in depth. The proportion of signal dots among noise dictated the signal strength. Noise dots were drawn at random binocular disparities in the range -1.5 to 1.5°. Before signal onset, the stimulus contained only noise dots, which were drawn at disparities in the same range. This stimulus was also drawn with a 3-frame *motion* lifetime even though the direction of motion never changed. During signal onset, dots changed binocular disparity only upon being plotted in a new location. This permitted the noise stimulus to transition to the signal stimulus without any individual dot ever changing binocular disparity throughout its lifetime. As a result, the change occurred over the course of 3 video frames for the depth task, as in the motion task. As in the motion task, this eliminated the possibility that monitoring any single dot might reveal the signal onset. Unlike with the motion stimuli, these stimuli could attain a maximum binocular disparity signal strength of 100% during the signal epoch. Stimuli for both tasks were confined to fixed

apertures of equal size in the two eyes to eliminate monocular cues to the depth change. If one of the dots of a disparity pair fell outside of that aperture, it was not drawn, leaving the other unpaired.

It is important to note that the stimuli used for each task did not contain both motion *and* depth noise. The motion task stimuli were drawn at a fixed disparity throughout the entire trial and the depth task stimuli were drawn at a fixed direction. Therefore, the two starting stimuli had a different appearance, which may have functioned as an additional cue to the dimension of the expected change.

During neuronal recording sessions, the speed of the stimulus as well as its signal direction and disparity were matched to the preference of the neuron. On days when there was no neuronal recording, the stimulus parameters were arbitrarily chosen from a set by the experimenter.

Electrophysiological Recording

We recorded in MT using standard electrophysiological techniques. Briefly, tungsten microelectrodes (impedance, 0.5-3 MΩ at 1 kHz) were advanced through a trans-dural guide tube, the signals were amplified with a conventional amplifier and passed through a band pass filter and window discriminator (BAK electronics) for on line spike detection. The analog voltage signals from the extracellular recordings were digitized at 25 kHz and saved to a computer disk by using a Cambridge Electronic Design 1401 data acquisition system. Spike2 software was used to confirm single-unit isolation and stability, which was particularly important because of the long duration of these recordings (typically 2-3 hours).

Area MT was located by using structural MRI scans aligned to the approach through the recording cylinder, transitions between gray and white matter, the established relationship between receptive field width and eccentricity, and the high incidence of direction- and binocular disparity-tuned neurons.

Cooling

Cooling was actuated by passing chilled fluid through small loops of metal tubing—"cryoloops"—chronically implanted in the lunate sulcus (Figure 3). The cryoloops were made of 23-guage stainless steel hypodermic tubing with an attached thermocouple, as previously described (Lomber et al., 1999; Ponce et al., 2008). Three of these loops were implanted into the right lunate sulcus of each animal and spaced to cover an area approximately 8 mm deep into the sulcus and 18 mm medio-lateral. Chilled methanol was pumped through the cryoloops to cool the surrounding brain tissue to 10-15 °C, which took approximately five minutes. This temperature is sufficient to eliminate visually evoked activity in the immediately surrounding cortex (Lomber et al., 1999). Temperature at each loop was monitored via an externally located connector and was independently controlled for each cryoloop by changing the flow rate of methanol from its dedicated pump.

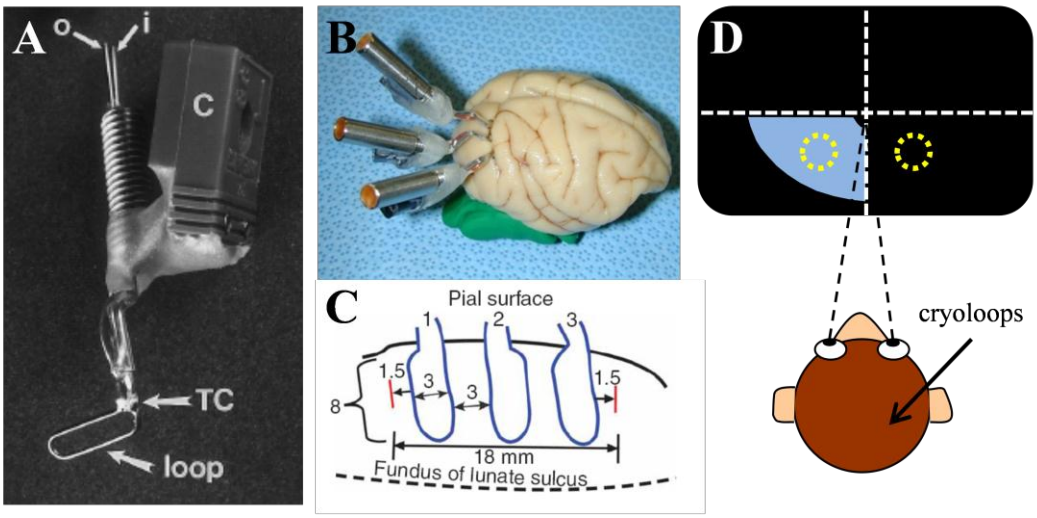

Figure 3: Cooling methods
(A) Photo of a cryoloop, the device used to cool local cortical tissue. The "loop" is the part inserted into the lunate sulcus. The attached thermocouple (TC) allows measurement of temperature at the loop via the external connector (C). Tubing supplying chilled fluid is connected to the input (i) and output (o) tubes of the loop. Image adapted from Lomber, Payne, and Horel 1999.
(B) Placement of three cryoloops in the right lunate sulcus of a macaque brain.
(C) Schematic of the spacing of the cryoloops once implanted in the lunate sulcus. They are spaced approximately 3cm apart, covering a space about 18 mm wide. Image from Ponce, Lomber, and Born 2008.
(D) Illustration of the monkeys' field of view and the scotoma—the portion affected by cooling. The black screen represents the virtual image of the monitors through the stereoscope. The dashed lines represent the horizontal and vertical meridians. The blue region in the lower left visual field corresponds to the scotoma, the part we expect to be affected by cooling of V2 and V3. The yellow circle in the scotoma indicates the placement of the visual stimulus. The right visual hemifield serves as the ipsilateral control, which we do not expect to be affected by cooling. The stimulus in the ipsilateral field was placed mirror-symmetric to the stimulus in the scotoma (yellow circle on the right).

Experimental Protocol

Each day's experimental timeline is schematized in Figure 4. The color and naming conventions in this figure will be used throughout this text. Experiments began with the isolation of a single MT neuron at physiological brain temperatures (35-38 °C) and collection of basic tuning data. The neuron's preferred location, size, and speed were qualitatively determined by

hand mapping but direction tuning and binocular disparity tuning were collected quantitatively using stimuli presented for 400 ms with a 300 ms inter-stimulus interval, for at least 6 repetitions. Direction tuning was obtained from a range of 8 directions spaced 45° apart and disparity tuning from 11 disparities with the following values: ±1.2, ±0.8, ±0.6, ±0.4, ±0.2, 0. If a neuron did not have a clear tuning preference for either direction or binocular disparity, it was not studied further. Properties of the change detection task stimuli were matched to the preferences of the neuron. Pre-cool task data were collected as monkeys performed the detection tasks for approximately one hour. Cooling was initiated by pumping chilled methanol through the loops and cooling-period data collection began after the temperature had stabilized at 10-15°C for at least 5 minutes. During cool-down animals either continued to perform the tasks (data not included in analyses) or rested. The cooling-period data set was collected in the same

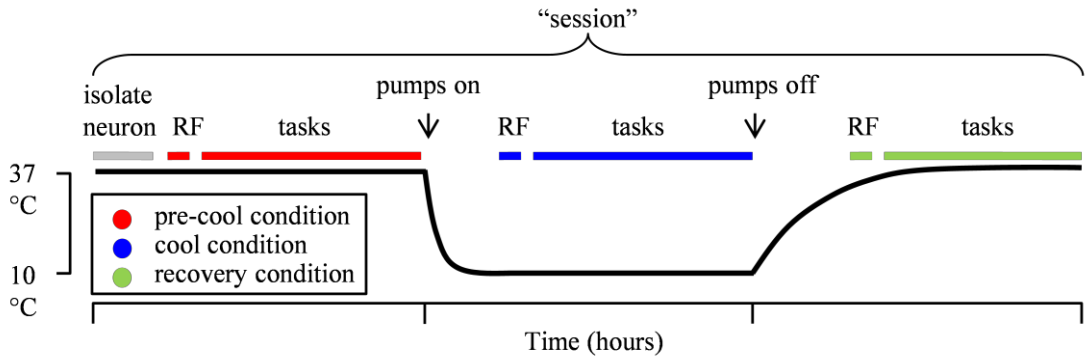

Figure 4: Session Timeline
For all conditions (pre-cool, cool, and recovery), we measured basic receptive field tuning properties ("RF") for approximately five minutes and then the animal performed interleaved motion and depth tasks ("tasks") for approximately one hour. The red, blue, and green colored bars correspond to pre-cool, cool, and recovery conditions, respectively. These color conventions will be used throughout this text. Arrows indicate when the cooling pumps were turned on and off. Cool data was collected only after temperature at the cryoloops had stabilized between 10-15°C for five minutes. Recovery data was collected approximately 15 minutes after cooling offset, when the temperature was at least 30 °C but often when it had not yet fully returned to physiological baseline (37-39 °C). Temperature recovery (black curve) is intentionally drawn with a longer time constant than cool-down.

way as the pre-cool data, with repeated quantitative measures of tuning properties followed by about an hour of task performance. Cooling lasted at most one hour and was never done more than once per day. In some sessions, continued isolation of a neuron and the animal's continued motivation permitted us to collect "recovery" data, which began at least 15 minutes after cooling was stopped, when temperatures were at least 30°C at the loops, sufficiently warm to resume visually evoked activity at the cooling site (Lomber et al., 1999). Usually, recovery data comprised repeated quantitative measures of tuning and occasionally sufficient data to measure task performance and rarely task-related neuronal activity.

Data set

A total of 144 cooling sessions were performed with monkey Q and 48 with monkey S. Behavioral sessions shown here are those after performance during cooling had stabilized (see below). Cooling data was often collected concurrently with electrophysiological recording in MT.

Monkey Q's behavioral performance was ~0% correct during both tasks during the first several cooling sessions (data not shown). Since this could have been due to non-task specific changes in the appearance of the stimulus (*e.g.* apparent changes in color resulting from inactivation of portions of the ventral stream), we temporarily introduced luminance cues in addition to the normal noise-to-signal changes and also increased the dot lifetime in some sessions. These changes led to rapid improvements in performance and as performance remained high, we eventually were able to phase out the luminance cues entirely by the tenth cooling session and reduce the dot lifetime back to three frames after the fourteenth. These cues were never re-introduced and we only report sessions after the fourteenth cooling session from this

animal. Importantly, behavioral performance in the ipsilateral visual hemifield was never impaired during any of these early sessions.

Unlike monkey Q, monkey S' performance did not drop to 0% correct during the first cooling session, therefore, we did not add additional cues to assist his performance during cooling. The results presented here are from all of monkey S's behavioral sessions with cooling.

Neuronal data were only recoded if the neuron's receptive field was mostly confined to the expected scotoma—the site affected by cooling—and if it had a clear tuning preference for direction and binocular disparity. Furthermore, since low spike counts violate the assumptions of many of our analyses (e.g. ROC), we often did not record neurons with responses to the preferred stimulus that were below 50 spikes/s to avoid extremely low spike rates during the cool condition. Recorded neurons with a peak firing rate below 15 spikes/s in the cool condition were excluded from analysis. Since MT neurons are typically well modulated by our stimuli, it was not difficult to find cells with higher rates.

The data presented here is from a pool of 150 single neurons: 104 from monkey Q and 46 from monkey S. Of all of these, 98 had sufficient quantitate tuning data for analysis of both direction and disparity in both pre-cool and cool conditions, and 78 neurons (44 from monkey Q, and 34 from monkey S) had sufficient task-related data during both tasks in both conditions. This task related data also met the criteria for behavior inclusion described above.

Analysis

Behavioral performance

There were four possible outcomes to each task trial: 1) a correct detection if the animal responded to the change within the allowed reaction time, 2) a miss if the animal did not respond

to the change within the allowed reaction time, 3) a false alarm if animal responded before signal onset, and 4) a break in fixation at any time during the trial. Behavioral performance was measured as a proportion of correct detections out of the sum of correct detections and misses (*i.e.* false detections and breaks in fixation were excluded). The proportion correct as a function of signal strength ($f(x)$) for each task was fit with a logistic function of the form

$$f(x) = \gamma + \frac{1 - \gamma - \delta}{1 + e^{-\left(\frac{\alpha - x}{\beta}\right)}}$$

using the psignifit toolbox version 2.5.6 for Matlab (see http://bootstrap-software.org/psignifit/) which implements the maximum-likelihood method described by Wichmann and Hill (2001a). Performance data was fit independently for each task in each condition with the free parameters α, β, and δ, which describe the offset, slope, and saturation of the sigmoid, respectively. The γ parameter sets the lower saturation for the function and corresponds to the animal's guess rate. The guess rate can skew measures of the animal's performance: a high guess rate can make the animal appear to perform better than his sensitivity allows and therefore changes in the guess rate between conditions can hinder our ability to measure changes in behavioral performance. Therefore, we needed to account for any changes in this value between conditions and sessions. The animal's ability to correctly guess the signal onset time depends on the frequency and temporal distribution of his attempts to guess, the temporal distribution of signal onset times, and the allowed reaction time window. For example, if signal onset can occur during one of two times and the animal always responds during the first one, he will perform at a rate of 50% correct. We simply extended this calculation to the continuous distribution of possible signal onset times and guesses. Our access to the animal's attempted guess rate comes from the false alarms—trials when the animal reported signal onset but it had not happened yet. These trials

consist of some unknown combination of real perceived detections and random guesses and therefore represent both his sensitivity to small random fluctuations in the stimulus and monkey "jumpiness". We used the temporal distribution of these responses throughout the trial to determine the probability with which the animal can correctly detect the signal onset during a false alarm. In other words, since the false alarms were not uniformly distributed throughout the trial duration, we first determined the probability of a false alarm at each time point in the trial. We then convolved this temporal distribution with the temporal distribution of possible signal onset times to give the probability that the animal would correctly guess as a function of time throughout the trial. These were then summed across all time points to give the probability of guessing correctly in any given trial or across all trials. More specifically, the estimation of guess rate in each condition was performed using the following equation:

$$p_{guess} = \sum_{t_i=tMin}^{tMax} p_{FA} \times p_{change}$$

where $tMin$ and $tMax$ correspond to the minimum and maximum possible change time, respectively and p_{change} corresponds to the probability of a change happening at time t_i. p_{FA} corresponds to the probability that the animal made a false alarm during all trials longer than t_i in the allowed reaction time window for a change at t_i (i.e. from $t_i + 200\ to\ t_i + 650$). Using this estimate, we determined that the animals could correctly guess signal onset with a frequency of 5-15%. For each condition and task, we fixed the γ parameter of the psychometric function to the estimated value of the guess rate.

Measurement of behavioral threshold and slope were obtained from the point on the psychometric function where the animal performed at 80% correct. Confidence intervals for

threshold and slope estimates were found by bootstrapping the fit 1999 times as implemented by the psignifit toolbox (Wichmann and Hill, 2001b). Note that although the motion stimulus strength could not exceed 66%, the behavioral *threshold* was not restricted to be below this value.

Reaction times for correct trials were determined from the time of saccade onset, defined as the time when the eye velocity first exceeded a threshold that depended on the saccade magnitude.

Standard statistical methods were used to compare changes between pre-cool and cool parameters.

Neuronal tuning properties

Spiking activity during the period 100-400 ms after stimulus onset was used to construct time-averaged direction and disparity tuning curves. ANOVA was used to determine whether a neuron's activity was reliably modulated by variations in stimulus features. Cells were included in subsequent analyses only if they were significantly tuned for either direction of motion or binocular disparity. Tuning was quantified by a discrimination index (DI):

$$DI = \frac{(R_{max} - R_{min})}{(R_{max} - R_{min}) + 2\sqrt{SSE/(N - M)}}$$

where R_{max} and R_{min} are the responses to the preferred and null direction or disparity, SSE is the sum squared error for the mean of the response to each trial type, N is the number of trials, and M is the number of stimuli used for tuning. Thus the DI is a measure of modulation by the preferred feature, normalized by the variability. As previously reported, there was no appreciable change in preferred direction or binocular disparity during inactivation when tuning could be

measured (Ponce et al., 2008). Therefore, in order to directly compare DIs collected during both pre-cool and cool conditions, the values of R_{max} and R_{min} were fixed at the values of direction and disparity that were calculated during the pre-cool condition.

Task-related neuronal activity

Spiking activity of single neurons was also collected as the animals performed the behavioral tasks described above. For all analyses, neuronal data were aligned to the onset of the signal stimulus. Only correct and missed trials were used in the following analyses.

Neurometric performance. We measured task-related cell sensitivity of single neurons by constructing a "neurometric function". For trials at each signal strength, we compared the distribution of responses immediately before signal onset to those shortly after signal onset with a receiver operating characteristic (ROC) curve ($e.g.$ Bosking & Maunsell, 2011). The area under the ROC curve corresponds to the probability with which an ideal observer can correctly determine whether a firing rate chosen randomly from these two distributions belongs to the pre-change or post-change epoch. Thus, it can be used as a measure of the probability with which the neuron can correctly detect the signal onset. As a neuron's response to the signal stimulus gets stronger, this value approaches 1; if the responses to the noise and signal stimuli are indistinguishable, it is 0.5; and if the neuron is less active upon signal onset the value will be below 0.5. Firing rates were compared between the 450 ms window immediately before the change and the window 50-650 ms after the change. For correct trials, spikes were only included up to 100 ms before the reaction time to exclude some post-decision signals ($e.g.$ Cook & Maunsell, 2002b). Thus, the post signal onset window varied with the animals' reaction time, which allowed us to include spikes from most of the signal epoch used by the animal. However, results were similar for a variety of window lengths and start times.

To determine the effect of cooling on cell sensitivity we aimed to compare neurometric performance between the pre-cool and cool conditions using data that fell along the steep portion of a neuron's neurometric function. Like the psychometric threshold, this is often determined at the neurometric threshold: the signal strength at which the neuron's performance is 0.8 (*i.e*. 80% correct). Analogously, the neurometric threshold is typically obtained from a function fitted to the neurometric data. However, no single function described a large majority of our data well; therefore we simply approximated the neurometric threshold by choosing the signal strength at which the neurometric performance was closest to 0.8 in the pre-cool condition and calculating the change in neurometric performance due to cooling *only* at that signal strength (see Figure 20). This near-threshold value was used to compute the percent change in neurometric performance relative to the pre-cool value. Since 0.5 is the chance level for neurometric performance, all values were first converted to distances from 0.5 by subtracting 0.5 as shown below:

$$NP_{shift} = \frac{(NP_{cool} - 0.5) - (NP_{pre-cool} - 0.5)}{(NP_{pre-cool} - 0.5)} \times 100\%$$

where $NP_{pre-cool}$ and NP_{cool} are the neurometric performance values at the near-threshold signal strength in the pre-cool and cool conditions, respectively. This calculation allows us to preserve the sign of the effect—values of NP_{shift} between -100% and 0% are decreases of neurometric performance toward chance, positive values are increases away from chance—and also to distinguish changes in sign, which will result in NP_{shift} value less than -100%.

We also attempted to estimate a more precise neurometric threshold by fitting a line to the neurometric data and comparing estimated thresholds from the fit (i.e. the signal strength at

which the neurometric performance is exactly 0.8). The results for neurons that were reasonably well fit by a line were qualitatively similar with either method.

Detect probability. We used the detect probability (DP) metric to measure the trial-to-trial co-variation between fluctuations in single-neuron firing rates and behavioral reports (Cook and Maunsell, 2002b). DP is a version of the more commonly used choice probability metric, adapted for detection tasks. DP was calculated for a given signal strength by comparing firing rates between correct and missed trials after signal onset. We constructed an ROC curve for the two distributions of rates (correct and missed trials) and measured the area under the curve to give the DP. This provides an estimate of the probability that an ideal observer can determine whether the monkey detected the signal onset by relying only on the firing rate of a single neuron. It is important to note that the stimuli are virtually identical for all trials of a given signal strength so a DP that deviates from the chance value of 0.5 indicates firing rate differences that are largely independent of differences in the visual stimulus and therefore are due to differences in the behavioral outcome.

Individual neurons' DP was calculated in a time window beginning 50 ms after signal onset and ending 100 ms before the reaction time during that trial. The results did not vary with reasonable size variations of this window, provided it was large enough to include more than a couple of spikes. DP was calculated using only responses that had at least 5 completed trials and, to reduce bias in the DP calculation, in which one trial outcome (*i.e*. correct or miss) did not occur more than 75% of the time (Uka & DeAngelis, 2004; I.Kang, personal communication). For neurons where multiple signal strengths met these criteria, responses were z-scored within each signal strength and combined. This procedure normalizes each rate to units of standard deviation and is commonly used to combine responses across conditions with different mean

rates. DP values from z-scored responses were similar at all signal strengths for each cell. A single ROC curve was constructed for all z-scored rates and the area under the resulting curve gives the neuron's DP. We used a permutation test to determine whether individual DP values were significantly different from 0.5. For the distribution of firing rates used to calculate the DP for each cell, we permuted the relationship between firing rate and choice, while preserving their relative frequencies. A new DP was calculated from the permuted data and this was repeated 2000 times to construct a distribution of DPs expected by chance. We rejected the null hypothesis that the DP was not significantly different from 0.5 if the measured DP fell outside the 95% confidence interval of the mean of the permuted distribution.

The time course of detect probability for the entire neuronal population was computed using the same basic method described above, but repeated within a 100-ms sliding time window that moved in 20 ms steps. First, each neuron's responses were z-scored within eligible signal strengths for each time window and then combined across signal strengths and neurons. To allow for fair comparison, only neurons with both pre-cool and cool data contributed to the DP time course. The DP at each time point was given by the area under the ROC curve for the combined z-scored responses at that point. The standard error of the mean (SEM) for the time series was computed via a bootstrap procedure (Efron and Tibshirani, 1998). At each time point, we sampled with replacement unpermuted pairs of z-scored rate and behavioral response to compute a new DP value. This was repeated 1000 times to generate a distribution of sample DP. The standard deviation of this distribution was taken to be the SEM.

To determine whether changes in DP were significant between pre-cool and cool conditions, we used the metric where we had the greatest statistical power: the detect probability computed from the combined z-scored rates across all neurons in a single time window. For this

analysis, we used a window 100-450 ms following signal onset, which was chosen to encompass the peaks of the DP time course for both tasks in pre-cool and cool conditions. To determine whether DP values were significantly different between pre-cool and cool conditions, we computed a distribution of re-sampled DPs for each condition and task with a similar bootstrap procedure as was described above. We then obtained a sampled distribution of DP differences ($DP_{cool} - DP_{pre\text{-}cool}$) from the generated DP values for each task. If the 95% confidence interval of this difference distribution included zero, then we concluded that there was no significant difference between the pre-cool and cool DP for that task.

Spike count mean to variance relationship. We determined the relationship between a neuron's mean spike count and the associated spike count variance by computing the ratio between the variance and the mean—a metric called the Fano factor. Spike counts were measured in a window 50-300 ms after signal onset, only from trials with a reaction time of at least 350 ms. Mean spike count and variance was computed from the responses to each signal strength for each task and condition. The relationship between spike count and variance did not differ between tasks so the data were combined in the presented analyses. Since responses from each neuron were collected at multiple signal strengths during each task, each neuron contributed 2-14 data points. The population Fano factor for each condition was estimated from the slope of the best-fit line to the mean-to-variance scatter plot (see Figure 26). The line was not constrained to pass through the origin. Fano factor was also computed for each data point in that plot (*i.e.* each signal strength in each condition) by taking the ratio of spike count variance to spike count mean.

Prediction of DP given changes in firing rate and variance. The relationship between DP, the sensitivity index, d', and their mutual dependence on changes in mean firing rate and

variance are discussed in Chapter 2. To determine the effect of our observed changes in mean rate and variance on DP, we calculated a predicted d':

$$d'_{pred} = \frac{\sqrt{pRate}}{\sqrt{pVariance}} d'_{pre-cool}$$

where $pRate$ and $pVariance$ are the ratio of cool to pre-cool firing rate and variance, respectively, and $d'_{pre-cool}$ is the d' value computed in the pre-cool condition. $pRate$ was determined from the change in mean firing rate *during the task* by calculating the ratio of rates in the 50-300 ms window after signal onset (same window as used for Fano factor estimation). $pVariance$ was computed as the ratio of the population Fano factor measured in the cool to pre-cool conditions.

Threshold model. To examine the relationship between the MT population response and the animals' reaction times, we adapted a threshold model that has previously been used for a motion detection task (Cook and Maunsell, 2002b). This model had two free parameters, threshold and motor preparation time, and was used to predict reaction times from the responses of the neuronal population. First, we sorted spike rates from individual neurons into 20 bins based on each trial's reaction time such that each bin contained the same number of trials from each neuron. Since reaction times varied day-to-day, quantile binning ensured that every neuron contributed to each time bin but resulted in differently sized bins. We then averaged the responses within each time bin across neurons. Responses were smoothed with an exponential filter (τ = 100 ms) and normalized by the mean firing rate 400 ms prior to signal onset. Every binned response was normalized by the same value across time so the normalization procedure simply scaled all the responses and did not change their relationship to each other. The predicted reaction time for each firing rate bin was the time that bin's response crossed the model's

threshold, plus the motor preparation time. Threshold and motor preparation time were simultaneously fit to data from both the pre-cool and cool conditions for each task. The model fit was performed using maximum likelihood estimation under normal assumptions for the mean reaction time estimates and attempted to minimize the error between the predicted and measured reaction times (with the use of the fminsearch function in MATLAB's Optimization Toolbox V6.1 (R2011b)). This method was robust to starting threshold and motor preparation time.

Chapter 1: Effects of V2 and V3 inactivation on behavioral performance during motion and depth detection tasks

The data presented in this chapter was collected with the assistance of Alexandra A. Smith. A.A.S performed the experiments in Figure 16 and Figure 17. I performed the remainder of the experiments and analyzed all of the data.

Introduction

We trained two monkeys on motion and depth detection tasks optimized for MT neurons. Previous electrophysiological results indicate that inactivation of V2 and V3 leads to a selective impairment in binocular disparity tuning but not direction tuning in MT (Ponce et al., 2008). We might therefore expect that cooling V2 and V3 would affect behavioral performance more during the depth task than the motion task. However, although we are generally interested in the effects of V2 and V3 inactivation in the context of neuronal responses in MT, the behavioral effects of inactivation need to be considered more broadly. In addition to providing major input to MT and the dorsal ("where") processing stream, V2 is the major source of input to the ventral ("what") processing stream (Ungerleider and Mishkin, 1982; Van Essen and Gallant, 1994). It is therefore likely we are also affecting processing in its downstream areas, such as V4 and IT. Therefore, we might also expect that changes in the animals' basic visual abilities or appearance of the stimulus (*e.g.* color) may have detrimental effects on their behavioral performance during motion or depth tasks.

Importantly, we do not expect the animal to be blind in the affected part of the visual field—the "scotoma". In a previous study, Merigan and colleagues placed chemical lesions in parts of V2 and V3 in the lunate sulcus (Merigan et al., 1993), the region targeted by our

cryoloops. They found that animals were not impaired in their acuity or contrast sensitivity, indicating that not only were the animals able to see, but important aspects of basic visual sensitivity were not significantly affected.

Neurons in V2 are sensitive to a variety of basic visual properties including color, orientation, complex edges, motion direction, motion speed, and binocular disparity (DeYoe and Essen, 1985; Hubel and Livingstone, 1985; Peterhans and von der Heydt, 1993; Levitt et al., 1994; Gegenfurtner et al., 1996; Hegdé and Van Essen, 2000). Consistent with its role as a major contributor to the "what" visual processing stream, most outputs from V2 that proceed to V4 originate in V2 compartments that contain color and form information (DeYoe and Essen, 1985); V2's major projections to MT originate predominately in compartments with orientation, binocular disparity, and some direction sensitivity. The dorsal portion of V3, the part adjacent to our cryoloops, has somewhat larger receptive fields than V2 neurons (Gattass et al., 1988) but is selective for a similar array of visual features including orientation, direction, color, binocular disparity, and speed (Felleman and Van Essen, 1987; Gegenfurtner et al., 1997; Adams and Zeki, 2001). Based on these properties, it may be expected that aspects of form, color, and motion, and depth perception may be affected by inactivation of V2 and V3. This may explain why Merigan and colleagues (1993) observed a decrement in one animal's ability to discriminate isoluminant chromatic gratings, indicating some impairment in color processing. The other animal was not affected, suggesting such impairments can be variable. Since inactivation of V2 and V3 by cooling did not impair direction selectivity in MT (Ponce et al., 2008), the major site of motion processing, we expected behavioral performance during the motion task to be less affected. As suggested by Ponce and colleagues, motion information is likely reaching MT via direct

projections from V1.Therefore, in the context of our study we expected behavioral performance to be impaired more during the depth task than the motion task.

Interestingly, neurons in V2 and V3 have also been implicated in more complex visual processing. For example, neurons in V2 are sensitive to illusory contours, which are created by flaking objects outside the neurons' receptive field (von der Heydt et al., 1984). Neurons in V3 can have multi-peaked orientation and direction tuning curves (Felleman and Van Essen, 1987) and respond to particular combinations of color and motion (Gegenfurtner et al., 1997). Indeed Merigan and colleagues' (1993) major finding was that lesions of V2 and parts of V3 lead to impairments in visual grouping. However, our experiments were not designed to address these remarkable properties.

Results

Signal Detection Tasks

We trained two macaque monkeys to perform both a motion and a depth reaction time detection task in which they were rewarded for detecting onset of either coherent motion or depth(Figure 5). Trials for both tasks began with a fixation period of 500 ms, followed by a noise stimulus that lasted a random time between 500 and 5,500 ms before signal onset. The animals' task was to detect this onset and make an eye movement toward the stimulus within the 650 ms

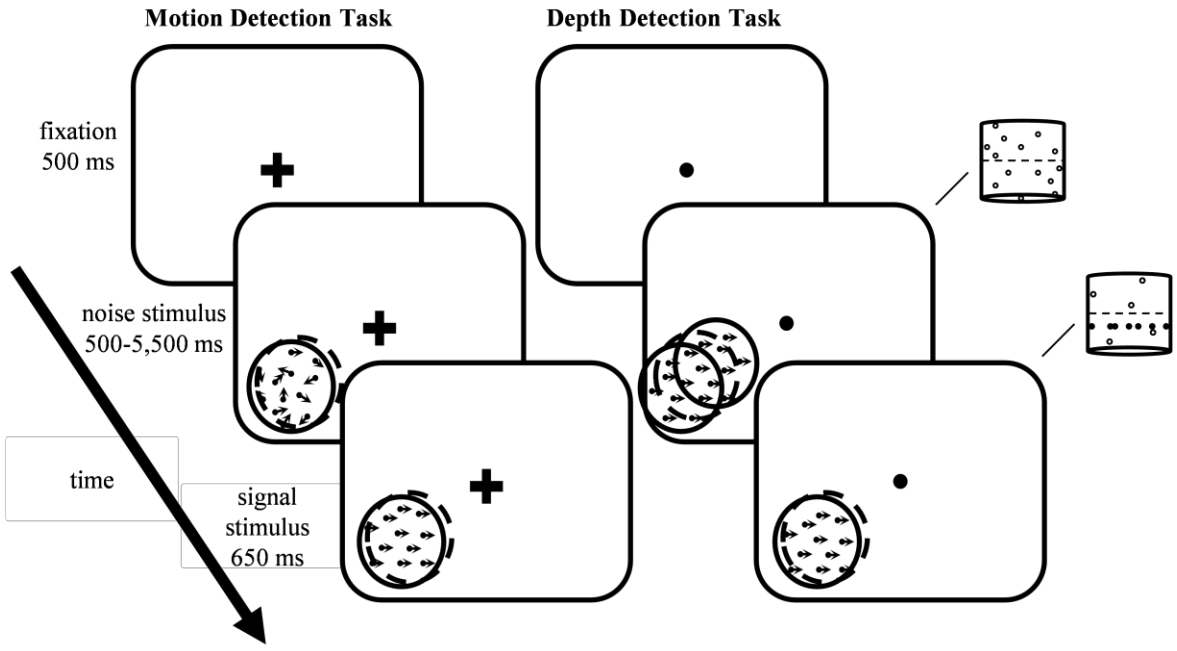

Figure 5: Motion and depth task design
After the animal acquired fixation on the central marker for 500 ms, a noise stimulus was presented for a random time between 500 and 5,500 ms and was followed by the signal onset. Animals were rewarded for reporting signal onset by making an eye movement toward the patch of dots between 200 and 650 ms after onset. If no response was made, the trial was labeled as missed and no reward was given. Any response after noise stimulus onset but prior to 200ms (minimum plausible reaction time) after signal onset was labeled a false alarm. Difficulty of both tasks was titrated by changing the proportion of signal dots in the signal stimulus. Lines in the depth task point to a top-down view of the stimulus in each stimulus epoch. The dashed line represents the plane of fixation.

presentation period. We titrated difficulty of both tasks by varying the proportion of signal dots—the signal strength—in the signal stimulus. The two tasks were interleaved in blocks of 25 trials per task. At the beginning of each block the animal had to correctly complete two practice trials before difficulty increased; these were not included in the analyses.

Effects of inactivation

In every cooling session, immediately before cooling, we measured the animals' behavioral performance. Visual stimuli were restricted to the part of the visual field affected by cooling based on the anatomical placement of the cryoloops and previous electrophysiological results (Ponce et al., 2008). This region, "the scotoma", extended approximately 10° into the periphery and excluded the fovea (Figure 3D). Unlike a scotoma created by a corresponding lesion in V1, this was not a blind spot; instead, this site is the location of the higher order deficits described below and in previous experiments (Merigan et al., 1993). During some sessions the animals also performed both tasks in the part of the visual field ipsilateral to the cryoloops, which we did not expect to be affected by cooling, thus allowing us to monitor any non-specific changes in performance. For simplicity, we will call this region the "ipsilateral visual field". The behavioral effects of cooling differed between the two animals so their results will be presented separately.

A representative behavioral session during cooling from monkey Q is shown in Figure 6. This animal's behavioral performance in the scotoma was degraded on both tasks during inactivation of V2/V3 (Figure 6A). This is evidenced by the reduction in his performance at most signal strengths (blue points are below the red points at the weaker signal strengths) and can be summarized by an increase in behavioral threshold, which we took as the signal strength at which the animal performed at 80% correct. Further evidence for degraded performance is the

increase in reaction time shown in Figure 6B. On this day, the median reaction time increased by 63 ms during the motion task and by 53 ms during the depth task. Importantly, the monkey was able to perform both tasks during cooling with reasonable success and there was no evidence of decreased trial initiation or general lack of motivation. Behavioral performance in the ipsilateral visual field was not significantly affected (Figure 6C-D). Also shown in this example is the

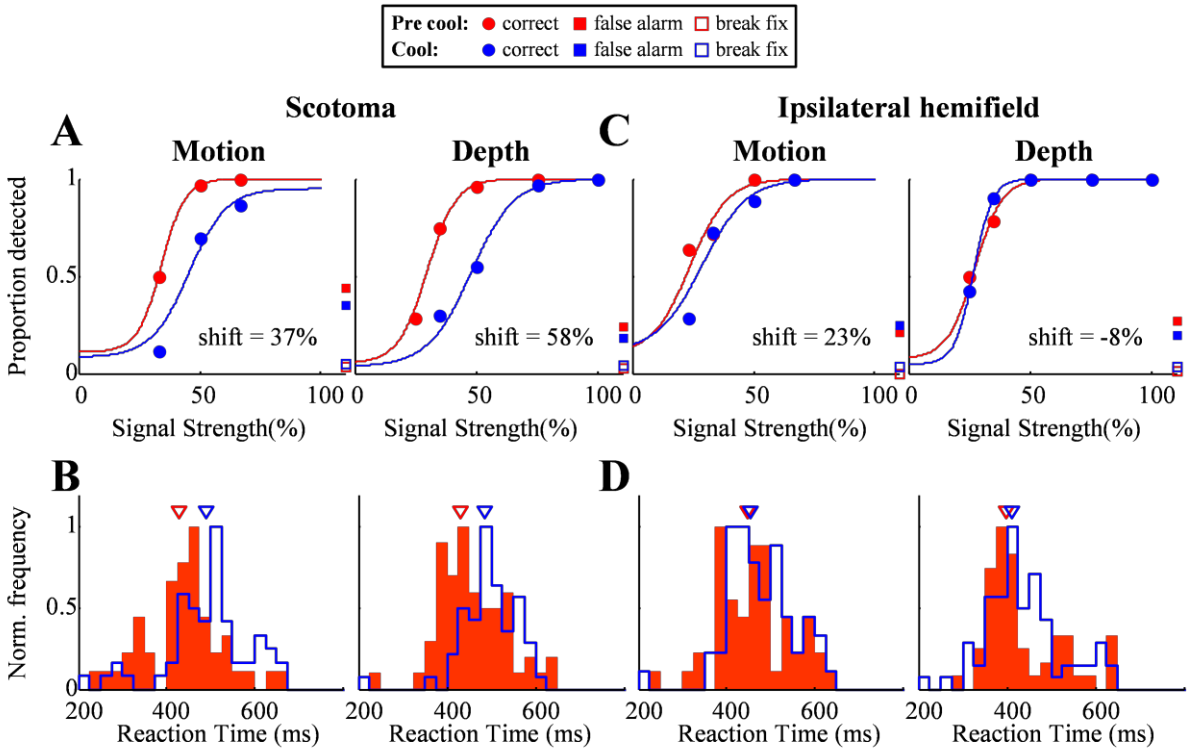

Figure 6: Monkey Q example behavioral performance
(A) Behavioral performance and fitted psychometric functions for the motion task (left) and depth task (right) in the scotoma during a single session. Data shown in red is from the pre-cool condition and data shown in blue is from the cool condition. The "shift" is the percent increase in behavioral threshold as compared to the pre-cool value ($i.e.\frac{cool-pre-cool}{pre-cool}$). Points shown at signal strengths greater than 100% correspond to proportion of breaks in fixation (□) and false alarms (■) across all trials.
(B) Reaction times in the scotoma. Median reaction times (▽) on the motion task (left) were 429 ms in the pre-cool condition and 492 ms in the cool condition. Median reaction times on the depth task (right) were 432 ms in the pre-cool condition and 485 ms in the cool condition.
(C-D) Behavioral performance (C) and reaction times (D) in the ipsilateral hemifield. Same conventions as in A-B. Median reaction times on the motion task were 447 ms in the pre-cool condition and 453 ms in the cool condition. Median reaction times on the depth task were 397 ms in the pre-cool condition and 412 ms in the cool condition.

proportion of breaks in fixation and proportion false alarms during both conditions (Figure 6A, C). Across all behavioral sessions for this animal, the proportion of false alarms and breaks in fixation was not significantly different during inactivation from those made in the pre-cool condition ($p>0.05$, sign test on paired data). The behavioral thresholds for this animal in sessions where thresholds could be measured are shown in Figure 7. Thresholds increase during most cooling sessions for both the motion and depth tasks (mean increase = 54% of pre-cool for the motion task, $p<<0.01$ sign test; mean increase = 53% of pre-cool for the depth task, $p<<0.01$ sign test). The threshold change was not significantly different between the two tasks within each session (Figure 7C; median shift difference = -11%, $p > 0.05$, paired sign test). Performance on either task was not significantly affected in the ipsilateral visual field (Figure 7B, D). Since we did not observe an effect of cooling on the ipsilateral side in the first 35 cooling sessions (including first 14 sessions, not shown, see Methods) we did not always test performance in the ipsilateral visual field in subsequent sessions in order to increase the number of trials completed with the stimulus in the scotoma.

In several behavioral sessions, we could not get an estimate of behavioral threshold because either there were insufficient data points to fit a psychometric function or the fit was poor. For monkey Q there were 20 such sessions with motion task performance and 10 with depth task performance. To include these sessions in a metric of behavioral performance, we generated a grand psychometric function by averaging performance across signal strengths in all sessions. Performance data at a particular signal strength was included only if there were data from both the pre-cool and cool conditions on the same day to allow for direct comparisons of performance in both conditions. The resulting performance data and fitted function are shown in Figure 8. Across 94 cooling sessions, the combined psychometric functions show a decrease in

performance over the full range of tested signal strenghts. The increase in grand threshold was 69% during the motion task and 67% during the depth task, indicating that, for monkey Q, performance on both tasks was similarly affected even when all experiments are taken into

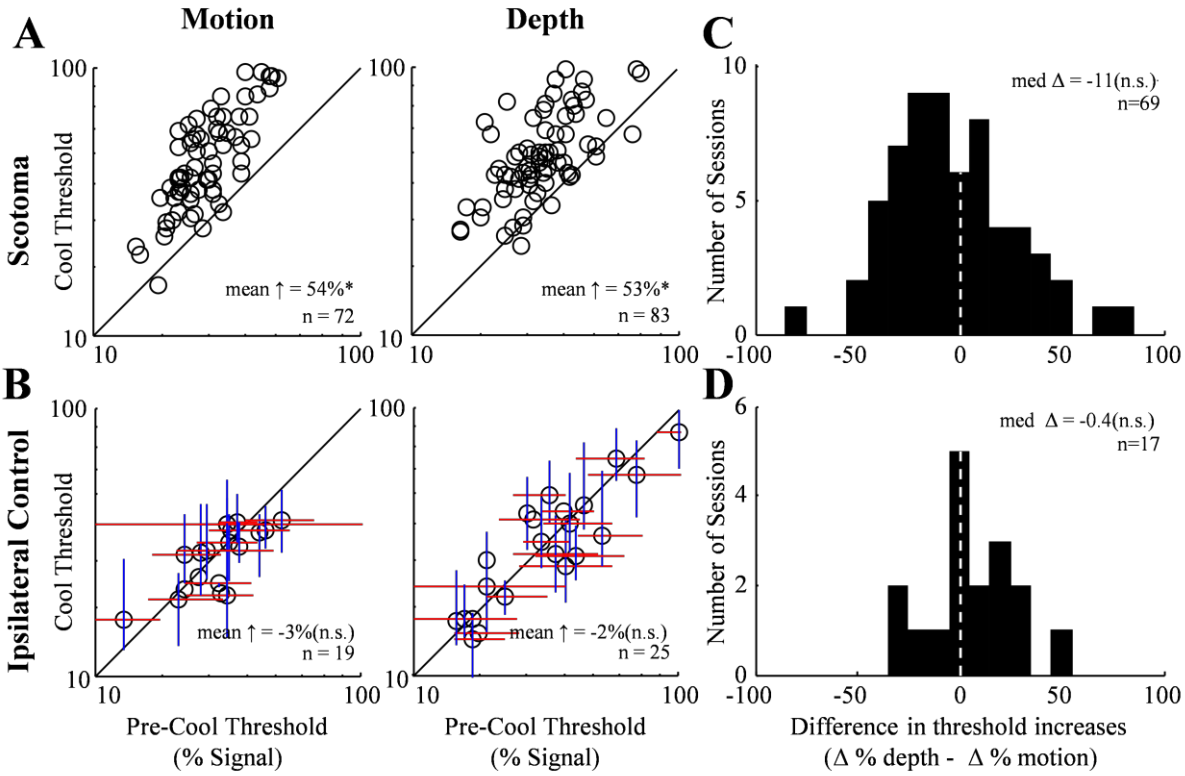

Figure 7: Population behavioral thresholds for monkey Q
(A-B) Behavioral thresholds (○) compared pre-cool to cool in the scotoma (A) and in the ipsilateral visual field (B). Data points lying above the unity line indicate an increase in threshold and therefore a decrement in behavioral performance. Error bars on the ipsilateral control data are 95% confidence intervals on the estimated threshold, derived from a parametric bootstrap procedure (Wichmann and Hill, 2001b); red = pre-cool, blue = cool. These were similar for behavioral performance in the scotoma and are not shown for clarity. Mean ↑ = mean increase in threshold during the cool condition expressed as a percent of pre-cool threshold. * = $p<0.05$; n.s. = not significant.
(C-D) Comparison of threshold increases between the depth and motion tasks in the scotoma (C) and in the hemifield not affected by cooling (D). For the subset of sessions for which we had estimates of threshold on both tasks we first computed the percent threshold increase from the pre-cool value for each task (same value as indicated within the axes of panels A-B). The values shown are the histogram of differences between motion and depth increases (Δdepth - Δmotion) within each session. Values greater than zero indicate the depth threshold shift was greater and performance affected more on the depth task. The median difference is shown in the upper right corner. Neither was significantly different from zero, sign test.

consideration. We also observed a decrease in slope in the grand psychometric function, which corresponds to a decline in sensitivity to increasing signal strengths. There was a significant decrease in slope across individual experiments as well, with a median slope decrease of 34% on the motion task and 22% on the depth task. These were not significantly different from each other when compared pairwise within sessions ($p>0.05$; data not shown). We observed no significant changes in slope during trials when the stimulus was presented in the ipsilateral visual hemifield.

Across all behavioral sessions, monkey Q's reaction times also increased during both tasks during inactivation. The median increase was 42 ms and 37 ms during the motion and depth tasks, respectively (Figure 9). Across all sessions, this increase was slightly bigger during the motion task (Figure 9C; median difference = -9ms, $p = 0.02$, sign test on paired means). There was no significant change in reaction times in the ipsilateral visual

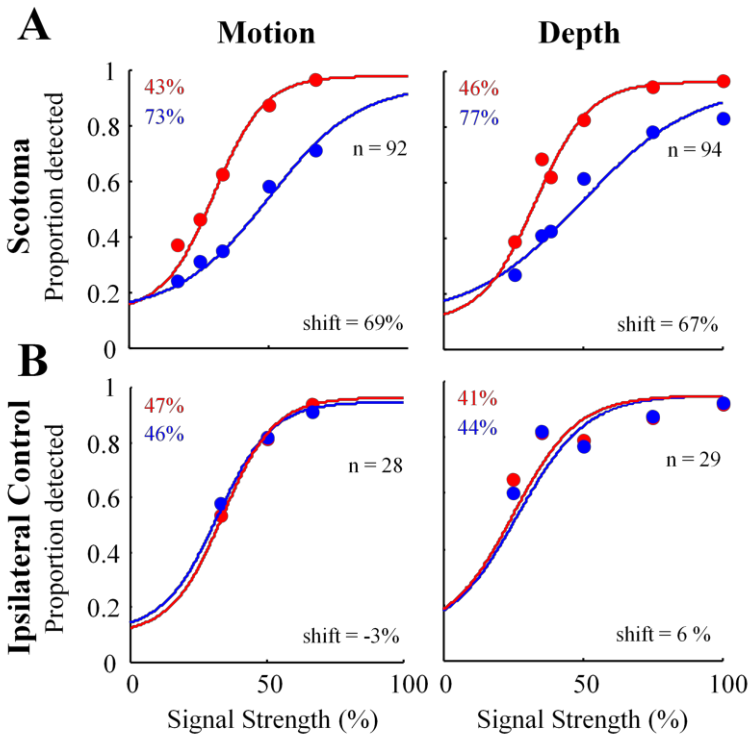

Figure 8: Grand psychometric function for monkey Q Behavioral performance combined across all behavioral sessions with cooling in the scotoma (A) and in the ipsilateral visual field (B). Performance from any given session was pooled only for signal strengths tested in both pre-cool and cool conditions. Values in the upper left corners indicate threshold and the value in the lower left corner ("shift") corresponds to the percent increase in threshold relative to the pre-cool value.

field on either the motion task (median increase = 5 ms, $p > 0.05$, sign test) or the depth task (median increase = -3 ms, $p > 0.05$) and these effects were not significantly different from each other (Figure 9D; median difference = 9ms, $p > 0.5$). Thus we concluded that monkey Q was impaired very similarly on both the motion and depth tasks.

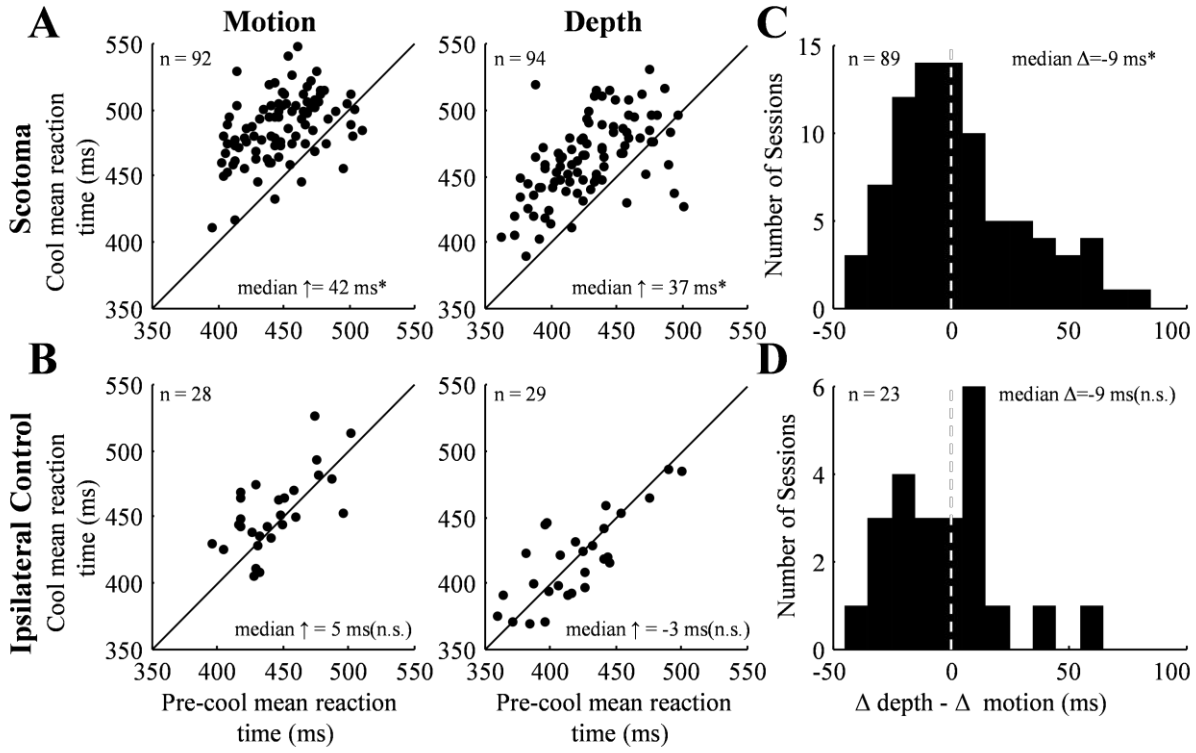

Figure 9: Reaction times for monkey Q

(A) Mean reaction times compared pre-cool to cool for the motion (left) and depth (right) tasks in the scotoma. Both motion and depth reaction times are significantly longer in the cool condition ($p<<0.01$ sign test on paired data for both tasks) with a median increase of 42ms on the motion task and 37 ms on the depth task. Asterisk indicates that the increase was statistically significant.

(B) Mean reaction times in the ipsilateral hemifield were not significantly different during the cool condition on either task ($p>0.05$ sign test on paired data). Same conventions as in (A). n.s. = not significant.

(C-D) Comparison of mean reaction time shifts between the motion and depth tasks in the scotoma (C) and in the ipsilateral visual field (D). For each session, we first compute the increase in mean reaction time between pre-cool and cool conditions ($\Delta = RT_{cool} - RT_{pre\text{-}cool}$) for the motion and depth tasks. The histogram of difference between the increases (Δdepth-Δmotion) for each session is shown in C-D. Differences less than zero indicate that reaction times increased more during the motion task than the depth task. The median differences are shown in the top right corner; * = $p<0.05$; n.s. = not significant.

The behavioral effects for monkey S were somewhat different, but were more in line with our initial expectations based on changes to tuning curves (their Figure 4, Ponce et al., 2008). A representative behavioral session is shown in Figure 10. Monkey S's performance was more affected during the depth task than during the motion task, with a threshold increase of 60% during the depth task and 3% during the motion task (Figure 10A). This was true in most sessions: on average, depth threshold increased significantly more than did the motion threshold

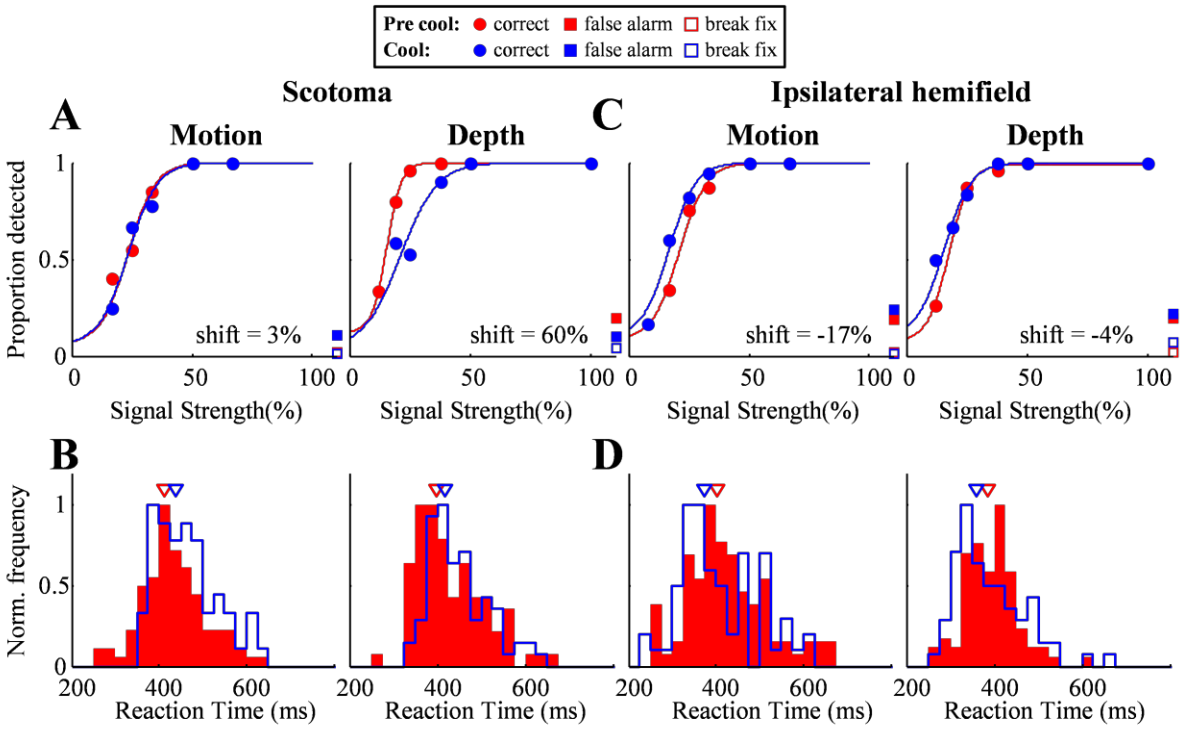

Figure 10: Monkey S example behavioral performance
(A) Behavioral performance in the scotoma. Same conventions as in Figure 6.
(B) Reaction times in the scotoma. Same conventions as in Figure 6. Median reaction times (▽) during the motion task were 414 ms in the pre-cool condition and 439 ms in the cool condition. Median reaction times during the depth task were 399 ms in the pre-cool condition and 418 ms in the cool condition.
(C-D) Behavioral performance (C) and reaction times (D) in the ipsilateral hemifield. Median reaction times during the motion task were 402 ms in the pre-cool condition and 372 ms in the cool condition. Median reaction times on the depth task were 385 ms in the pre-cool condition and 359 ms in the cool condition.

(Figure 11A, C; median depth increase = 46%; median motion increase = 18%, p<<0.01 paired sign test on difference). When performance in the ipsilateral hemifield was tested, there was no significant increase in threshold during either the motion or depth task and the small differences were not significantly different from each other (Figure 11B, D). In this example session, the median reaction time increased by 25 ms during the motion task and 19 ms during the depth task. Across all behavioral sessions the median increase was similar during the two tasks: 43 ms during the motion task and 45 ms during the depth task; the distributions were not significantly different between the tasks (Figure 12; p>0.05, sign test paired data). This animal also exhibited a significant decrease in the proportion of false alarms (5% decrease, p<<0.01; depth task 2%

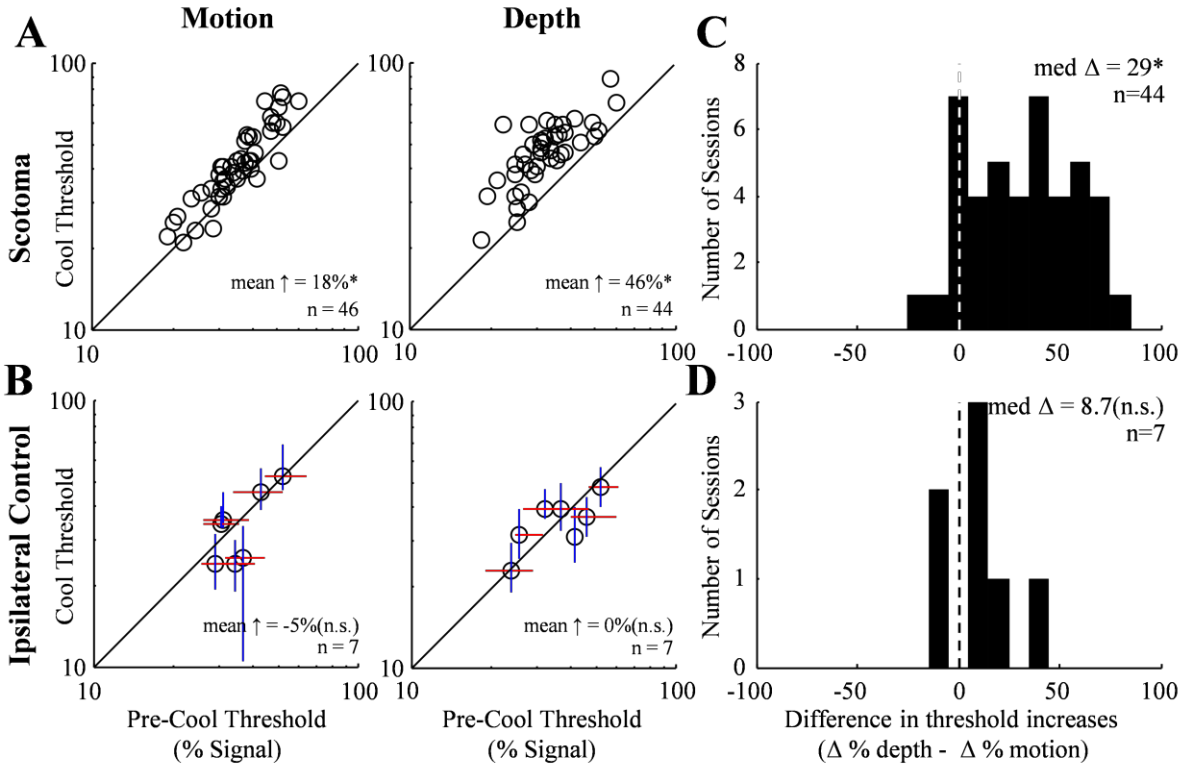

Figure 11: Population behavioral thresholds for monkey S
(A-B) Behavioral thresholds (○) compared pre-cool to cool in the scotoma (A) and in the ipsilateral visual field (B). Same conventions as in Figure 7.
(C-D) Comparison of threshold increases between the depth and motion tasks in the scotoma (C) and in the hemifield not affected by cooling (D). Same conventions as in Figure 7. Values greater than zero indicate the depth threshold increase was larger.

decrease, $p<<0.01$) and a slight increase in the proportion of breaks in fixation (motion task 2% increase, $p<<0.01$; depth task 3% increase, $p<<0.01$). Since the false alarm rate has an effect on the animal's guess rate, and thus the shape of the psychometric function, we always included the estimated guess rate in the psychometric function fit for both animals (see Methods).

There were only two sessions in which psychometric functions could not be fit to Monkey S's performance but we computed a grand psychometric function for comparison to monkey Q. The results confirm what we observed on individual sessions, which is that inactivation of V2 and V3 impaired the animal more during the depth task than during the motion task (Figure 13). As in monkey Q, we observed a decrease in slope that was also evident in individual sessions. The median slope decrease was 21% and 24% for the motion and depth task, respectively. These differences were not significantly different within sessions ($p >0.05$). There were no significant changes in slope in the visual hemifield unaffected by cooling.

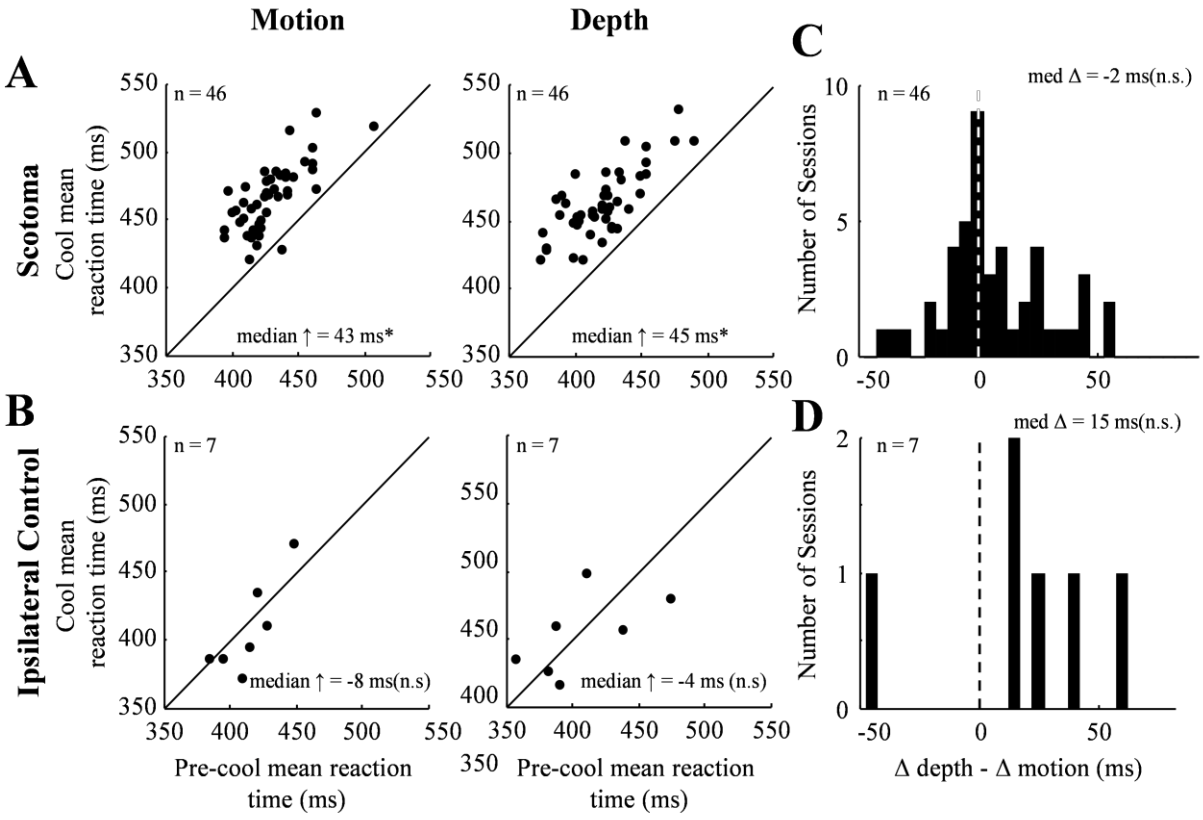

Figure 12: Reaction times for monkey S
(A) Mean reaction times compared pre-cool to cool during the motion (left) and depth (right) tasks. Both motion and depth reaction times are significantly longer in the cool condition ($p<<0.01$ sign test on paired data for both tasks) with a median increase of 42ms on the motion task and 37 ms on the depth task. Solid line is line of unity.
(B) Mean reaction times in the visual hemifield not affected by cooling were not significantly different in the cool condition on either task ($p>0.05$ sign test on paired data).
(C-D) Comparison of mean reaction time shifts between the motion and depth tasks. For each session, we compute the increase in mean reaction time between pre-cool and cool conditions for the motion and depth tasks. The difference between the increases (Δdepth-Δmotion) is shown here. Same conventions as in Figure 9.
(C) Comparison of mean reaction time shifts between the motion and depth tasks in the visual hemifield affected by cooling.
(D) Comparison of mean reaction time shifts between the motion and depth tasks in the visual hemifield not affected by cooling.

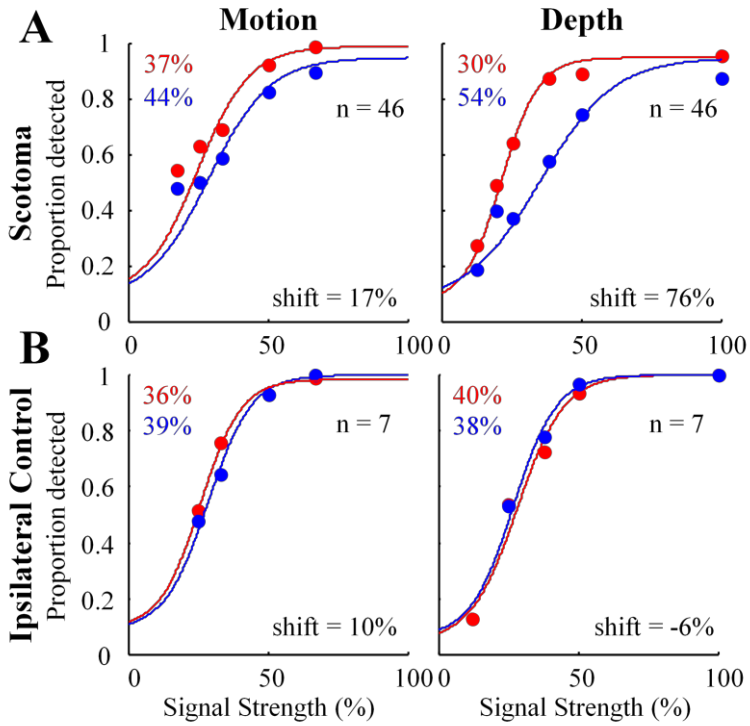

Figure 13: Grand psychometric function for monkey S
Behavioral performance combined across all behavioral sessions with cooling in the scotoma (A) and in the ipsilateral visual field (B).

Recovery from inactivation

During some sessions, the animals' continued motivation permitted us to get an accurate estimate of his behavioral performance in the scotoma upon recovery from inactivation. Recovery data were collected beginning 15 minutes after cooling was stopped or when the temperature at the loops had reached at least 30°C (sufficiently warm for visually evoked activity to resume in the region adjacent to the cryoloops). An example recovery session form monkey S is shown in Figure 14. Although the animal's performance during both tasks is impaired somewhat by cooling on this day, both his behavioral performance and reaction times return to pre-cool values during the recovery period. This was true for both monkeys in most sessions where we were able to measure behavioral performance (Figure 15), although monkey Q's mean

reaction times tended to be slightly but significantly elevated during the recovery period (median reaction times were 13 ms longer during the depth task and 19 ms longer on the motion task, $p<0.05$ for both values being significantly different from zero).

We also looked for changes in pre-cool values of threshold and reaction time as a function of session number to determine whether there were any long-term behavioral effects of inactivation. Experimental testing spanned a total of 12 months for monkey Q and 3 months for

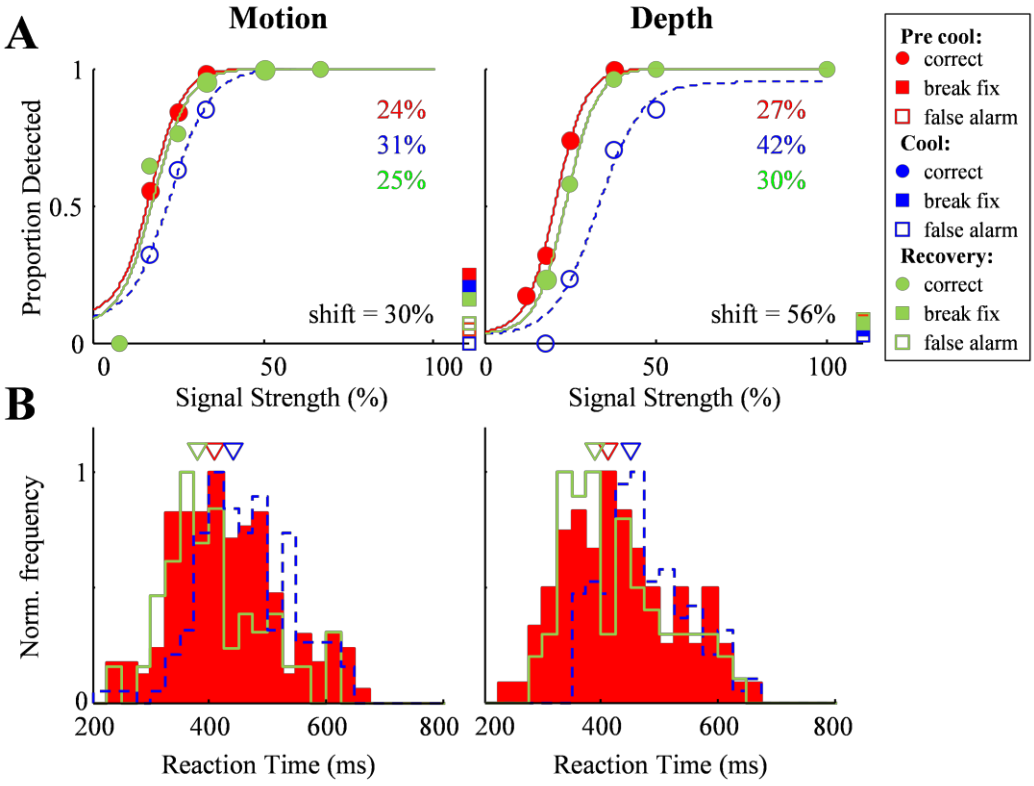

2

Figure 14: Example behavioral session with recovery
(A) Psychometric functions and threshold estimates (numbers in upper right corener) shown in all three conditions in a single session. Left: motion task, right: depth task. Data in green corresponds to the recovery period, which began 15 min after cooling offset when temperature at the loops was at least 32°C.
(B) Reaction distributions. Median reaction times (▽) in the motion task were 411 ms, 441 ms, and 381 ms in the pre-cool, cool, and recovery periods, respectively. Median reaction times in the depth task were 412 ms, 452 ms, and 389 ms in the pre-cool, cool, and recovery periods, respectively.

monkey S. We found no significant change in pre-cool reaction times in the first third of the sessions compared to the last third for either monkey. We found a significant increase in pre-cool depth threshold in monkey Q but additional experiments indicated that this was due to a decrease in the stimulus size in later sessions to accommodate those sessions' MT receptive fields. The depth task is selectively more difficult with small stimuli because a higher proportion of dots is near the perimeter of the aperture and therefore unpaired, thereby reducing the proportion of signal dots (see Methods: Visual Stimulus). We found no changes in the motion task thresholds or in pre-cool thresholds during either task for monkey S. Furthermore, we found no difference

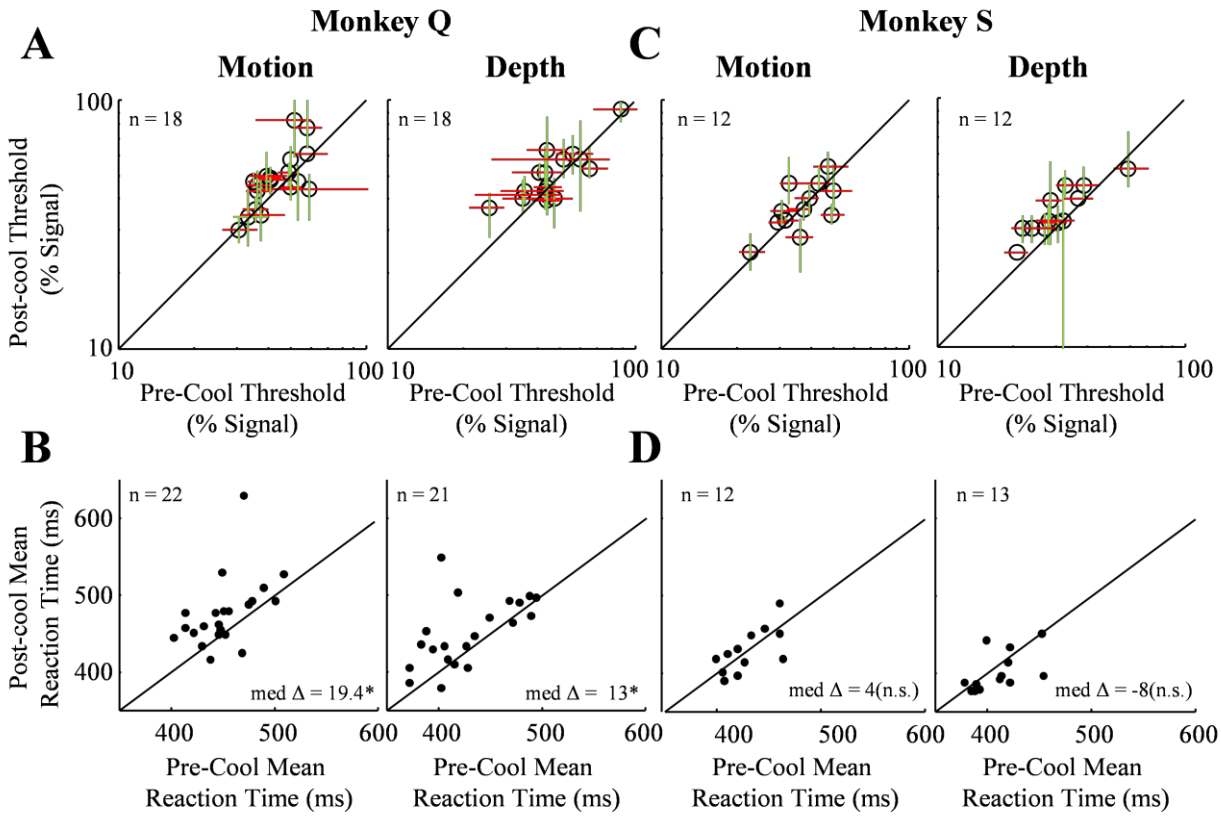

Figure 15: Recovery from inactivation population summary
(A) Monkey Q behavioral thresholds compared pre-cool to recovery in the scotoma. Same conventions as in Figure 7.
(B) Monkey Q mean reaction times compared pre-cool to recovery in the scotoma. Same conventions as in Figure 9.
(C) Monkey S behavioral thresholds compared pre-cool to recovery in the scotoma.
(D) Monkey S mean reaction times compared pre-cool to recovery in the scotoma.

in the magnitude of the cooling effect on either task over the several months of testing with each animal. Therefore, we conclude that the behavioral effects we observed were reversible on a daily basis and not due to long-term damage or other permanently disruptive effects of cooling.

Fine Change Detection Tasks

Our finding that monkey Q was equally impaired during both motion and depth signal detection tasks was somewhat unexpected given previous results suggesting the disparity-heavy contribution of the V2/V3 pathway to MT. In an additional attempt to uncover differential effects of inactivation on tasks involving the two modalities in this animal, we tested his behavioral performance during a task that required a slightly different cortical computation. Performance on the signal detection tasks we initially employed depends on neurons' ability to discriminate signal stimuli from noise stimuli. Subsequent analysis of concurrent MT neuron recordings revealed that MT neurons are indeed impaired more in disparity signal-from-noise discrimination than motion signal-from-noise discrimination (see Chapter 2). Furthermore, we found that MT neurons *tuning* selectivity was degraded more for disparity than direction of motion, as previously reported by Ponce *et al*. (2008). Tuning selectivity, unlike signal-to-noise sensitivity, is measured as the differences in neuronal responses to 100% signal stimuli at different directions or binocular disparities for direction and disparity tuning, respectively. Since tuning selectivity does not depend on whether neurons can discriminate noise from signal, it represents a different cortical computation. Therefore, we tested monkey Q's behavioral performance on tasks that more closely depend on the tuning properties of MT neurons rather than their ability to discriminate noise from signal. In this "fine change" task, the animal was rewarded for detecting a small change in the direction or depth of random dot stimuli. All stimuli were presented at the maximal signal strength and only changed in either direction or disparity. Task difficulty was

titrated by varying the change amount in degrees direction or disparity rather than by manipulating the overall signal strength. Thus, the animal's ability to do this task depends on the tuning selectivity of the underlying sensory pool, which we know is also disrupted during inactivation. Since tuning for binocular disparity is also degraded more so than for direction of motion, we would again predict that the animal would be more impaired during the depth fine change task than the motion fine change task.

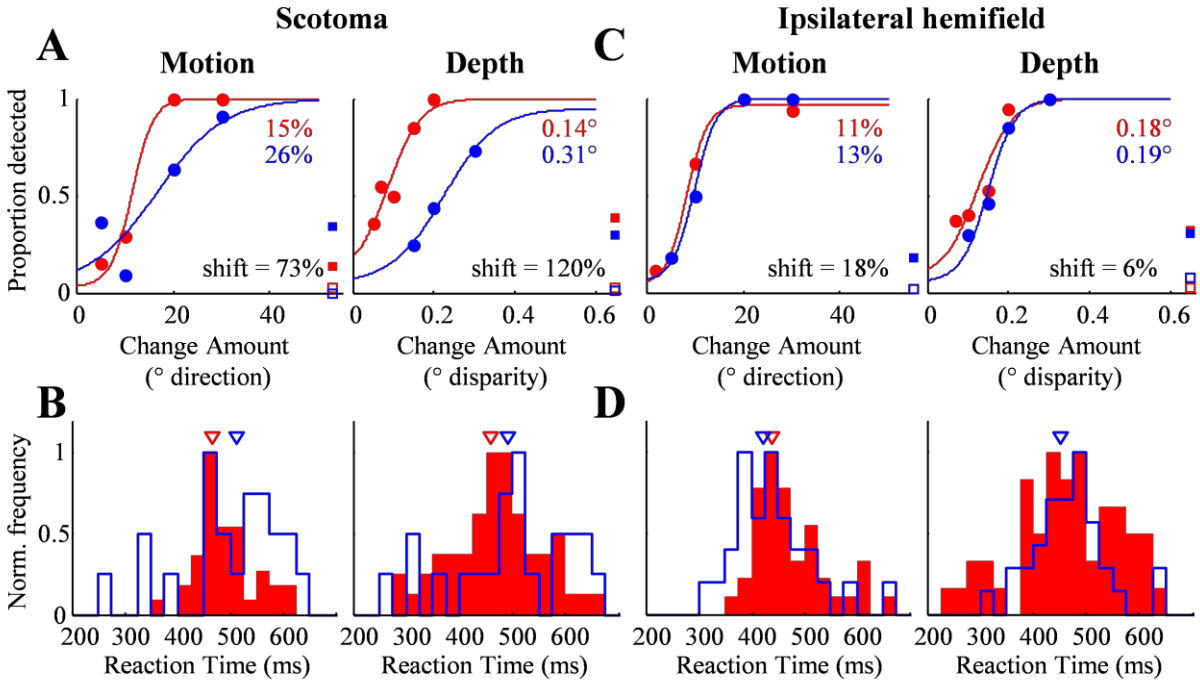

Figure 16: Fine change motion and depth tasks example behavioral session
(A) Behavioral performance in the scotoma. Example performance and fitted psychometric functions for the motion task (left) and depth task (right) from a single session. Note the axes for the motion and depth tasks are different. Otherwise, same conventions as in Figure 6.
(B) Reaction times in the part of the visual field affected by cooling. Median reaction times (▽) during the motion task (left) were 466 ms in the pre-cool condition and 513 ms in the cool condition. Median reaction times during the depth task (right) were 460 ms in the pre-cool condition and 491 ms in the cool condition.
(C-D) Behavioral performance (C) and reaction times (D) in the ipsilateral hemifield. Same conventions as in A-B. Median reaction times on the motion task were 439 ms in the pre-cool condition and 424 ms in the cool condition. Median reaction times on the depth task were 451 ms in the pre-cool condition and 452 ms in the cool condition.

We performed a total of 16 cooling sessions while the animal performed the fine change versions of the motion and depth tasks, two of which were excluded due to insufficient data. An example behavioral session from this task is shown in Figure 16.

As in the signal detection tasks, this animal appears to be impaired during both the motion and depth tasks with a 73% increase the fine motion task threshold and 120% increase in the fine depth task threshold. This experiment is representative of the population effects, which are shown in Figure 17. Although there are too few sessions to determine whether there are small differences in the magnitude of the effects during the two tasks, it is clear that the animal's performance is impaired substantially on both tasks: the median threshold increase was 81% during the motion task and 115% during the depth task. Furthermore, the median reaction time across experiments increased by 34 ms on the motion task and 51 ms on the depth task, although this difference was not significant (data not shown). Therefore, we conclude that this animal was similarly impaired on fine-change versions of both motion and depth tasks as well.

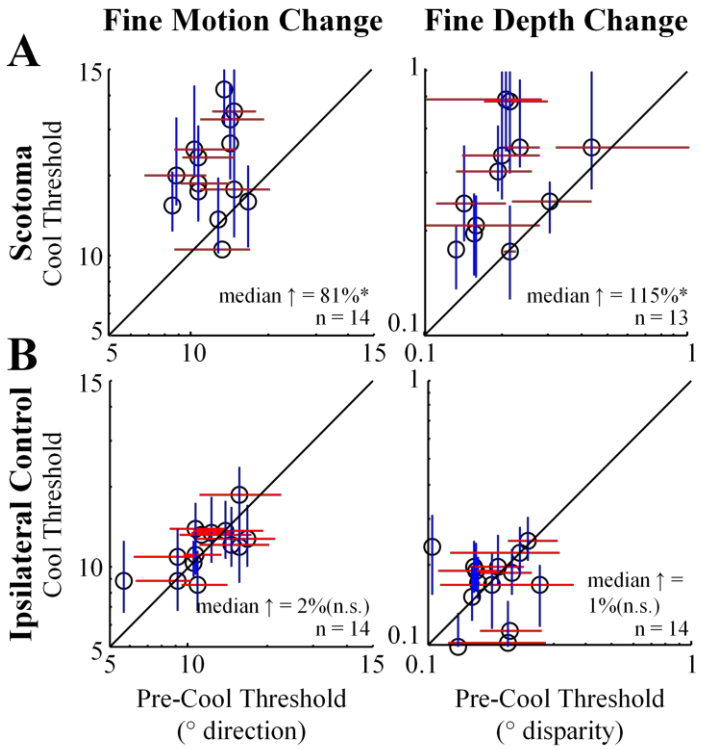

Figure 17: Fine change task population thresholds
(A-B) Behavioral thresholds (○) compared pre-cool to cool in the scotoma (A) and in the ipsilateral visual field (B). Note axes are different between the motion and depth tasks. Otherwise, same conventions as in Figure 7.

Discussion

We measured behavioral performance of two animals during motion and depth signal detection tasks tailored to the preferences of MT neurons while we inactivated V2 and V3. Previous anatomical and neuronal studies of MT inputs suggested we might see a bigger impairment during the depth task than the motion task. This is indeed what we saw in one of our animals, monkey S but not in the other, monkey Q. We found that monkey S' performance was degraded more during the depth than motion signal detection task, as evidenced by much larger increases in behavioral threshold as well as reaction times during the depth task. However, monkey Q's performance was similarly impaired during two versions of motion and depth tasks: a signal detection task and a fine-change task.

The non-specific impairment of monkey Q presents a bit of a mystery, especially in light of monkey S's specific behavioral effects. It is unlikely that this is simply due to reduced motivation or alertness for several reasons: 1) performance remains unaffected for the interleaved trials in the visual hemifield not affected by cooling, 2) the typical shape of the psychometric function during cooling rejects the idea that the animal adopted a mixed strategy (e.g. ignoring the difficult trials), 3) we observed no changes in the rate of trial initiation. Furthermore, it is unlikely that the animal simply can't see. In a previous study, permanent lesions in V2 and parts of V3 did not lead impairments in basic visual processing such as contrast sensitivity and spatial acuity (Merigan et al., 1993). In our experiments, monkey Q often continues to do well during the easiest trials (e.g. performance at 100% signal on the depth task and 66% signal on the motion task in Figure 6A), indicating that his ability to resolve the dots is not impaired.

However, as discussed in the introduction to this chapter, it is likely that inactivating V2 and V3 affected a variety of visual processes. For example, it is likely that we affected color and form processing and thereby the appearance of the task stimuli. In fact, Merigan and colleagues observed color processing deficits in one of their two animals following lesions of V2 and V3 (Merigan et al., 1993). Such changes in the appearance of the stimulus may have led to the non-specific impairments that we observed in monkey Q. It is also possible these behavioral results reflect real deficits in motion processing. For example, many neurons in V3 are sensitive to motion, some similarly to MT neurons (Gegenfurtner et al., 1997), so their inactivation may explain the effects on the behavioral performance during the motion task. As a result, perhaps the selective results of monkey S are most surprising. However, since they are in line with the predictions from the MT neuronal data, they likely reflect underlying deficits in depth processing that exceed those of motion processing.

Chapter 2: Effects of V2 and V3 inactivation on neuronal activity during motion and depth detection tasks

Introduction

Reversible inactivation of V2 and V3 by cooling has been shown to lead to a larger reduction in MT neurons' tuning selectivity for binocular disparity than motion direction, suggesting that these areas convey a disproportionate amount of binocular disparity information to MT (Ponce et al., 2008). We implemented this technique to determine whether changes in neuronal sensitivity on a short time scale (the hour-long cooling session) can lead to changes in the contribution of MT neurons to behavioral reports during motion and depth detection tasks. Previous work indicates that choice probability—a metric of neurons' correlation with behavior—is often highest for the neurons most sensitive to the task demands and that this relationship can evolve over months as animals' performance gradually improves during a complex task (Britten et al., 1996; Law and Gold, 2008, 2009). These results reveal a level of flexibility in the decision circuitry that can accompany learning on a long timescale. We set out to use a choice probability-like metric, called detect probability (DP), to determine whether the decision circuitry could adapt on a short timescale if we suddenly changed MT neurons' "informativeness" for binocular disparity more than motion.

First, it is important to note that although the selective changes in tuning strength indicate that the indirect pathway through V2 and V3 is necessary for recovering one aspect of disparity but not motion information in MT, we did not know how these changes in tuning properties would affect neurons' performance in the context of the motion and depth signal detection tasks we used. To clarify: behavioral performance during both tasks depends on a group of neurons'

ability to encode signal as being distinct from noise—*i.e*. signal detection. In contrast, when we evaluate a neuron's tuning strength, we measure the differences in the neuron's response to a range of values of a feature presented only at 100% signal strength. Thus a neuron's tuning strength does not necessarily reflect how well it can distinguish signal from noise at its preferred direction or disparity, the neuronal computation necessary for the tasks. Since the signal from noise discrimination also depends on the availability of binocular disparity and direction information, we hypothesized that weakened tuning for binocular disparity in MT would also lead to greater impairments in neuron's ability to discriminate signal from noise stimuli during the depth task than the motion task. This, in turn, could lead to a larger reduction in MT neurons' involvement in behavioral judgments during the depth task than the motion task.

Therefore, our two major goals were to determine whether: 1) the previously observed selective effects of inactivating V2 and V3 on MT tuning curves extend to neurons' sensitivity during the signal detection tasks and 2) to determine the effects of inactivation on MT correlations with behavior (DP).

Results

We observed several effects of inactivation on MT neurons' sensory representation: a non-specific global reduction in firing rate, a larger impairment in binocular disparity tuning selectivity than direction tuning selectivity, a larger reduction of cell sensitivity during the depth task than the motion task, and a reduction in spike count variability (Fano factor) across both tasks. Furthermore, we found that choice-related activity, as measured by detect probability (DP), was reduced during the depth task and not the motion task, suggesting that the impairments we induced in cell sensitivity during cooling led to a selective restructuring of the depth but not motion task-related decision circuitry. We also found that a simple integrate-to-bound model of

MT read-out can account for a large proportion of the variability in the animals' reaction times during both tasks in both conditions. All neuronal results were similar between the two animals so their data will be presented together.

Firing Rate and Tuning

We observed marked changes in the basic visual responses of MT neurons during reversible inactivation of V2 and V3 by cooling. Many of these effects are similar to those previously reported by Ponce and colleagues (2008). First, we observed a global reduction in visually-evoked firing rate. The median effect was a 36% reduction as measured from the response to the preferred direction of motion (100% signal strength) in the pre-cool vs. cool conditions. Secondly, we observed a greater reduction in tuning strength for binocular disparity than for direction of motion. An example cell's tuning curve for binocular disparity and direction is shown in Figure 18A. Despite overall decrease in firing rate during inactivation (18% reduction for this cell), this neuron continued to be strongly selective for direction of motion but became less selective for binocular disparity. We quantified the tuning selectivity for both direction and disparity with a discrimination index (DI) for each feature (see Methods). The DI is 0 when the responses to the preferred feature value are indistinguishable from the responses to the null value (*i.e*. the cell is not tuned) and it approaches 1 as the responses to the preferred feature become more distinguishable from the responses to the null feature. The DI was measured at the same stimulus values in both the pre-cool and cool conditions. For this example cell, the DI decreased by 3% for direction tuning and 11% for disparity tuning. This pattern of results is representative of the population of recorded neurons in that the disparity DI declined more than the direction DI in most cells (Figure 18B-D). The median DI change for direction tuning was a reduction of 5% and a reduction of 26% for disparity tuning, both of

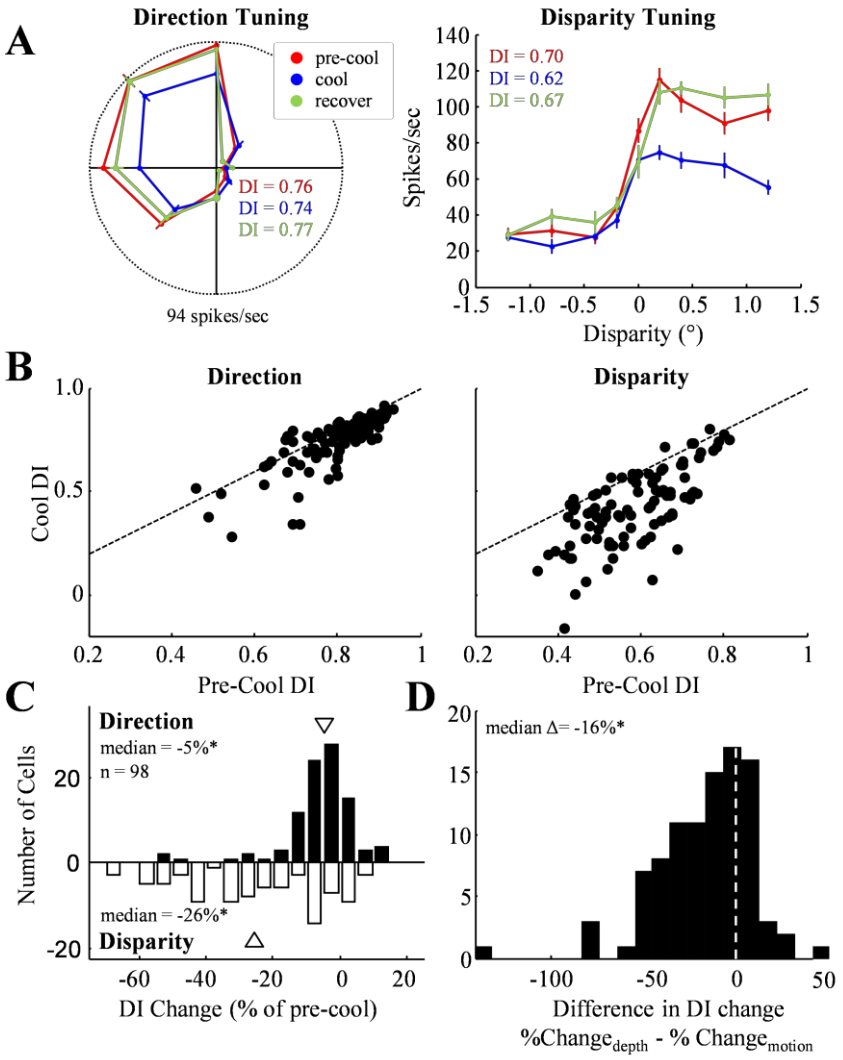

Figure 18: Binocular disparity tuning is impaired more than direction tuning
(A) Example direction (left) and disparity (right) tuning curve for a single neuron during the pre-cool, cool, and recovery periods. Tuning selectivity is quantified by a discrimination index (DI), which is shown for each condition next to the tuning curve. Data from the pre-cool, cool, and recovery periods are shown in red, blue, and green, respectively.
(B) Population comparison of DI pre-cool to cool for direction (left) and disparity (right). Dashed line is line of unity. Values below zero in the cool condition (in the disparity DI plot) indicate that tuning modulation inverted such that the neuron now responded more to the null stimulus than the preferred.
(C) Comparison of DI changes for cells in which both direction and disparity tuning data was collected in both pre-cool and cool conditions. Asterisks indicate that each distribution was significantly different from zero ($p < 0.01$, sign test).
(D) Pair-wise comparison of DI changes between the two features. The percent change in DI for direction tuning is subtracted from the change in DI for disparity tuning. Values less than zero indicate that disparity tuning was impaired more than direction tuning. (* = $p<0.01$, sign test)

which were significantly different from zero (Figure 18C). The decrease in disparity DI was significantly greater than the decrease in direction DI in a pair-wise comparison within each session (Figure 18D; median difference = 16%, $p<0.01$ sign test). This confirms the earlier findings of Ponce and colleagues (2008) and indicates that the indirect pathway to MT convey a disproportionate amount of disparity information. The global reduction in firing rate likely reflects the removal of input to MT neurons.

Also shown in the example in Figure 18A is the tuning curve measured during the recovery period (in green), which in this case was obtained 23 minutes after cooling was discontinued, when the temperature had returned close to physiological temperature (> 36.6°C at each of the three cryoloops, normal physiological temperature was 38-39°C for this animal). For this example cell, the firing rates at all directions and binocular disparities had returned to the pre-cool values by this time. Accordingly, the DI calculated during the recovery period was similar to the pre-cool DI value. We were able to collect recovery tuning data for 49 MT neurons. Recovery-period data was always collected at least 15 minutes after the cooling period had ended, when temperatures were at least 30°C at the loops, which is sufficiently warm to resume normal visually evoked activity (Lomber et al., 1999). The recovery DI for direction and disparity for these cells is plotted against the pre-cool values in Figure 19. Many cells have recovered completely by this time and the median DI difference between pre-cool and recovery is -3% and -7% for the motion and depth tasks, respectively. Although these are both significantly less than zero, the difference in DI is smaller than it was during cooling, indicating that these cells are on their way to complete recovery. Additional evidence supports that the neuronal effects of inactivation were fully reversible. First, we did not observe any change in the distribution of pre-cool direction or disparity DIs as a function of experimental session, most of

which were on consecutive days, indicating complete recovery by the next day. We also observed no difference in the magnitude of the inactivation effect over time (3-12 months of experiments in the two animals) which suggests that long term damage or reorganization was unlikely. Taken together, these results indicate that the neuronal effects of inactivation were repeatable and reversible on a daily basis.

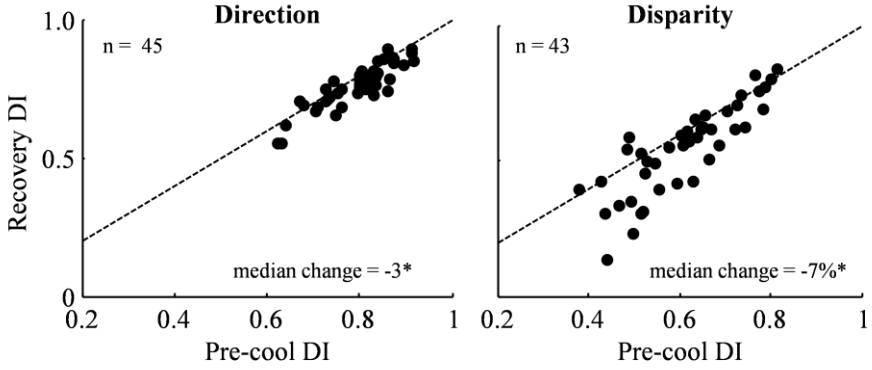

Figure 19: Recovery of tuning DI
Tuning DI during the recovery period is shown plotted against the pre-cool DI for direction (left) and disparity (right) tuning. The median percent difference $\left(\frac{DI_{recovery} - DI_{pre-cool}}{DI_{pre-cool}} \times 100\%\right)$ is shown in the bottom right corner. The asterisk indicates that the median difference is significantly different from zero ($p<0.01$, sign test).

Task-related cell sensitivity

To assess the effects of inactivation on the neurons' performance during each task, we constructed a neurometric function for each neuron (see Methods). This is analogous to a psychometric function and describes how well each *neuron* would be able to discriminate signal from noise during the task and thereby detect signal onset. This allowed us to measure the effects of inactivation on the neurons informativeness as it pertains to the tasks. For each task, the neurometric function was computed by comparing neuronal responses at each signal strength immediately prior to signal onset to the responses shortly after signal onset. The area under the ROC curve for these two distributions corresponds to the probability with which an ideal

observer can correctly determine whether a randomly selected rate belongs to the pre- or post-signal onset epoch. Thus it gives the probability with which the neuron can correctly detect the change. This metric is likely an overestimate of the neuron's performance because we specify the time windows in which to compare responses, removing the temporal ambiguity that is present in each trial. It is therefore an upper bound on how sensitive each neuron is to the change the monkey must detect. The neurometric functions for four example neurons are shown in Figure 20. In both conditions, MT neurons' responses increased as a function of signal strength in both

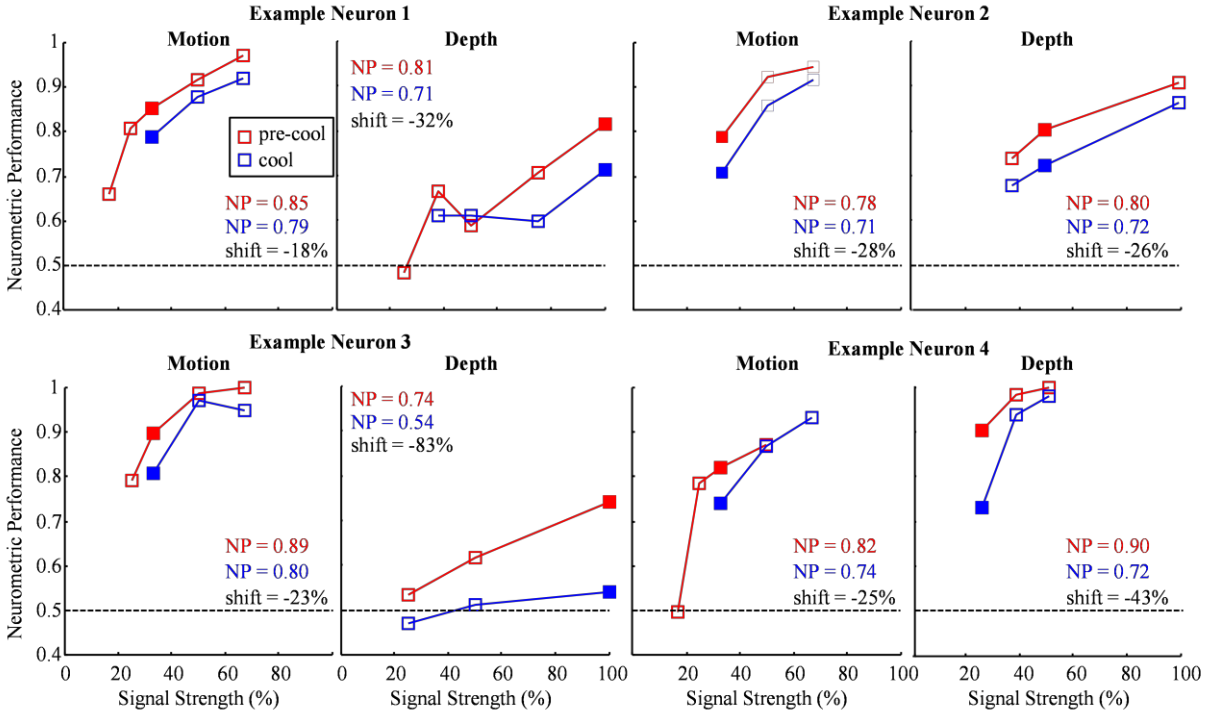

Figure 20: Example neurometric functions
(A-D) Neurometric performance during the motion (left) and depth (right) tasks for four example neurons (numbered 1-4). Squares correspond to the neurometric performance at each tested signal strength. Not all signal strengths were tested in all conditions. Of the signal strengths tested in both conditions, the signal strength at which the neuron's performance was nearest to 0.8 (i.e. 80% correct) in the pre-cool condition was chosen as the comparison point for the cool condition. Responses to this signal strength are shown as filled squares. The neurometric performance values and percent change in neurometric performance relative to the pre-cool value are shown in the corner of each panel. Dashed horizontal line at 0.5 indicates the chance rate of performance.

motion and binocular disparity. In the pre-cool condition, neurons often reached near-perfect performance at the highest signal strengths during the motion task; however, they tended to perform poorly during the depth task even though the maximum available signal strength was higher (100% on the depth task versus 66% on the motion task). This is largely because MT neurons are modulated more by direction than binocular disparity, leading to smaller differences in the firing rate distributions pre- and post-signal onset on the depth task (DeAngelis and Uka, 2003).

To determine the effect of cooling on the neurometric performance, we approximated the neurometric threshold (the signal strength at which neurometric performance was nearest to 0.8. *i.e*. 80% correct) in the pre-cool condition. We then calculated the neurometric performance during inactivation at that same signal strength. This near-threshold signal strength is indicated by the filled markers for each neurometric performance function in Figure 20. Neurons with pre-cool neurometric performance below 0.55 were excluded from this analysis since they were effectively insensitive to the task prior to inactivation (1 excluded for motion, 9 excluded for depth; total number of neurons = 78). Individual cells' near-threshold neurometric performance during both conditions and for both tasks is plotted in Figure 21A. The median decrement in neurometric performance during inactivation was 18% during motion task and 41% during the depth task. This difference was significant in a pair-wise comparison within each session, such that for most neurons, the decrement in performance was greater during the depth task than the motion task (Figure 21C; median difference = 20%, $p<0.05$). Note that for many neurons, the neurometric performance nearest 0.8—the signal strength defined to be the threshold—was often substantially below 0.8 (as evidenced by the spread along the abscissa in the right panel of Figure 21A). This was usually the case when the neurons maximal performance was below 0.8 at

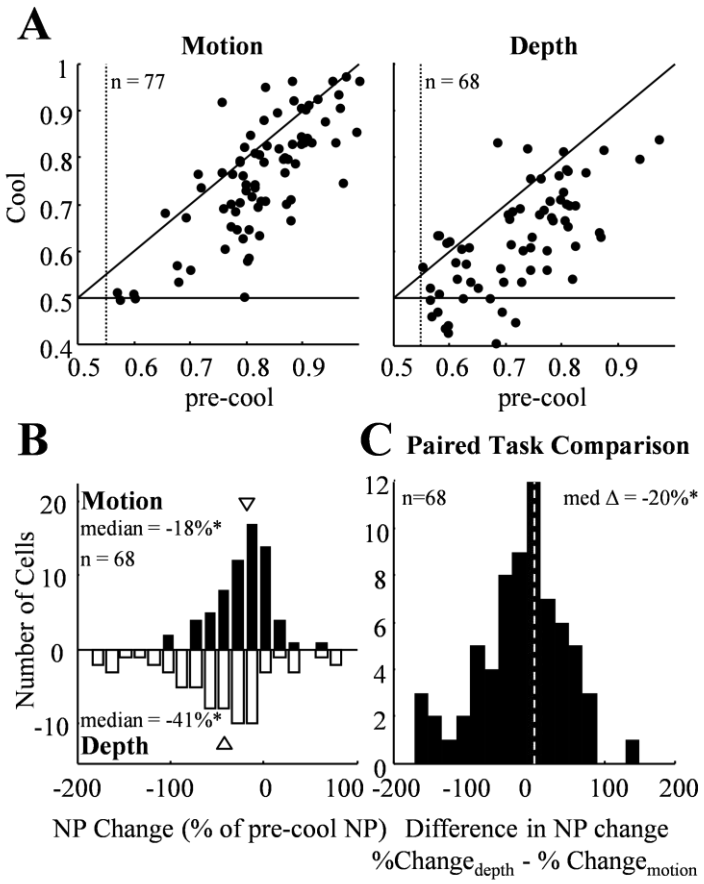

Figure 21: Neurometric performance population summary
(A) Neurometric performance of individual neurons compared pre-cool to cool for the motion (left) and depth (right) tasks. Diagonal line is line of unity. Dashed vertical line indicates the threshold below which neurons were excluded from the neurometric performance analysis (1 excluded point in the motion plot and 9 excluded points in the depth plot are not shown).
(B) Comparison of the percent change in neurometric performance for each task. Only neurons that contributed to both histograms are included. The median reduction was 18% during the motion task and 41% during the depth task. Values below -100% indicate sign changes in performance relative to 0.5 (see Methods).
(C) Pair-wise comparison of the performance changes during the two tasks for each neuron. The percent change in neurometric performance during the motion task is subtracted from the change in neurometric performance during the depth task. Values below zero indicate that depth neurometric performance was impaired more than motion neurometric performance. (* = $p<0.01$, sign test)

all signal strengths. Since this was more common during the depth task, one concern is that if lower-performing neurons were more sensitive to the effects of inactivation (*e.g.* the computation was more fragile to begin with) we might see disproportionate effects on the tasks simply due to differences in pre-cool neurometric performance. However, restricting the analysis to the subset of neurons with the highest neurometric performance during the depth task did not lead to qualitative changes in this effect: neurometric performance was still affected significantly more during the depth task than the motion task. This was true for all tested subsets of the data. Furthermore, we found no significant correlation between the magnitude of the effects of inactivation on neurometric performance and pre-cool neurometric performance during the depth task ($\rho = 0.1$, $p > 0.05$) indicating that lower-performing cells were not affected more strongly by inactivation.

Although neurometric performance was impaired more during the depth task than the motion task, there was still a significant impairment during the motion task. Unlike direction tuning, neurometric performance during the motion task was often affected by cooling: the median decrease in direction tuning DI was only 5% but neurometric performance on the motion task declines by 18%, on average. However these results are not in conflict since tuning and task-related neurometric performance reflect different aspects of the neurons' encoding of direction information, as discussed above. Therefore, our results indicate that input from V2 and V3 also affects MT neurons' representation of noisy motion stimuli, albeit less than noisy disparity stimuli.

Choice-related activity in MT

The discovery that cortical neuronal responses are weakly correlated with behavioral reports has been used to suggest that a neuron, or a set of neurons, contribute to perceptual

decisions. Such correlations with behavior occur when the animal is presented with identical visual stimuli, even one with no signal strength, suggesting that small fluctuations in neuronal firing influence perceptual decisions. Experimenters often search for these effects under experimental conditions where task parameters are tailored to the preferences of the neuron under study in order to give the neuron its "best chance" of being involved. Neurons in MT exhibit this kind of choice-related activity during motion and depth discrimination tasks (Britten et al., 1996; Uka and DeAngelis, 2004) and in the motion detection task we used (Cook and Maunsell, 2002b; Bosking and Maunsell, 2011). However, choice related activity in MT neurons had not previously been examined in the context of a depth detection task.

We measured these correlations, termed "detect probability" (DP) for detection tasks, for individual neurons as monkeys alternated between the two tasks. DP was measured at intermediate signal strengths where there were sufficient numbers of both correct and missed trials (see Methods). Neuronal responses after the signal onset were z-scored within each stimulus (*i.e*. signal strength) and then combined, across stimuli, for each neuron. Responses were sorted into two distributions: one containing trials when the animal correctly detected the change and one for trials when the animal missed the change. The area under the ROC curve for these two distributions is the DP, which indicates the probability with which an ideal observer can determine whether the animal reported detecting the signal onset from a firing rate chosen randomly from the two distributions. This value will differ from chance (0.5) if the two distributions are somewhat non-overlapping. Such a difference would indicate that neuronal responses differed on the basis of the animal's choice. Like any ROC measure, possible values range from 0 to 1, where a DP of 1 signifies that the neuron always fired more when the animal detected the change than when it missed the change. Conversely, when the value approaches 0,

the neuron fires *less* when the animal correctly detected the change than when it missed the change.

We found that MT neurons exhibit choice-related activity during both motion and depth detection tasks during the pre-cool condition (Figure 22). Individual neuron DPs had a median value of 0.54 during the motion task and 0.54 during the depth task, both of which were significantly greater than 0.5 ($p<0.05$, sign test). Such small values are typical and perhaps not surprising when one considers that we are measuring the activity of only a single neuron at a time, while it is likely that hundreds, if not thousands, of neurons are being used to solve these tasks. The finding that the population's DP is significantly greater than chance during both tasks suggests that MT neurons contribute to perceptual decisions involving both motion and depth stimuli. Importantly, individual neurons' DP values for the motion and depth tasks were not correlated, indicating the perceptual contributions could be determined independently for different modalities.

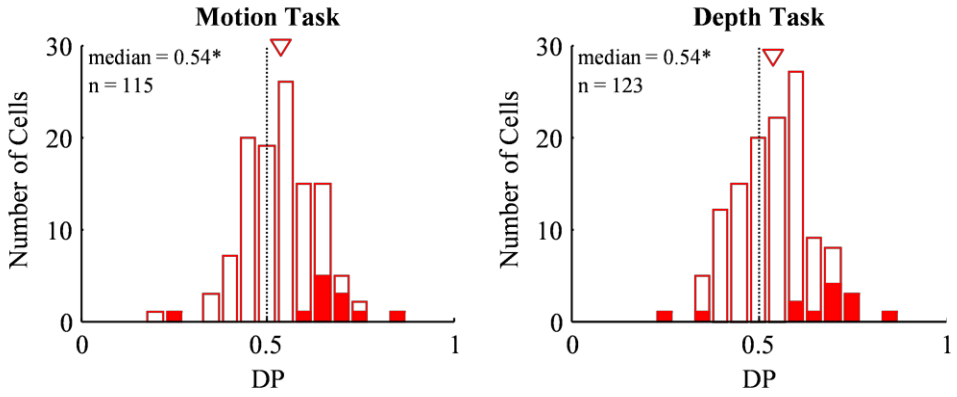

Figure 22: Population DP histograms
Detect probability during the pre-cool condition from all recorded single neurons for the motion (left) and depth (right) tasks. Filled in bars indicate individual neurons that had DPs significantly different from 0.5 as determined by a permutation test. Triangles indicate median values. * = $p<0.05$, sign test

Relationship between detect probability and neuronal sensitivity

We found that DP was significantly correlated with neurometric performance, suggesting that the most informative neurons had the strongest correlations with behavioral reports. For this analysis, neurometric performance was determined across all signal strengths tested in the pre-cool condition. The correlation was 0.25 for the motion task and 0.25 for the depth task, both of which were significant ($p<0.01$, Figure 23). Recent experiments show that this relationship does not exist at the beginning of training on a motion discrimination task, but develops over many months as animals' performance improves (Law and Gold, 2008). We set out to determine whether such changes can occur on the time scale of an hour by reversibly degrading neuronal sensitivity for both direction and disparity stimuli, but more so for disparity.

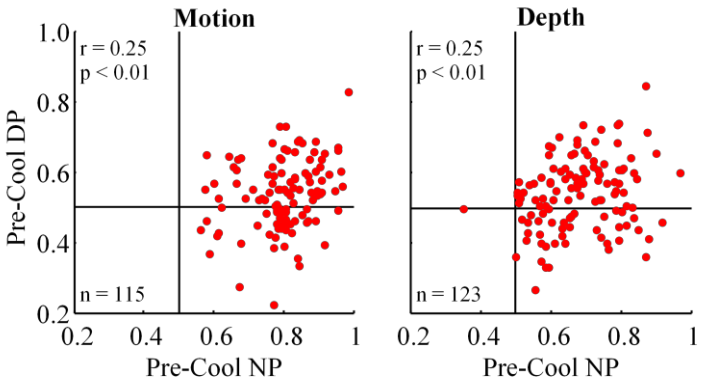

Figure 23: Relationship between neurometric sensitivity and detect probability
DP plotted against neurometric performance for all recoded neurons during the motion (left) and depth (right) tasks. r = Pearson's correlation coefficient; p = p value; n = number of neurons.

Effects of inactivation of V2 and V3 on choice-related activity in MT

To compare choice-related activity between the pre-cool and cool conditions we computed the DP time course aligned to the signal onset, for the entire population of recorded MT neurons (Figure 24). This allowed us to examine the dynamics of choice-related activity and provided sufficient statistical power to compare DP between conditions. In the pre-cool condition, DP

during the motion and depth tasks shared a similar time course. Before signal onset, DP is at the chance value of 0.5, indicating that there were no anticipatory biases in activity prior signal onset. DPs rose shortly after signal onset and peaked at similar times for the two tasks, beginning approximately 300 ms after signal onset. The comparable time courses indicate that MT firing rates were most predictive of the animals' responses at similar times throughout the trial. DP

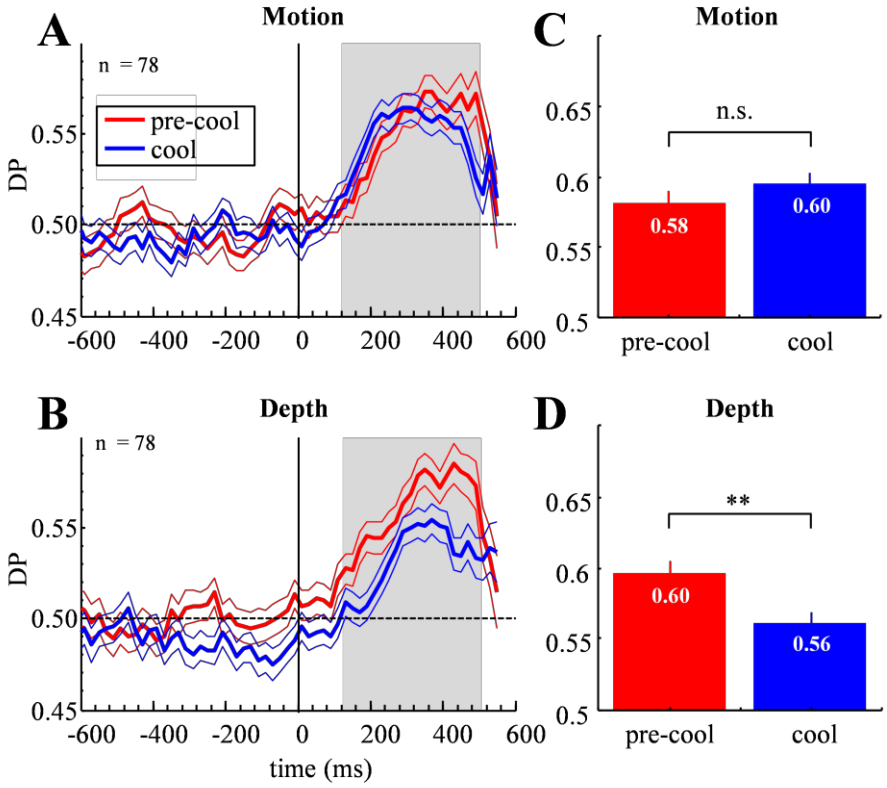

Figure 24: DP time course
(A-B) DP time course plotted aligned to the signal onset at time 0. Thick lines are DP value computed in a sliding window and thin lines are SEM obtained via a bootstrap procedure. Gray box indicates time window used to compute population DP value in C-D. n = number of neurons.
(C-D) Population DP computed by combining z-scored responses in a single time window (100-500 ms after signal onset) from all neurons with both pre-cool and cool data for both tasks. Error bars are SEM from bootstrap. The measured DP value is printed in each bar. The difference between DP changes during the depth task and motion task was significant ($p < 0.01$, data not shown). ** = $p < 0.01$; n.s = not significant.

during both tasks began to fall before the monkey's behavioral response, possibly reflecting that the movement constituting the behavioral response depended on later areas. These time courses are similar to those that have previously been observed in reaction-time or short duration motion and depth tasks (Cook and Maunsell, 2002b; Cohen and Newsome, 2009; Sasaki and Uka, 2009; Bosking and Maunsell, 2011). During inactivation we observed a selective reduction of DP during the depth task but not the motion task. This is evident throughout most of the DP time course following signal onset. The difference first became statistically significant approximately 175 ms following signal onset and remained until ~275 ms following signal onset. However, because statistical significance is sensitive to trial numbers and spike rate, we do not take these times to be the definitive start of DP differences. Interestingly, we found that during cooling, depth DP was significantly lower than 0.5 in the brief period immediately before the change (~400 ms before the change). This cannot be explained by non-selective changes like the reduction in firing rate or change in motivational state since those would tend to bring the DP value toward 0.5. Instead, a drop in DP below 0.5 indicates that the animal tended to correctly detect the signal when the firing rate before the change was slightly lower than average. This may reflect a decoding strategy where, to facilitate detection of the change, the neurons' responses are being compared in a sliding time window throughout the trial (*e.g*. Cook and Maunsell, 2002b). During trials where the firing rate is slightly lower than average before the change, the signal onset would lead to a larger modulation than average and it would be easier for the neuron—and the monkey—to detect the signal.

To summarize the effect of reversible inactivation on DP, we also pooled DP values across time in a fixed 400 ms window after signal onset (indicated by the gray area in Figure 24). A bootstrap procedure revealed that DP during the depth task decreased significantly between pre-

cool and cool conditions from 0.60 to 0.56 ($p<0.01$). The change in motion DP from 0.58 to 0.6 was not statistically significant ($p>0.05$). Importantly, depth DP was affected significantly more than motion DP, as measured by a separate bootstrap procedure that compared the distributions of re-sampled effect magnitudes ($p<0.01$, see Methods). Although a seemingly small change, the drop in depth DP during cooling represents a 40% decrease when measured relative to chance (0.5) and could have substantial implications for downstream decision mechanisms.

We were able to collect sufficient recovery data from 11 single neurons to measure DP during both tasks in all three conditions. This data could not be collected for most neurons because it required continuous isolation of a single neuron's electrical response for approximately three hours, a task that proved difficult. For these 11 neurons, we found that DP during the depth task returned to values similar to those in the pre-cool condition during the recovery period (Figure 25), demonstrating the changes in DP during inactivation are reversible on a similar timescale.

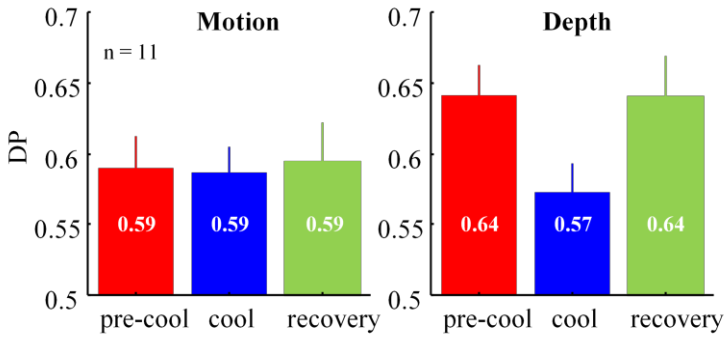

Figure 25: DP recovery
Population DP computed in the same way as in Figure 24C-D. Only the 11 neurons with recovery data contributed to the pre-cool and cool DP estimate. Same conventions as in Figure 24C-D.

Changes in DP and neurometric performance are not due to changes in firing rate

Measures that depend on the receiver operating characteristic (ROC) curve, such as DP and neurometric performance, are sensitive to both the mean and standard deviation of the

distributions being compared. This is evident by examining the relationship between the area under the ROC curve and the sensitivity measure, d':

$$aROC = \Phi\left(\frac{d'}{\sqrt{2}}\right)$$

where $aROC$ is the area under the ROC curve, Φ is the transformation by the cumulative normal distribution function, and d' is the sensitivity index, which depends on the mean and standard deviation in the following way:

$$d' = \frac{m_1 - m_2}{\sqrt{\sigma^2}}$$

where $m_1$and m_2 are the means of the two distributions being discriminated and σ is their standard deviation, which is assumed to be the same for both distributions (Macmillan and Creelman, 2004). For DP measures, m_1 and m_2 usually differ by only a few spikes (which is why $aROC$ is close to 0.5) so this is a fair assumption. Of course, the denominator reduces to the standard deviation (σ) but it is easier to think about this problem in terms of the variance, σ^2. Cortical neurons typically exhibit a constant relationship between their mean spike count and variance across all firing rates (Softky and Koch, 1993). This relationship can be quantified by the Fano factor, which is simply the ratio of spike count variance to mean spike count. As a result, as long as $m_1 \approx m_2 \approx \sigma^2$ in all conditions, we would have expected that, given a reduction in firing rate, d'should decrease simply because the mean rates $m_1$and m_2 decline faster than the square root of the variance (σ^2) in the denominator. Therefore we were surprised that DP did not decrease during both tasks solely due to the lower mean firing rate in MT caused by inactivation of V2 and V3. This prompted us to examine the relationship between the mean spike count and the variance during inactivation.

For each neuron, we computed the mean spike count and associated variance in response to each unique stimulus type—*i.e*. signal strength—separately for each condition. Since neuronal responses were collected at multiple signal strengths for each task, each neuron contributed 2-14 data points. A scatter plot of the calculated mean spike counts and associated variance is shown in Figure 26. The slope of the best-fit line gives the Fano factor for the entire population of neurons. The Fano factor declines from a pre-cool value of 1.19 to 0.76 during inactivation. This decrease was similar when the data were analyzed separately for each task, across different signal strengths (including the noise epoch immediately before signal onset), and in response to the 100%-signal stimuli used for quantitative tuning. This decrease persisted when we matched mean spike counts and numbers of data points between conditions. We also computed the Fano factor for each data point in Figure 26A individually by computing the variance to mean ratio (rather than the fit to all the data) and found that there is no significant correlation between mean spike count and Fano factor in any condition or task. Similarly, we found that the median Fano factor computed in this way was significantly lower during cooling, even when restricted to points with lower mean spike counts (Figure 26C). Thus, we observed a decrease in Fano factor even when we accounted for the difference in spike rate. This finding has several important implications that will be elaborated upon in the general Discussion. In the context of our other findings, our estimation of the Fano factor allowed us to generate expected DP values given the reduction in both firing rate and variance.

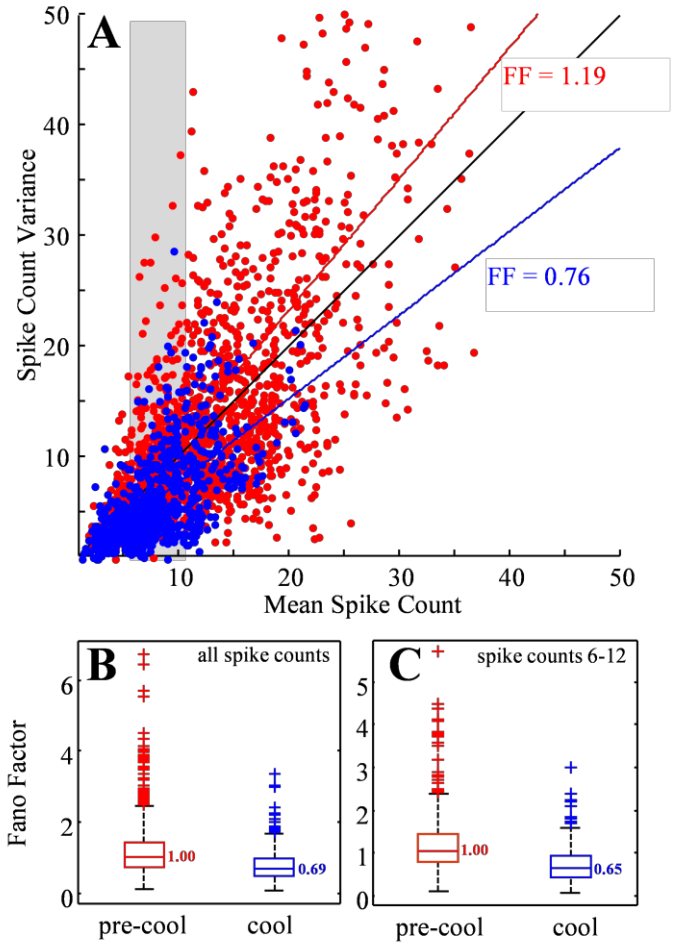

Figure 26: Fano factor
(A) Scatter plot of mean spike count vs. spike count variance. Each point is the mean spike count and variance measured at one signal strength during one task. Data from each neuron was only included if the neuron contributed to both pre-cool and cool data sets. One cell contributes 2-14 points, one for each signal strength in each task. The gray region indicates data used for comparison in (C). FF is the Fano factor, which is the slope the best fit line to each data set (pre-cool and cool). The black diagonal line is the unity line, which corresponds to the Poisson prediction of FF = 1.
(B) Box plot of the Fano factor computed for each point in (A) by dividing the variance by the mean spike count. The central mark is the median and the edges of the box are the 25^{th} and 75^{th} percentiles. Whiskers include approximately 95% of the distribution and crosses are remaining points. The median Fano factor is shown adjacent to each box plot. The distributions are significantly different from each other ($p<<0.01$, rank sum test).
(C) Same as (B) but only showing Fano factor for points where the mean spike count was between 6 and 12 (gray area in (A). For this subset, the number of points in each distribution is approximately equal (~450). These distributions are also significantly different ($p<0.01$, rank sum test).

We estimated the expected DP in the cool condition by adjusting the pre-cool DP (*i.e.* its underlying *d'*, see Methods) by the measured reduction in firing rate and variance (Figure 27). We also show the predicted DP based on the firing rate reduction alone. As discussed above, the predicted DP when we only accounted for the change in mean rate (dashed light blue line) was lower than the DP we observed during cooling during the motion task and was similar to the measured DP during the depth task. However, when we accounted for the changes in both mean and variance we found that the expected DP is very similar to the pre-cool value on both tasks. Thus the reduced variance effectively counteract the reduced firing rate we observed. Therefore, the changes we see in depth DP during cooling are larger than would be expected given the reduction in firing rate alone. Since this decline in variability was constant across all stimulus strengths and stimulus configurations, all other ROC-based measures such as neurometric performance should also not be affected by the change in mean rate.

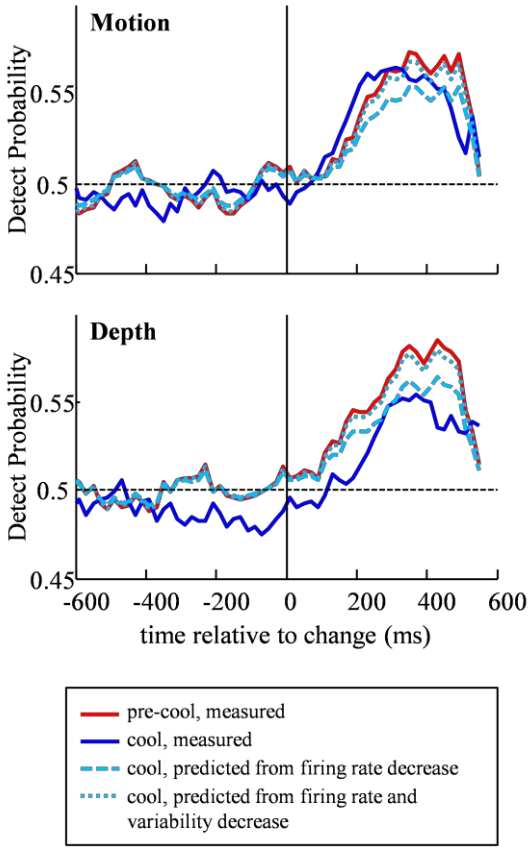

Figure 27: DP prediction
Predicted DP time courses for the motion (top) and depth (tasks). Predictions were obtained by adjusting the measured d' in the pre-cool condition by the observed reduction in firing rate (dashed light blue line) and by the combined reduction in firing rate and variance (dotted light blue line). The measured DP in the cool condition is also shown (solid blue line).

Neuronal population dynamics

Although DP declines during the depth task during inactivation, it continues to be significantly greater than chance level in both tasks. This suggests that the MT population continues to be involved in depth decisions in addition to motion decisions, albeit at reduced levels. However, the changes in firing rate during both tasks that we observed during inactivation of V2 and V3 present a challenge to downstream decision circuitry. Most models of MT read-out posit an integrate-to-bound mechanism where information from relevant MT neurons is accumulated until a fixed threshold is reached, which in turn triggers a behavioral response (Cook and Maunsell, 2002b; Roitman and Shadlen, 2002).

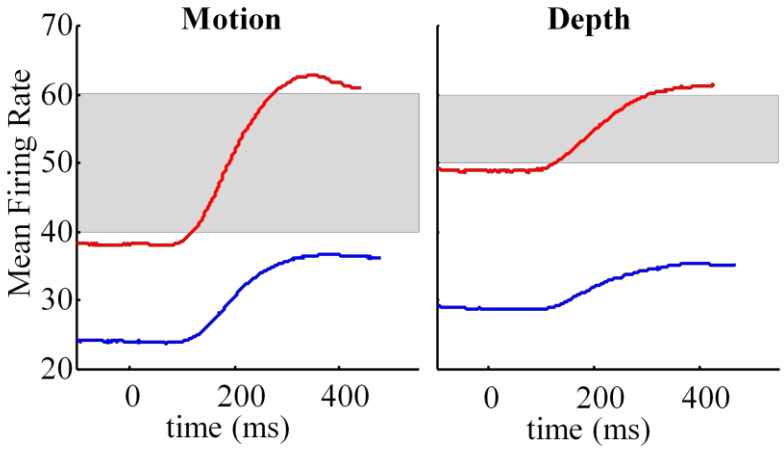

Figure 28 Average firing rates in the recorded MT population For each neuron, responses to all signal strengths were filtered with exponential filter (τ = 100 ms) and averaged across all neurons. Responses are aligned to signal onset at t = 0. Gray area indicates possible threshold values that could be used to detect signal onset in the pre-cool condition. No threshold established in the pre-cool condition and expressed as an absolute firing rate can be used to perform either task in the cool condition.

If this threshold were expressed in terms of absolute firing rate, the population response in our experiments would rarely reach this threshold during inactivation since few neurons ever fire enough spikes to approach even the responses to pre-signal onset stimuli in the pre-cool condition. This is evident in the response averaged across all of our recorded neurons, which is shown, aligned to the signal onset, in Figure 28. For example, if increases in firing rate in the population were used to detect signal onset via a threshold crossing, any threshold established

during the motion task in the pre-cool condition would be somewhere between 40 and 65 spikes per second (indicated by the gray area in Figure 28); clearly, this threshold would never lead to detections during the motion task during cooling. The same is true for the depth task. However, the animals continue to be able to perform both tasks, at least partially from the neuronal signals in MT, suggesting the need for some flexibility in how the population response informs behavioral decisions. One simple way to allow for such flexibility is to implement a *relative* threshold, rather than a fixed one, across different conditions; *e.g.* rather than make the behavioral response when the neuronal population response reaches 40 spikes per second, wait for it to reach a 40% increase, relative to some baseline rate. This could provide a mechanism for the downstream read-out mechanism to detect the signal in our signal detection tasks under two very different spike rate regimes (pre-cooling and cooling) and, furthermore, to be responsive during the variety of spike rate regimes encountered during different tasks (*e.g.* compare mean pre-cool motion rates to pre-cool depth task rates). We should note that few experimenters, if any, have argued that this threshold is expressed as an absolute firing rate; however, few have had opportunities to explore the possibility of a relative threshold explicitly.

To determine whether such a relative threshold can be used to predict behavioral responses from responses of the population of MT neurons, we implemented a model of MT read-out that has previously been used with great success to account for the observed variability in reaction times during a motion detection task (Cook and Maunsell, 2002b). This model assumes two stages: a perceptual processing stage and a motor preparation stage that leads to the behavioral output, in our case an eye movement to the stimulus. A schematic of this model is shown in Figure 29C. The perceptual processing stage includes filtering of the MT population responses by a leaky integrator to simulate the integration of MT population responses in a

down-stream area. These responses are then passed through a threshold detector and the time at which responses cross the threshold is used to predict reaction time. The additional motor preparation time is added to account for the post-decision processing needed to generate the operant response.

We implemented this model for our population of MT neurons by sorting responses by reaction time separately for each task and condition. We sorted responses from each neuron into 20 bins based on reaction time, such that each neuron contributed an equal number of trials to each bin. Sorted responses were then averaged across neurons and filtered with an exponential filter to simulate the responses of a leaky integrator. To explore the possibility of a relative threshold, we simply normalized the population responses to the mean firing rate in the epoch preceding signal onset. Since every bin's response was simply divided by the same value, the end result was just a change in y-axis units; there was no change in the relative relationship between the responses. As a result, rather than being expressed as an absolute firing rate, this threshold would be expressed as a constant multiple of the pre-signal onset response in the pre-cool and cool conditions for each task independently.

We found that responses' rate of rise increased with shorter reaction times for both the motion and depth task under both cool and pre-cool conditions (Figure 29). This suggests that a threshold model might be sufficient to predict reaction times during both tasks and therefore that MT may contribute to motion and depth processing in a similar manner. Although the absolute firing rates during each task were very different between conditions, they reach a similar peak value in the cool condition when normalized, suggesting a relative threshold could be used.

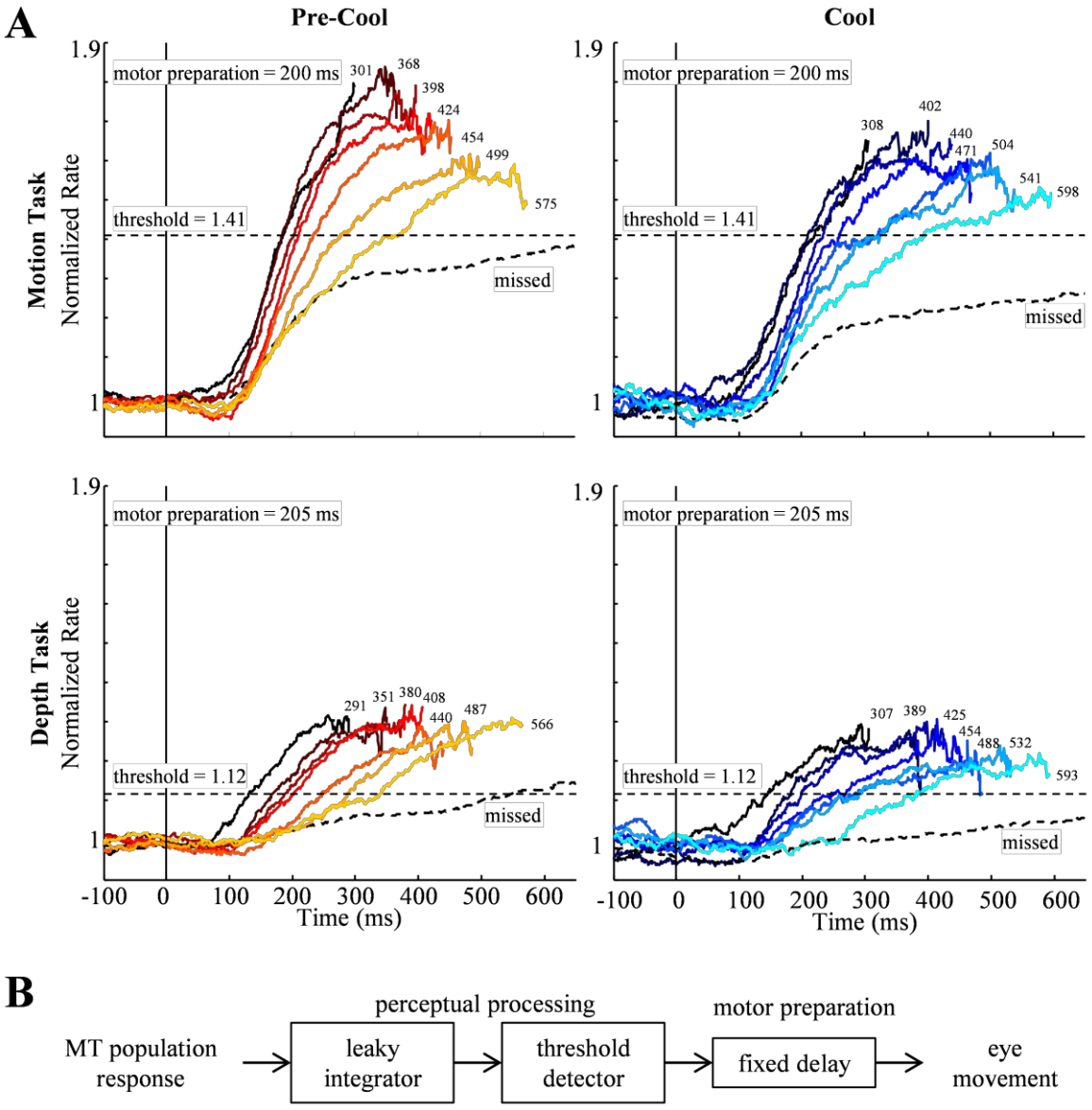

Figure 29: Threshold model
(A) Individual neuron responses during each task and condition were filtered by a leaky integrator, binned by the animals' reaction time, and averaged across neurons. Responses were normalized to the mean response across all bins the 400 ms period prior to signal onset. A total of 20 bins were used but only every third (i.e. bins 1, 3, 6, 9, 12, 15, and 18) is shown, for clarity. Each bin's median reaction time is shown near the end of every trace. Thresholds and motor preparation times were fit simultaneously to data from both conditions from each task. The resultant values are indicated in each plot. Also shown are the responses during missed trials, which were not used in model optimization. Note that although the missed responses cross threshold during the depth task in the pre-cool condition, the predicted RT given the motor preparation time would exceed the allowed RT window (max 650 ms).
(B) Schematic of the threshold model (adapted from Cook and Maunsell 2012b)

To determine whether a single threshold could account for measured reaction times in all conditions, we fit a single threshold and motor preparation time to each task under both conditions. The threshold and motor preparation time were optimized to best predict the measured reaction times for each response bin. The resultant threshold is indicated by the dashed lines in Figure 29A: 41% for the motion task and 12% for the depth task. Optimized motor preparation times were 200 ms for the motion task and 205 ms on the depth task. The similarity in motor preparation times suggests that MT may be similarly positioned from the motor processing stage in both decision circuits. The motor preparation time during the motion task is slightly faster than that of 264 ms obtained by Cook and Maunsell (2002b), likely because our animals were making an eye movement response, which tends to be faster than the lever release used in their study.

We found that this single threshold and motor preparation time provide a good prediction of the observed reaction times for each task in both conditions (Figure 30). The model could explain at least 82% of the variance in reaction times, and as much as 98% in the depth task during the pre-cool condition. Allowing either parameter to vary between conditions did not improve the proportion of explained variance by more than 2%. Allowing both parameters to be free in each condition also did not improve the proportion of explained variance by more than 2%. As a result, it seems that a constant relative threshold can be used to account for the variability in reaction times, providing a mechanism by which the decision circuitry can be robust to changes in mean firing rate.

Notably, we did not see evidence of a speed-accuracy tradeoff in the population data. Since reaction times during inactivation were longer during both tasks for both animals, a lower threshold could have allowed for faster reaction times and a faster rate of reward (e.g. Gold &

Shadlen, 2002). This would have been manifest in the data by an over-prediction of reaction time in the cool condition and/or an under-prediction in the pre-cool condition, since the data were fit simultaneously. A lack of consistent bias in both conditions indicates that the internal threshold was likely similar under the two conditions. However, averaging an arbitrary number of trials and neurons, as we did, obscures two important aspects of the data: 1) the possibility of day-to-day variability of the threshold and 2) the level of noise that might be present for any given read-out neuron's inputs. It is likely that our averaging procedure smoothed out any day-to-day fluctuations in this threshold between or within sessions and obscured more minute dynamics. Alternatively, the level of threshold we observed for each task may be necessary to distinguish responses to signal among noise from a pool of neurons during a single trial. For example, at the other extreme, when this model is applied to individual neurons, they are very

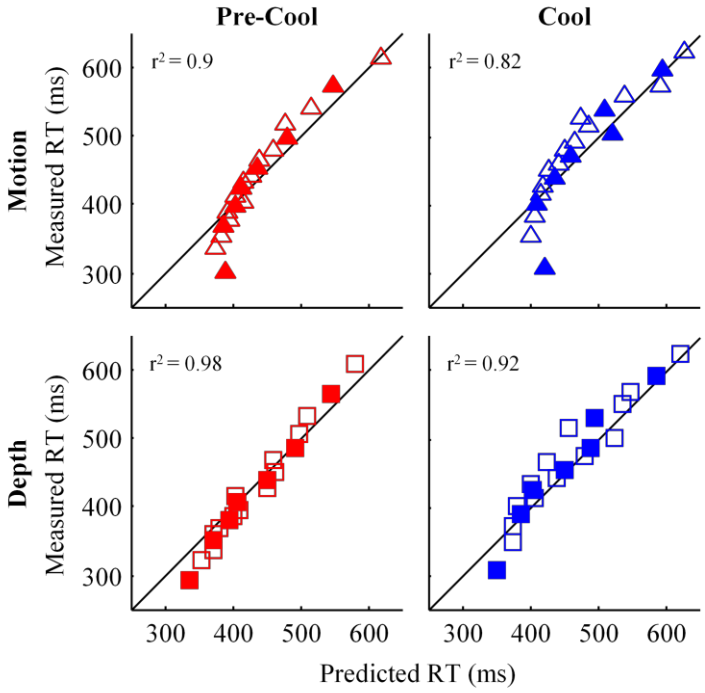

Figure 30: Predicted reaction times
Optimized threshold model parameters were used to determine predicted reaction times from the MT population response. The predicted reaction time was determined from the first time each binned population response crosses the threshold plus the motor preparation time. r^2 is the proportion of variance explained by the model. Filled symbols correspond to the traces shown in Figure 29.

poor detectors of signal during both motion and depth based tasks because of the large response fluctuations (*i.e*. noise) in the response to the visual stimulus during a single trial (data not shown; also see Cook & Maunsell, 2002b). If the integrator neuron was receiving only a few noisy inputs during any given trial, a higher threshold would allow the animal to avoid making false alarms in response to this noise in the pre-signal onset epoch. Nonetheless, the data indicates that, on average, a relative threshold can be used for each task under a variety conditions.

Although this threshold was the same across conditions for each task, it was different between tasks. Looking at the data, it is clear why this was the case: the neuronal modulation during depth task was much smaller than the modulation during the motion task. This flexibility between the two decision circuits indicates that, not only can the threshold be robust to different firing rates within a task, but it can be robust to firing rate differences between tasks.

We should point out that when the data was analyzed separately for each monkey, the model did not do a good job predicting monkey Q's reaction times during the motion task in the cool condition (Figure 31A, gray panel). The proportion of explained variance was only 54%, substantially lower than in all other cases: the minimum explained variance for this monkey in the other conditions was 79% and the minimum for monkey S in all conditions was 90%. This was mostly because the rate of rise of most MT responses did not differ when sorted by reaction time in this condition, which is evident in the vertical clustering of the predicted reaction times in the gray panel. That is, for most reaction time bins MT responses increased at a similar rate and were therefore not predictive of reaction time. Since DP values remained high for this animal during the motion task in this condition, MT neurons likely continued to be involved in the decision but this data suggests that there was a change in how MT responses were used to make

the decision. Importantly, this animal was significantly impaired in his performance during the motion task during cooling, as discussed in Chapter 1. It is therefore possible that his impaired performance was due to a disruption in how MT responses were used during the motion task in the cool condition.

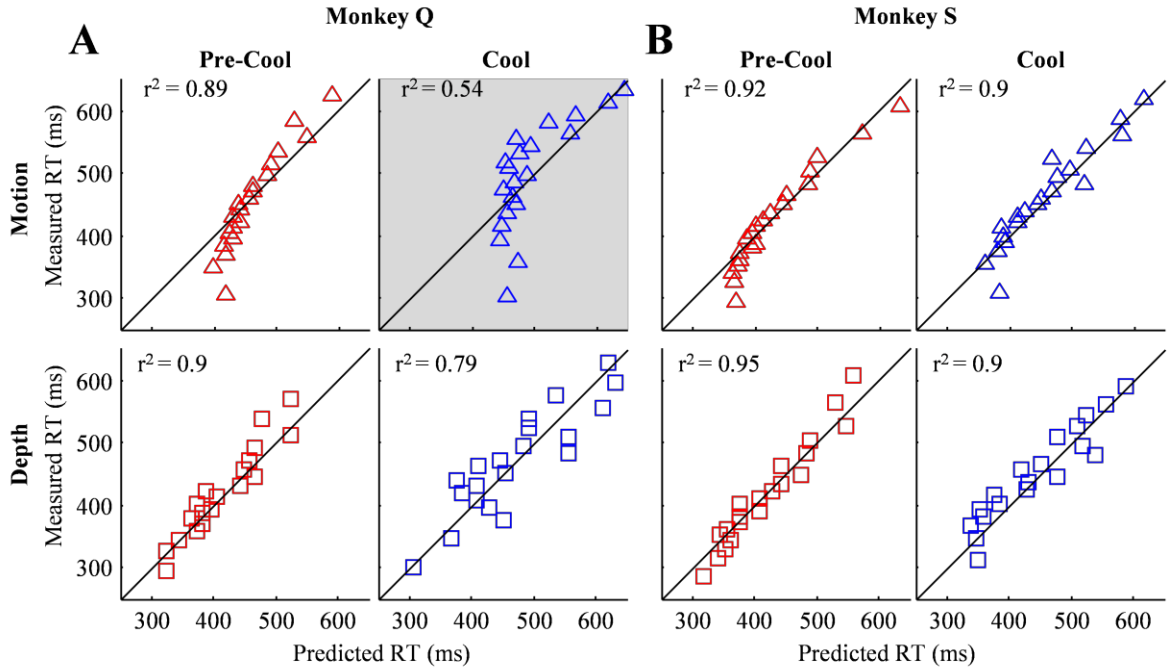

Figure 31: Predicted reaction times, shown separately for each monkey
The threshold and motor preparation time were fit simultaneously for both pre-cool and cool conditions for each task, but separately for each monkey. Same conventions as in Figure 30
(A) Comparison of predicted and measured reaction times for monkey Q.
(B) Comparison of predicted and measured reaction times for monkey S.

Summary

We found that neuronal sensitivity in MT was degraded during both motion and depth signal detection tasks during reversible inactivation of V2 and V3, but significantly more so during the depth task. Furthermore, we found that detect probability decreased selectively during the depth task and not the motion task, possibly reflecting the disproportionate reduction in neuronal sensitivity during the depth task. Taken together, these data reflect re-structuring in the

MT-related decision circuitry during the depth task but not the motion task. This change occurred on the timescale of the approximately one-hour daily cooling sessions and was reversible on a similar timescale. Furthermore, we found that an integrate-to-bound model with a fixed relative threshold can account for the observed variability in reaction time under most conditions. Since the absolute firing rates under these conditions vary drastically, this finding reflects the flexibility of the decision bound.

Discussion

In the experiments described here, we used reversible inactivation to inactivate V2 and V3, visual cortical areas along one of the two major cortical pathways to MT—the indirect pathway. Previous work indicates that information passing through these areas is necessary to recover binocular disparity information in MT (Ponce et al., 2008). We found that inactivation of V2 and V3 impaired behavioral performance during depth signal detection, indicating that these areas are also involved in perception of depth. One of the two animals was also similarly impaired during a motion signal detection task. Furthermore, we found that the activity of MT neurons was correlated with behavioral reports during both depth- and motion-detection tasks, indicating that they are involved in the perceptual decision process. When we disproportionately impaired MT *neurons'* sensitivity for binocular disparity, we found that these correlations —*i.e.* detect probability—declined during the depth task, suggesting that these neurons became less involved in the decision. This is notable for the short timescale over which it occurred—the hour-long inactivation sessions—and for its specificity to decisions on the depth task but not motion task.

Behavioral effects of inactivation of V2 and V3

We found that inactivation of V2 and V3 led to impairments in the ability of MT neurons to discriminate signal from noise in both motion and binocular disparity, but significantly more so for binocular disparity. Given MT's involvement in these tasks, it is therefore not surprising that there was some degree of behavioral impairment during the motion task in both animals. However, if behavioral performance during these tasks was based solely on MT processing, we would expect a bigger behavioral impairment during the depth task than the motion task. This is indeed what we observed in one animal, monkey S, but not monkey Q, who was about equally

impaired during motion- and depth-based detection tasks. Monkey Q was also about similarly impaired during fine change motion and depth tasks. There are several possible reasons for the non-specific impairment in monkey Q: first, there may have been non-specific changes in the animal's overall motivation or alertness; second, he may have been less robust to changes in stimulus appearance that may have occurred due to changes in processing in other visual areas (*e.g.* V4); third, the difference may due to real underlying impairments in both motion and depth processing in this animal, perhaps in visual areas other than MT.

As discussed in Chapter 1, there are multiple reasons to believe that it is unlikely that monkey Q was simply unmotivated during inactivation: his performance remained unaffected in the ipsilateral visual field and we observed no changes in the rate of trial initiation. Furthermore, his high success rate during the easy trials of both tasks indicates that it is unlikely that the animal simply could not see. Instead, his deficits should be considered in the broader context of the effects of V2 and V3 inactivation. V2 and V3 neurons are themselves selective for orientation, color, motion, and binocular disparity (DeYoe and Essen, 1985; Hubel and Livingstone, 1985; Peterhans and von der Heydt, 1993; Levitt et al., 1994; Gegenfurtner et al., 1996). Furthermore, V2 and V3 provide a major sources of input to V4, the major conduit to the ventral processing stream (reviewed in Maunsell and Newsome, 1987 and Van Essen and Gallant, 1994). Therefore, it is likely that cooling also affected processing in V4 and downstream areas. Given the response properties of V4 neurons (reviewed in Roe et al., 2012) and the ventral stream's role in object recognition, inactivation may have led to changes in processing of features such as color and form. The resultant changes in the appearance of the stimulus may have made both tasks equally difficult for monkey Q. Monkey S may have not been affected by these changes if the magnitude of these effects varied between the animals or if monkey S was

more robust to these changes in appearance. Alternatively, it is possible that motion processing in areas other than MT was also affected in monkey Q, leading to the similar behavioral impairment during the two tasks. For example, humans with damage to V2 and possibly V3 exhibit deficits in motion processing similar to the kind we measured here (Vaina et al., 2000). However, this damage may have also extended to fibers of passage of other areas. Furthermore, transcranial magnetic stimulation (TMS) of human V2 has been shown to lead to disruptions of motion perception (Cowey et al., 2006); although this may be due to indirect disruption of activity in connected areas such as MT (Ilmoniemi et al., 1997). In either case, this does not account for the lack of substantial impairment during the motion task in monkey S. Instead, results from our attempts to model the read out of the MT population response (Chapter 2) suggest that MT responses during the motion task were used differently during inactivation in this animal: unlike in all other conditions, MT responses were not good predictors of monkey Q's reaction time. This was true even though the activity of MT neurons continued to be correlated with behavioral reports, indicating that these neurons continued to be involved in the task. It therefore seems to have been a change in how MT responses were used to inform behavior—whether because of a change in monkey Q's strategy or a change in how MT responses were pooled. Such changes may have led to the decrement in this animal's performance during the motion task during inactivation of V2 and V3. Ultimately, since we do not have access to the effects of inactivation on ventral stream processing or the underlying MT population read out mechanisms, we cannot distinguish between the relative contributions of these effects to monkey Q's behavioral impairment during the motion task. We therefore conclude that the results reflect some combination of differences in cooling effects between the

two animals such that additional visual processing such as color, form, or motion (in MT or other areas) were more affected in monkey Q than in monkey S.

Our finding that both animals are impaired during the depth detection task is similar to a previous study in which removal of the foveal representation of V2 led to increases in stereoacuity thresholds (Cowey and Wilkinson, 1991). However, subjects' eye movements were not monitored and it was not clear that the deficits were due to lesions in V2 alone. Indeed, few studies have monitored eye movements and none that we are aware of monitored vergence (reviewed in Cumming and DeAngelis, 2001). In one study where monkeys performed a depth discrimination task, lesions in the foveal V2 representation led to no behavioral impairment (Cowey and Porter, 1979). However, eye movements were not monitored and it is possible monkeys used their peripheral vision to perform the task. In a subsequent study, Cowey and Wilkinson (1991) found up to 10-fold increases in behavioral thresholds during the same task (although fixation was not enforced in this study either, as mentioned above). Our study therefore serves as the first attempt to monitor the effects of V2 and V3 inactivation on behavioral performance during a depth task while also monitoring eye position.

Changes in neuronal variability

We were surprised to find that neuronal variability in MT—as measured by the Fano factor—declines during inactivation of V2 and V3. Fano factor is typically considered to be a property of the local cortical circuit and several groups have previously reported a decrease in Fano factor in response to changes in visual stimulation or behavioral state (*e.g.* attention) (Churchland et al., 2006, 2010; Cohen and Maunsell, 2009; Mitchell et al., 2009). However, in all of these cases the Fano factor rarely, if ever, declined below a value of 1. The earlier observation that Fano factor tends to be near 1 for cortical neurons, regardless of firing rate,

contributed to the characterization of spike generation as a Poisson-like process (Softky and Koch, 1993). However, the Poisson-like variability of cortical neurons is difficult to explain with a simple integrate-and-fire model with only excitatory inputs, one of the more basic approximations for cortical neurons. Any such model that averages inputs that are themselves random should produce increasingly regular firing patterns (*i.e*. lower variability) as input—and the output firing rate—increases (Softky and Koch, 1993). To account for the observed variability in visual cortex, Shadlen and Newsome (1994) proposed a model that posits balanced excitatory and inhibitory input to each model cortical neuron, a property that has recently been corroborated in vivo (Okun and Lampl, 2008). This balanced input predicts spike rate variability that is as high as what is observed *in vivo* and may account for Poisson-like properties of cortical neurons. It is therefore possible that the decrease in variability that we observed is due to changes in this excitatory and inhibitory balance. In collaboration with Camille Gomez and Gabriel Kreiman, we are currently investigating whether our observed decrease in Fano factor can be explained by a change in the excitatory/inhibitory balance with the use of a relatively simple integrate-and-fire model neuron whose number of excitatory and inhibitory inputs can be manipulated. We find that certain changes in the excitatory/inhibitory balance can lead to a decline in Fano factor and mean rate, similar to what we observed experimentally. However, these simulations are still in the preliminary stage and require further exploration before we can draw any conclusions.

Dynamics of cortical decision circuitry

We found that inactivation of V2 and V3 led to a larger degradation of MT neuron's performance during the depth signal detection task than the motion signal detection task. These changes were accompanied by a selective reduction in choice-related activity—as measured by

detect probability (DP)—during the depth task but not the motion task. This finding corroborates the main hypothesis for our experiments: that cortical decision circuitry can adapt on a short timescale to changes in the "informativeness" in the underlying sensory pool of neurons. But what does "adapt" mean in this case?

As noted in the Introduction, because of correlated variability between groups of MT neurons, DP likely reflects the contribution of a local group of neurons rather than any individual neuron. Therefore, a reduction in DP likely reflects a decrease in weighting of the neurons in the local MT pool. This can happen as a result of dilution of the decision across a larger population of neurons within MT or in other areas. For example, since the effects of inactivation on neurometric performance were heterogeneous and some neurons maintained high sensitivity, pooling across a larger number of MT neurons may have increased the sensitivity of the population as a whole. Alternatively, binocular-disparity sensitive neurons in other visual areas may have been recruited instead (*e.g*. Chowdhury and DeAngelis, 2008).

It has also recently been proposed that decision-related activity partially reflects non-causal top-down effects such as attention (Nienborg and Cumming, 2009). Using a fixed-duration (*i.e*. non-reaction time) discrimination task, Nienborg and Cumming found that choice-related activity peaked at a later time relative to the when the stimulus contributed most to the decision, indicating a non-causal component to the choice-related response. However, it is not clear how much such top-down signals such as those proposed by Nienborg and Cumming contribute to DP for reaction-time detections tasks with more unpredictable timing, such as the ones we used. For example, Smith *et al*. (2011) trained animals to detect a very brief (50ms) motion pulse and showed that peak DP was coincident with the availability of sensory information. Furthermore, the DP reached similar peak values to those reported in longer duration studies, indicating that

any post-decision contribution may be small. It is therefore unlikely that the changes we observe are entirely due to changes in top-down processing.

Finally, changes in the inter-neuronal correlation structure in MT may have also led to changes in DP. However, any global changes in correlation structure should have similarly affected motion DP, which we did not observe. Nevertheless, since we did not record the activity of multiple neurons simultaneously, we do not have access to the inter-neuronal correlation structure and our data cannot directly address this hypothesis. The simplest conclusion we can draw is that the reduced DP during the depth task reflects reduced weighting of the local pool of MT neurons in the decision.

The selective change in DP raises another interesting question: since neurometric performance was degraded somewhat during the motion task as well as during the depth task, albeit significantly less so, why didn't we observe changes to DP during the motion task? It is possible that the magnitude of the impairment was simply not sufficient to trigger changes in the decision circuitry. Alternatively, it may be that MT neurons are the only neurons ideally suited for the motion detection task we employed. Unlike neurons in any other visual cortical area, a large majority of neurons in MT are predominately tuned for direction of motion irrespective of shape or color (Albright, 1992; Seidemann et al., 1999). Furthermore, permanent and reversible lesions in MT lead to large deficits in motion perception and discrimination (Newsome and Pare, 1988; Chowdhury and DeAngelis, 2008). In contrast, previous work indicates that training history can change whether or not MT neurons are correlated with decisions during a depth task, suggesting that other areas can be recruited during this task (Chowdhury and DeAngelis, 2008). Therefore, changes in decision circuits may only occur when there are other available neurons to recruit for the task at hand.

Several other laboratories have reported short timescale changes in choice-related activity in individual MT neurons (Purushothaman and Bradley, 2005; Cohen and Newsome, 2009; Bosking and Maunsell, 2011). In all of them, choice-related activity declined (within a single session) when the stimulus properties were chosen to differ from the preferences of the neuron—*e.g.* if the direction of the stimulus was sufficiently different from preferred direction of the neuron. Thus, choice-related activity was largest for a neuron when it most informative for the upcoming trial. In these experiments the monkeys were cued to the properties of the upcoming stimulus, allowing for fast anticipatory mechanisms such as feature attention to "select" the most relevant neurons (Cohen and Newsome, 2008). Indeed, recent evidence from our laboratory indicates that feature attention effects are largest for the most strongly tuned neurons (Ruff and Born, in preparation). Although a feature attention-like mechanism can recruit neurons quickly, the relationship between the magnitude of feature attention effects and the neuronal informativeness likely relies on circuitry established throughout months of training. Our manipulation of neuronal sensitivity would have disrupted any such pre-existing relationship since neurons there were previously useful became less so during inactivation. Therefore, the changes we observe in DP reflect the ability of the circuit to adapt to changing sensitivity on a short timescale. Whether this adaptation is linked to changes in feature-attention mechanisms presents an interesting direction for future experiments.

Dynamics of the population response

Despite the changes in DP that we observed, neurons in MT continued to be correlated with decisions during both motion and depth tasks during inactivation of V2 and V3. To determine whether a single scheme could be used to inform behavioral decisions for both tasks under both pre-cool and cool conditions we implemented a simple population read-out model.

The model consists of two major stages: a perceptual processing stage where sensory evidence is accumulated by a later area, such as sensorimotor area LIP, until responses reach a decision bound and a motor preparation stage where the eye movement is generated (Cook and Maunsell, 2002b). A leaky integrator is used to model that accumulation of sensory responses. This serves as a sort of sliding window over neuronal responses in time and helps account for the temporal uncertainly in when to begin sensory integration. A fixed motor preparation delay is consistent with studies of eye movement generation that have suggested that most noise in the behavioral output can be attributed to variability in the sensory estimate—that is, the visual processing stage rather than the motor preparation stage (Osborne et al., 2005).

First, we found that this model accounted for a large proportion in the variability in our animals' reaction times during both motion and depth tasks, indicating that MT population responses were used in a similar way. Furthermore, the motor preparation time was similar between the two tasks, suggesting that they may require a similar number of subsequent processing steps. To our knowledge, this is the first attempt to determine how MT population responses may contribute to decisions during a depth detection task.

Moreover, we found that a single threshold could account for variability in the each tasks' reaction times in both pre-cool and cool conditions if the population responses were first normalized. In other words, the threshold can be expressed in terms of gain over the baseline response, which would provide a way for read-out circuitry to be robust to different firing rates. Remarkably, this flexibility allows neurons to contribute to the motion and depth tasks even when firing rates during a particular task are drastically reduced, which does not happen under normal physiological conditions. Although the mechanism for this process remains to be explored, one way this relative threshold could be implemented is by normalization of the

activity of neurons in the read-out pool. Divisive normalization—or gain control—in cortical circuits is a mechanism by which the response of a neuron is divided by the responses of the local pool of neurons (reviewed in Carandini and Heeger, 2011). This mechanism could effectively perform the same normalization on neuronal responses that we did and allow read-out neurons to respond to relative changes over baseline.

It is important to note that this model is likely an oversimplification of the underlying mechanisms used to decode the population response. In particular, the stimulus parameters were always tailored to the preferences of each neuron so we could only include responses from neurons tuned to each stimulus. However, previous work indicates that responses from neurons with opposite tuning preferences can be anti-correlated with decisions during a detection task, suggesting that their activity is used in comparison to that of other neurons (Bosking and Maunsell, 2011). Furthermore, we averaged MT responses over an arbitrary number of neurons over many days, likely smoothing out realistic noise levels and any short-term fluctuations in the underlying threshold. Nonetheless, the model provides a surprisingly good account of the variability in reaction times observed during both tasks during both pre-cool and cool conditions.

Conclusion

In summary, we found evidence for selective restructuring of decision circuitry during a depth task and not motion task following degradation of depth sensory information more than motion information. This reflects fast-timescale adaptation to reduced neuronal sensitivity and might mirror changes that occur when we rapidly learn new tasks.

Bibliography

Adams, D.L., and Zeki, S. (2001). Functional Organization of Macaque V3 for Stereoscopic Depth. Journal of Neurophysiology *86*, 2195–2203.

Albright, T.D. (1992). Form-Cue Invariant Motion Processing in Primate Visual Cortex. Science *255*.

Albright, T.D., Desimone, R., and Gross, C.G. (1984). Columnar organization of directionally selective cells in visual area MT of the macaque. Journal of Neurophysiology *51*, 16–31.

Born, R.T., and Bradley, D.C. (2005). Structure and function of visual area MT. Annual Review of Neuroscience *28*, 157–189.

Bosking, W.H., and Maunsell, J.H.R. (2011). Effects of Stimulus Direction on the Correlation between Behavior and Single Units in Area MT during a Motion Detection Task. Journal of Neuroscience *31*, 8230–8238.

Britten, K.H., Newsome, W.T., Shadlen, M.N., Celebrini, S., and Movshon, J.A. (1996). A relationship between behavioral choice and the visual responses of neurons in macaque MT. Visual Neuroscience *13*, 87–100.

Carandini, M., and Heeger, D. (2011). Normalization as a canonical neural computation. Nature Reviews Neuroscience.

Chowdhury, S.A., and DeAngelis, G.C. (2008). Fine discrimination training alters the causal contribution of macaque area MT to depth perception. Neuron *60*, 367–377.

Churchland, M.M., Priebe, N.J., and Lisberger, S.G. (2005). Comparison of the spatial limits on direction selectivity in visual areas MT and V1. Journal of Neurophysiology *93*, 1235–1245.

Churchland, M.M., Yu, B.M., Cunningham, J.P., Sugrue, L.P., Cohen, M.R., Corrado, G.S., Newsome, W.T., Clark, A.M., Hosseini, P., Scott, B.B., et al. (2010). Stimulus onset quenches neural variability: a widespread cortical phenomenon. Nature Neuroscience *13*, 369–378.

Churchland, M.M., Yu, B.M., Ryu, S.I., Santhanam, G., and Shenoy, K.V. (2006). Neural variability in premotor cortex provides a signature of motor preparation. The Journal of Neuroscience *26*, 3697–3712.

Cohen, M.R., and Kohn, A. (2011). Measuring and interpreting neuronal correlations. Nature Neuroscience *14*, 811–819.

Cohen, M.R., and Maunsell, J.H.R. (2009). Attention improves performance primarily by reducing interneuronal correlations. Nature Neuroscience *12*, 1594–1600.

Cohen, M.R., and Newsome, W.T. (2008). Context-dependent changes in functional circuitry in visual area MT. Neuron *60*, 162–173.

Cohen, M.R., and Newsome, W.T. (2009). Estimates of the contribution of single neurons to perception depend on timescale and noise correlation. The Journal of Neuroscience *29*, 6635–6648.

Cook, E.P., and Maunsell, J.H.R. (2002a). Attentional modulation of behavioral performance and neuronal responses in middle temporal and ventral intraparietal areas of macaque monkey. The Journal of Neuroscience *22*, 1994–2004.

Cook, E.P., and Maunsell, J.H.R. (2002b). Dynamics of neuronal responses in macaque MT and VIP during motion detection. Nature Neuroscience *5*, 985–994.

Cowey, A., Campana, G., Walsh, V., and Vaina, L.M. (2006). The role of human extra-striate visual areas V5/MT and V2/V3 in the perception of the direction of global motion: a transcranial magnetic stimulation study. Experimental Brain Research *171*, 558–562.

Cowey, A., and Porter, J. (1979). Brain damage and global stereopsis. Proceedings of the Royal Society of London *204*, 399–407.

Cowey, A., and Wilkinson, F. (1991). The role of the corpus callosum and extra striate visual areas in stereoacuity in macaque monkeys. Neuropsychologia *29*, 465–479.

Cumming, B.G., and DeAngelis, G.C. (2001). The Physiology of Stereopsis. Annual Review of Neuroscience *24*, 203–238.

DeAngelis, G.C., Cumming, B.G., and Newsome, W.T. (1998). Cortical area MT and the perception of stereoscopic depth. Nature *394*, 677–680.

DeAngelis, G.C., and Newsome, W.T. (1999). Organization of disparity-selective neurons in macaque area MT. The Journal of Neuroscience *19*, 1398–1415.

DeAngelis, G.C., and Newsome, W.T. (2004). Perceptual "read-out" of conjoined direction and disparity maps in extrastriate area MT. PLoS Biology *2*, E77.

DeAngelis, G.C., and Uka, T. (2003). Coding of horizontal disparity and velocity by MT neurons in the alert macaque. Journal of Neurophysiology *89*, 1094–1111.

DeYoe, E.A., and Van Essen, D.C. (1988). Concurrent processing streams in monkey visual cortex. Trends in Neurosciences *11*, 219–226.

DeYoe, E.A., and Essen, D.C.V. (1985). Segregation of efferent connections and receptive field properties in visual area V2 of the macaque. Nature *317*.

Dosher, B.A., and Lu, Z.-L.L. (1998). Perceptual learning reflects external noise filtering and internal noise reduction through channel reweighting. Proceedings of the National Academy of Sciences *95*, 13988–13993.

Dubner, R., and Zeki, S. (1971). Response properties and receptive fields of cells in an anatomically defined region of the superior temporal sulcus in the monkey. Brain Research *35*, 528–532.

Efron, B., and Tibshirani, R.J. (1998). An Introduction to the Bootstrap (New York: Chapman and Hall/CRC).

Van Essen, D.C., and Gallant, J.L. (1994). Neural mechanisms of form and motion processing in the primate visual system. Neuron *13*, 1–10.

Felleman, D.J., and Van Essen, D.C. (1987). Receptive Field Properties of Neurons in Area V3 of Macaque Monkey Extrastriate Cortex. Journal of Neurophysiology *57*.

Gattass, R., Sousa, a P., and Gross, C.G. (1988). Visuotopic organization and extent of V3 and V4 of the macaque. The Journal of Neuroscience : the Official Journal of the Society for Neuroscience *8*, 1831–1845.

Gegenfurtner, K.R., Kiper, D.C., Beusmans, J.M.H., Carandini, M., Zaidi, Q., and Movshon, J.A. (1994). Chromatic properties of neurons in macaque MT. Visual Neuroscience *11*, 455–466.

Gegenfurtner, K.R., Kiper, D.C., and Fenstemaker, S.B. (1996). Processing of color, form, and motion in macaque V2. Visual Neuroscience *13*, 161–172.

Gegenfurtner, K.R., Kiper, D.C., and Levitt, J.B. (1997). Functional Properties of Neurons in Macaque Area V3. Journal of Neurophysiology *77*, 1906–1923.

Ghose, G.M., Yang, T., and Maunsell, J.H.R. (2002). Physiological correlates of perceptual learning in monkey V1 and V2. Journal of Neurophysiology *87*, 1867–1888.

Girard, P., Salin, P.A., and Bullier, J. (1992). Response selectivity of neurons in area MT of the macaque monkey during reversible inactivation of area V1. Journal of Neurophysiology *67*, 1437–1446.

Glickstein, M., Cohen, J.L., Dixon, B., Gibson, A., Hollins, M., Labossiere, E., and Robinson, F. (1980). Corticopontine visual projections in macaque monkeys. The Journal of Comparative Neurology *190*, 209–229.

Gold, J.I., and Shadlen, M.N. (2002). Banburismus and the Brain : Decoding the Relationship between Sensory Stimuli, Decisions, and Reward. Neuron *36*, 299–308.

Hegdé, J., and Van Essen, D.C. (2000). Selectivity for complex shapes in primate visual area V2. The Journal of Neuroscience *20*.

von der Heydt, R., Peterhans, E., Baumgartner, G., and Baumbgartner, G. (1984). Illusory Contours and Cortical Neuron Responses. Science *224*, 1260–1262.

Hubel, D.H., and Livingstone, M.S. (1985). Complex-unoriented cells in a subregion of primate area 18. Nature *315*.

Hubel, D.H., and Livingstone, M.S. (1987). Segregation of Form , Color, and Stereopsis in Primate Area 18. The Journal of Neuroscience *7*, 3378–3415.

Ilmoniemi, R.J., Virtanen, J., Ruohonen, J., Karhu, J., Aronen, H.J., Näätänen, R., and Katila, T. (1997). Neuronal responses to magnetic stimulation reveal cortical reactivity and connectivity. Neuroreport *8*, 3537–3540.

Janssen, P., Vogels, R., Liu, Y., and Orban, G.A. (2001). Macaque inferior temporal neurons are selective for three-dimensional boundaries and surfaces. The Journal of Neuroscience *21*, 9419–9429.

Janssen, P., Vogels, R., and Orban, G. a (2000). Three-dimensional shape coding in inferior temporal cortex. Neuron *27*, 385–397.

Law, C.-T., and Gold, J.I. (2008). Neural correlates of perceptual learning in a sensory-motor, but not a sensory, cortical area. Nature Neuroscience *11*, 505–513.

Law, C.-T., and Gold, J.I. (2009). Reinforcement learning can account for associative and perceptual learning on a visual-decision task. Nature Neuroscience *12*, 655–663.

Levitt, J.B., Kiper, D.C., and Movshon, J.A. (1994). Receptive Fields and Functional Architecture of Macaque V2. Journal of Neurophysiology *71*.

Lomber, S.G., Payne, B.R., and Horel, J. a (1999). The cryoloop: an adaptable reversible cooling deactivation method for behavioral or electrophysiological assessment of neural function. Journal of Neuroscience Methods *86*, 179–194.

Macmillan, N.A., and Creelman, D.C. (2004). Detection Theory: A User's Guide (Psychology Press).

Maunsell, J.H.R., and Van Essen, D.C. (1983a). Functional properties of neurons in middle temporal visual area of the macaque monkey. I. Selectivity for stimulus direction, speed, and orientation. Journal of Neurophysiology *49*, 1127–1147.

Maunsell, J.H.R., and Van Essen, D.C. (1983b). Functional properties of neurons in middle temporal visual area of the macaque monkey. II. Binocular interactions and sensitivity to binocular disparity. Journal of Neurophysiology *49*, 1148–1167.

Maunsell, J.H.R., and Van Essen, D.C. (1983c). The connections of the middle temporal visual area (MT) and their relationship to a cortical hierarchy in the macaque monkey. The Journal of Neuroscience *3*, 2563–2586.

Maunsell, J.H.R., and Newsome, W.T. (1987). Visual processing in monkey extrastriate cortex. Annual Review of Neuroscience *10*, 363–401.

Merigan, W.H., and Maunsell, J.H.R. (1993). How parallel are the primate visual pathways? Annual Review of Neuroscience *16*, 369–402.

Merigan, W.H., Nealey, T.A., and Maunsell, J.H.R. (1993). Visual effects of lesions of cortical area V2 in macaques. The Journal of Neuroscience *13*, 3180–3191.

Mitchell, J.F., Sundberg, K. a, and Reynolds, J.H. (2009). Spatial attention decorrelates intrinsic activity fluctuations in macaque area V4. Neuron *63*, 879–888.

Movshon, J.A., and Newsome, W.T. (1996). Visual response properties of striate cortical neurons projecting to area MT in macaque monkeys. The Journal of Neuroscience *16*, 7733–7741.

Newsome, W.T., and Pare, E.B. (1988). A Selective Impairment of Motion Perception Following Lesions of the Middle Temporal Visual Area (MT). The Journal of Neuroscience *8*, 2201–2211.

Nienborg, H., and Cumming, B.G. (2009). Decision-related activity in sensory neurons reflects more than a neuron's causal effect. Nature *459*, 89–92.

Nienborg, H., and Cumming, B.G. (2010). Correlations between the activity of sensory neurons and behavior: how much do they tell us about a neuron's causality? Current Opinion in Neurobiology *20*, 376–381.

Okun, M., and Lampl, I. (2008). Instantaneous correlation of excitation and inhibition during ongoing and sensory-evoked activities. Nature Neuroscience *11*, 535–537.

Osborne, L.C., Lisberger, S.G., and Bialek, W. (2005). A sensory source for motor variation. Nature *437*, 412–416.

Pack, C.C., Born, R.T., and Livingstone, M.S. (2003). Two-dimensional substructure of stereo and motion interactions in macaque visual cortex. Neuron *37*, 525–535.

Pack, C.C., Conway, B.R., Born, R.T., and Livingstone, M.S. (2006). Spatiotemporal structure of nonlinear subunits in macaque visual cortex. The Journal of Neuroscience : the Official Journal of the Society for Neuroscience *26*, 893–907.

Parker, A.J., and Newsome, W.T. (1998). Sense and the single neuron: probing the physiology of perception. Annual Review of Neuroscience *21*, 227–277.

Peterhans, E., and von der Heydt, R. (1993). Functional organization of area V2 in the alert macaque. The European Journal of Neuroscience *5*, 509–524.

Ponce, C.R., Lomber, S.G., and Born, R.T. (2008). Integrating motion and depth via parallel pathways. Nature Neuroscience *11*, 216–223.

Purushothaman, G., and Bradley, D.C. (2005). Neural population code for fine perceptual decisions in area MT. Nature Neuroscience *8*, 99–106.

Rodman, H.R., Gross, C.G., and Albright, T.D. (1989). Afferent basis of visual response properties in area MT of the macaque. I. Effects of striate cortex removal. The Journal of Neuroscience *9*, 2033–2050.

Roe, A.W., Chelazzi, L., Connor, C.E., Conway, B.R., Fujita, I., Gallant, J.L., Lu, H., and Vanduffel, W. (2012). Toward a Unified Theory of Visual Area V4. Neuron *74*, 12–29.

Roe, A.W., Parker, A.J., Born, R.T., and DeAngelis, G.C. (2007). Disparity channels in early vision. The Journal of Neuroscience *27*, 11820–11831.

Roitman, J.D., and Shadlen, M.N. (2002). Response of neurons in the lateral intraparietal area during a combined visual discrimination reaction time task. The Journal of Neuroscience *22*, 9475–9489.

Ruff, D.A., and Born, R.T. The role of neuronal tuning in attention. In Preparation.

Salzman, D.C., Britten, K.H., and Newsome, W.T. (1990). Cortical microstimulation influcences perceptual judegements of motion direction. Nature *346*.

Sasaki, R., and Uka, T. (2009). Dynamic readout of behaviorally relevant signals from area MT during task switching. Neuron *62*, 147–157.

Schiller, P.H. (1993). The effects of V4 and middle temporal (MT) area lesions on visual performance in the rhesus monkey. Visual Neuroscience *10*, 717–746.

Seidemann, E., Poirson, A.B., Wandell, B. a, and Newsome, W.T. (1999). Color Signals in Area MT of the Macaque Monkey. Neuron *24*, 911–917.

Shadlen, M.N., and Newsome, W.T. (1994). Noise, neural codes and cortical organization. Current Opinion in Neurobiology.

Shipp, S., and Zeki, S. (1985). Segregation of pathways leading from area V2 to areas V4 and V5 of macaque monkey visual cortex. Nature *315*.

Shipp, S., and Zeki, S. (1989). The Organization of Connections between Areas V5 and V2 in Macaque Monkey Visual Cortex. The European Journal of Neuroscience *1*, 333–354.

Sincich, L.C., and Horton, J.C. (2003). Independent projection streams from macaque striate cortex to the second visual area and middle temporal area. The Journal of Neuroscience *23*, 5684–5692.

Sincich, L.C., Park, K.F., Wohlgemuth, M.J., and Horton, J.C. (2004). Bypassing V1: a direct geniculate input to area MT. Nature Neuroscience *7*, 1123–1128.

Smith, J.E.T., Zhan, C.A., and Cook, E.P. (2011). The Functional Link between Area MT Neural Fluctuations and Detection of a Brief Motion Stimulus. Journal of Neuroscience *31*, 13458–13468.

Smith, M. a, and Kohn, A. (2008). Spatial and temporal scales of neuronal correlation in primary visual cortex. The Journal of Neuroscience *28*, 12591–12603.

Softky, W.R., and Koch, C. (1993). The highly irregular firing of cortical cells is inconsistent with temporal integration of random EPSPs. The Journal of Neuroscience *13*, 334–350.

Stepniewska, I., Qi, H.X., and Kaas, J.H. (1999). Do superior colliculus projection zones in the inferior pulvinar project to MT in primates? The European Journal of Neuroscience *11*, 469–480.

Uka, T., and DeAngelis, G.C. (2004). Contribution of area MT to stereoscopic depth perception: choice-related response modulations reflect task strategy. Neuron *42*, 297–310.

Umeda, K., Tanabe, S., and Fujita, I. (2007). Representation of stereoscopic depth based on relative disparity in macaque area V4. Journal of Neurophysiology *98*, 241–252.

Ungerleider, L.G., and Desimone, R. (1986). Cortical connections of visual area MT in the macaque. The Journal of Comparative Neurology *248*, 190–222.

Ungerleider, L.G., and Mishkin, M. (1982). Two Cortical Visual Systems. In Analysis of Visual Behavior, D.J. Ingle, M.A. Goodale, and R.J.W. Mansfield, eds. (Cambridge, MA: MIT Press), pp. 549–586.

Vaina, L.M., Soloviev, S., Bienfang, D.C., and Cowey, A. (2000). A lesion of cortical area V2 selectively impairs the perception of the direction of first-order visual motion. NeuroReport *11*, 1039–1044.

Wheatstone, C. (1838). Contributions to the Physiology of Vision. Part the First. On Some Remarkable, and Hitherto Unobserved, Phenomena of Binocular Vision. Philosophical Transactions of the Royal Society of London *128*, 371–394.

Wichmann, F.A., and Hill, N.J. (2001a). The psychometric function: I. Fitting, sampling, and goodness of fit. Perception & Psychophysics *63*, 1293–1313.

Wichmann, F.A., and Hill, N.J. (2001b). The psychometric function: II. Bootstrap-based confidence intervals and sampling. Perception & Psychophysics *63*, 1314–1329.

Yang, T., and Maunsell, J.H.R. (2004). The effect of perceptual learning on neuronal responses in monkey visual area V4. The Journal of Neuroscience *24*, 1617–1626.